Synthesis and characterization of biodegradable polyesters : polymerization mechanisms and polymer microstructures revealed by MALDI-ToF-MS

Document Version:

Publisher's PDF, also known as Version of Record (includes final page, issue and volume numbers)

Please check the document version of this publication:

• A submitted manuscript is the version of the article upon submission and before peer-review. There can be important differences between the submitted version and the official published version of record. People interested in the research are advised to contact the author for the final version of the publication, or visit the DOI to the publisher's website.
• The final author version and the galley proof are versions of the publication after peer review.
• The final published version features the final layout of the paper including the volume, issue and page numbers.

Link to publication

Synthesis and characterization
of biodegradable polyesters

'Polymerization mechanisms and polymer microstructures revealed by MALDI-ToF-MS'

Saskia Huijser

Synthesis and characterization of biodegradable polyesters

'Polymerization mechanisms and polymer microstructures revealed by MALDI-ToF-MS'

PROEFSCHRIFT

ter verkrijging van de graad van doctor aan de
Technische Universiteit Eindhoven, op gezag van de
Rector Magnificus, prof.dr.ir. C.J. van Duijn, voor een
commissie aangewezen door het College voor
Promoties in het openbaar te verdedigen
op maandag 8 juni 2009 om 16.00 uur

door

Saskia Huijser

geboren te Eindhoven

Dit proefschrift is goedgekeurd door de promotoren:

prof.dr. C.E. Koning
en
prof.dr. A.M. van Herk

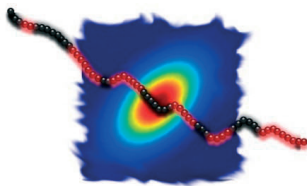Copromotor:
dr. R. Duchateau

Voor mijn ouders.

Table of Contents

1

Introduction

Abstract. *Polyesters constitute an important class of polymers and have earned their world fame as fiber material in bed linen and clothing, food containers and automotive parts. Currently, polyesters of lactones and lactides have drawn increasing attention as therapeutic devices due to their good biodegradability and biocompatibility. Homo- and copolymers of lactones and lactides can be synthesized by a ring-opening polymerization, which can proceed anionically, cationically, and by a metal-catalyzed coordination/insertion mechanism. Especially, the latter method is widely employed due to the capability of performing controlled stereospecific polymerizations resulting in high molecular weight polymers with low polydispersities. As many of the lactide and lactone polymers are nowadays predominantly used for medical applications, there is a strong interest in obtaining this polymer without the use of (toxic) metal catalysts. Enzymes and organic catalysts might be a feasible solution to circumvent the use of these metal catalysts. Due to their capability for stereo-, regio-, and chemoselective polymerizations under mild reaction conditions, enzymes have gained increasing appreciation in the world of polymer synthesis. However, due to their inherent characteristic to give relatively broad molecular weight distributions, the demand for other metal-free more controlled polymerization catalysts is pressing. In the past few years, N-heterocyclic carbenes have given the status of promising replacements of their metal-based colleagues due to the living character of the polymerizations catalyzed. Recently, an old pathway towards polyesters has been revived due to the development of new effective metal catalysts. The ring-opening polymerization of oxiranes and anhydrides no longer suffers from the formation of ether linkages by homopolymerization of the oxirane, but can be obtained in its purely alternating topology, thereby opening perspective for the synthesis of new polyesters with different properties.*

1.1 A brief history of plastics and polyesters

The development of plastics bloomed forty to fifty years ago in a time when the oil supply seemed infinite. It was not without reason that Benjamin Braddock (Dustin Hoffman) got a single word of advice 'Plastics' in the movie The Graduate in 1967.[1] The first truly synthetic polymer was discovered in 1909 by Leo Baekeland and was synthesized from phenol and formaldehyde. The polymer was launched as Bakelite and used mainly as casings of house appliances such as radios, telephones and door handles. During the Second World War, the development of plastics was mostly pushed by Germany and Russia out of necessity for warfare appliances. Nylon which was already discovered in the 1920s was produced on large scale for the manufacturing of parachutes. After the war the oil prices dropped, stimulating research in the petrochemical industry with as result some major breakthroughs. In the 1950s even domestic parties were being introduced for little plastic containers called Tupperware. At this time plastic had made its introduction into the homes of people. The advantage of plastics over traditional materials (wood, paper, glass, metal) became apparent and the production increased rapidly. The worldwide production of plastic over the last 60 years has grown from 1.3 million tons in 1950 to a predicted 230 million metric tons in 2008.[2,3]
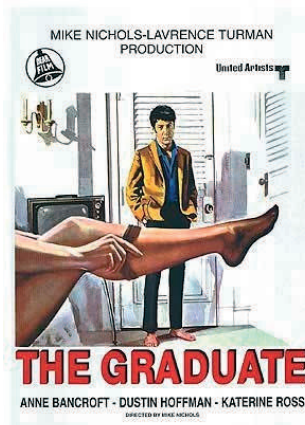
Polyesters form a particular class of polymers and probably the only polymer that got 'awarded' being the title of a movie released in 1981 directed by John Waters. Polyesters are well-known fiber materials for clothing and bed sheets. The first polyester was discovered by W.H. Carothers who found that fibers could be created by polycondensation of diols with dicarboxylic acids. Carothers' discovery was pursuit by two British scientists who patented polyethylene terephthalate (PET) in 1941 while working for Calico Printer's Association of Manchester. In 1946 DuPont took over the legal rights and in the years to follow, polyester became popular as textile fiber that would remain wrinkle-free upon wearing and washing.[3,4]

As the advice of Mr. McGuire in The Graduate nowadays still holds, the challenges in the field of plastics have changed due to the high oil prices and for most the environmental problems our planet is dealing with. The challenge is no longer only the result of the desire to find the ultimate polymer or composite material for a given goal or problem. The challenge lies in finding materials that can replace existing plastics in terms of physical properties and production scale but have no polluting effect on our ecosystems, in other words, plastics that can be produced from so-called renewable materials. Moreover, the research into plastics that can sustain health and youth or help to cure diseases has increased vastly as biomedical technology progresses.

Not only did plastic found its way into our homes, currently it also finds its way into our body. Typical examples are artificial kneecaps, hip joints, bone screws, breast implants and all kinds of therapeutic devices. The past decades, the polyester market got a small boost again when it was discovered that aliphatic polyesters as poly(lactide) and poly(ε-caprolactone) are biodegradable and non-toxic. The latter awakened a whole new era of polyester research.

1.2 Synthesis of polyesters

Polyesters can be synthesized in various ways as shown in Figure 1-1. Classically, bulk polyesters are synthesized by polycondensation of diols with diacids or of hydroxyacids. This method knows several disadvantages, *e.g.* high reaction temperatures are required, elimination side-products need to be removed and long reaction times are needed to obtain high molecular weight material.[4]
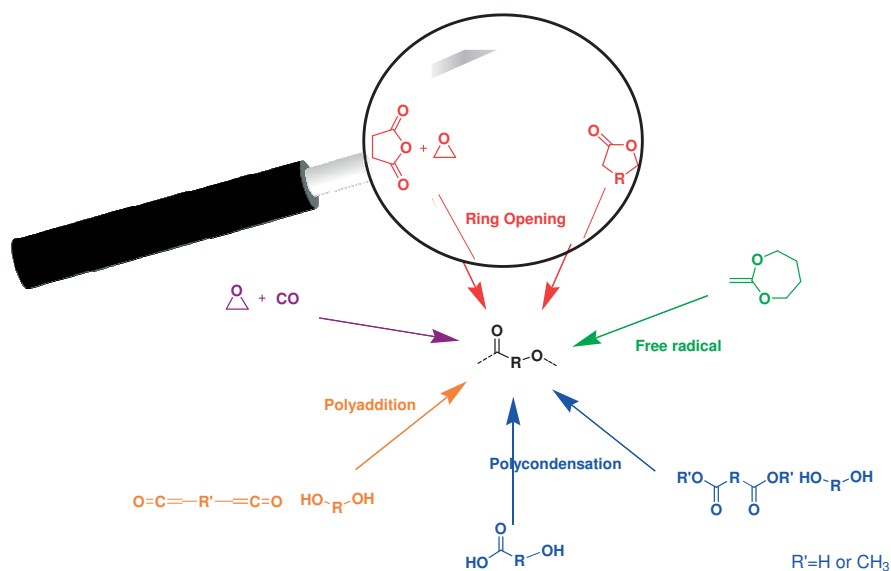
Figure 1-1. Different routes to synthesize polyesters.

The past two decades, the ring-opening polymerization of lactides and lactones has gained increasing attention, not only due to the biodegradable and biocompatible properties of the corresponding polyesters, but also due to the fact that the monomers used are often not petroleum based. Ring-opening polymerization (ROP) of lactides and lactones can be done enzymatically, ionically and by coordinative initiation. Although it is known for many years, a relatively unexplored field of research is the metal-mediated ring-opening polymerization of oxiranes with anhydrides. Other mechanisms than coordination/insertion often have the disadvantage of homopolymerization of the oxirane.

3

In this case a polyether or in some cases a poly(ester-*co*-ether) is obtained. Inoue *et al.* were the first to report on the successful polymerization by coordination catalysis of phthalic anhydride and amongst others cyclohexene oxide.[5,6] Recently, Coates' *β*-diketiminato zinc complexes have shown to be highly active in the perfect alternating copolymerization of amongst others succinic anhydride with cyclohexene oxide.[7] In this thesis more insight into both mentioned types of ring-opening polymerization is provided.

An example of a polyester which cannot easily be synthesized by ring-opening polymerization is poly(*γ*-butyrolactone) as a consequence of the stability of the five-membered ring.[4] A more effective way to synthesize this polyester is by free radical polymerization of 2-methylene-1,3-dioxolane, a cyclic ketene acetal.[8] This route has also been employed to synthesize poly(*ε*-caprolactone) from 2-methylene-1,3-dioxepane using AIBN as initiator.[9] Another less well-known polymerization is the reaction between a bisketene and a diol. The problem with these reactions is the tendency of the bisketene to dimerize or to homopolymerize and its reaction with oxygen or water. Sebacyl bisketene was reacted with bisphenol A resulting in polyesters with molecular weights up to 50,000 g·mol^{-1}.[10]

Finally, the carbonylation of an oxirane can lead to cyclic lactones but also to alternating polyesters.[11] Drent *et al.* [12] patented in 1993 the carbonylation of epoxides catalyzed by $Co_2(CO)_8$ / 3-hydroxypyridine with as aimed product the *β*-lactone, but it was later found by others that in fact the polyester was afforded as main product. The theory that the polymer was obtained from the ring-opening of the *β*-lactone appeared to be incorrect as discovered by the group of Rieger. They reported on the synthesis of poly(3-hydroxybutyrate) from propene oxide with carbon monoxide.[13] This route is not very popular due to the toxicity of carbon monoxide.

1.2.1 Ring-opening polymerization of lactones and lactides

The ring-opening polymerization of lactides and lactones was firstly reported by Carothers. Ring-opening polymerization of cyclic esters can be accomplished anionically, cationically, by a coordination / insertion mechanism and by enzymes. Anionic ring-opening polymerization is often initiated by alkali metal alkoxides.[14,15] The cationic polymerization often requires Lewis acids ($AlCl_3$, BF_3, $FeCl_3$, $ZnCl_2$) or Brønsted acids (HCl, RCOOH).[16,17] Due to their versatility, the other two mechanisms, coordination-insertion and enzymatic ring-opening, will be discussed separately in paragraphs 1.2.1.1 and 1.2.1.2 respectively. In paragraph 1.2.1.3 an interesting new class of catalysts will be discussed, namely the organic, metal-free catalysts.
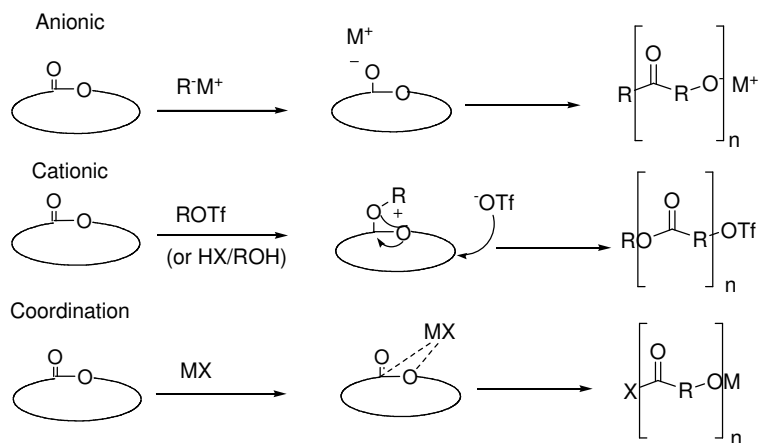
Figure 1-2. Different pathways to ring open a cyclic ester.[17]

1.2.1.1 Transition and main metal catalysts

The development of effective transition metal catalysts revolutionized mainly in the field of polyolefin synthesis. The rate of these developments naturally reflected also in other fields of polymer chemistry with as result that a large variety of polymers and polymer architectures were obtained using metal-based catalysts. Moreover the discovery of stereo-selective synthesis by metal complexes ever increased the popularity and the pool of desired physical properties could finally be bridged. Typical ligands for diverse metal complexes used to synthesize polyesters are given in Figure 1-3.
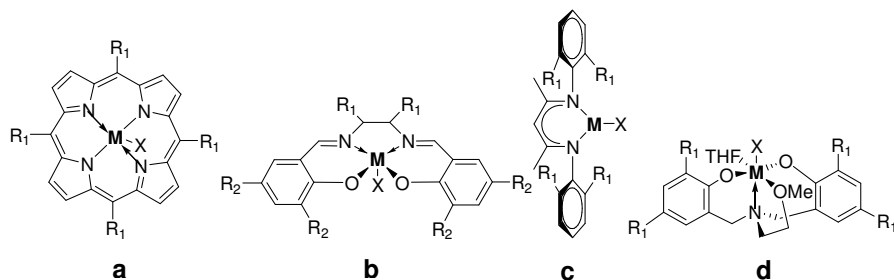
Figure 1-3. Catalytic complexes used in the ring-opening of lactones and lactides, a) porphyrin complex, b) salen complex, c) β–diketiminato complex, d) bisphenolate amine complex.[18-20]

Porphyrinato complexes have gained considerable interest due to their role as photosynthetic centers. The porphyrins coordinate to different metals and are nowadays applied in the living polymer synthesis of diverse monomers. Different lactones, epoxides, cyclic ethers, carbonates and siloxanes have been ring opened and polymerized by mainly aluminum porphyrins and later by their chromium analogues.[21] Metalloporphyrins were employed by Inoue *et al.* in the reaction of CO_2 with epoxides

based on their discovery in the late 1960s of the successful alternating copolymerization of carbon dioxide and epoxide to form polycarbonates.[22,23] Later they also reported the formation of polyester by ring-opening polymerization of an anhydride with an epoxide but unfortunately relatively low molecular weights were obtained at that time.[5,6]

The salen ligands can be considered as cheaper alternatives to the porphyrin complexes. The term salen stands for the *N,N''*-bis-(salicylidene)-1,2-ethylenediimine ligand and was firstly synthesized by Pfeiffer.[24] Jacobsen *et al.* reported the synthesis of a chiral salen ligand employed in the asymmetric epoxidation of simple olefins.[25] His discovery triggered research groups to use these complexes or similar ones in the synthesis of polycarbonates from epoxides and CO_2. The groups of Coates and mainly Darensbourg reported several different types of salen complexes to produce polycarbonates.[26-29] In parallel, the chiral ring-opening polymerization of lactide was firstly reported by Spassky using the (R)-SALBinaphtAlOCH$_3$ complex.[30] Since then other studies reported on the stereo-selective polymerization of lactide using (chiral) salen–type Schiff base complexes.[31-33] Lactide possesses two asymmetrical carbons and therefore has three different isomers, namely L-lactide, D-lactide and meso-lactide (Figure 1-4).
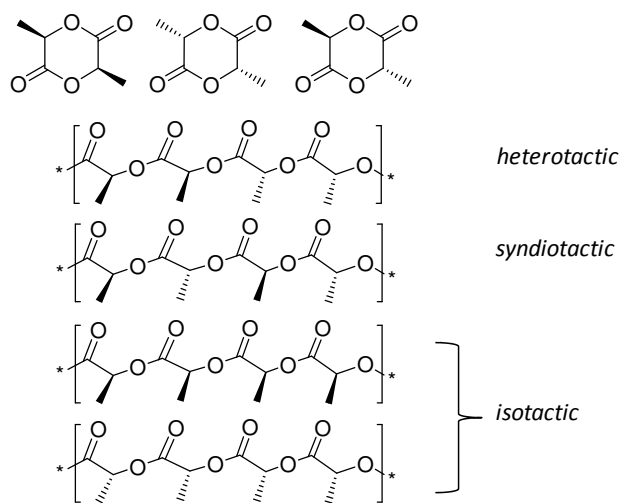
Figure 1-4. Different stereo-isomers of lactide.

Nomura and co-workers investigated for example stereo-selectivity induced by using *achiral* salen type complexes in a chain end control mechanism.[34] Moreover, they performed a systematic exploration on the steric effects by the substituents on achiral salen ligands. It was found that the substituents at the 3-position of the salicylidene moiety are decisive for stereoselectivity and that the backbone determines the rate of polymerization.[35]

Another well-known ancillary ligand applied for ROP catalysts is the β-diketiminate (BDI). Coates' complex with zinc is extremely powerful in the alternating copolymerization of epoxides and carbon dioxide but also in the ring-opening polymerization of lactones and lactides.[36-39] Additionally, calcium, magnesium, Group 3 metal and lanthanide BDI complexes have been investigated in the ROP of lactide. It was found that the reactivity towards ring-opening of an equivalent amount of lactide was in the order Ca>Mg>Zn, which corresponds to the degree of polar character of the metal amide bond. Nevertheless, in the actual polymerization of lactide the order of Ca and Mg was reversed. Most likely the ligand was not sufficiently sterically demanding due to the bigger calcium which explains the formation of atactic-PLA.[40,41] Recently, the zinc BDI complexes have also proven to be good homogeneous catalysts in the reaction of anhydride with epoxide to form polyesters.[7]

Bisphenolate-amine Group 3 metal complexes were examined by the group of Carpentier in the ring-opening of β-butyrolactone and lactide. The polymerizations proceeded rapidly at room temperature to afford highly stereospecific polymers.[42-44] Zwitterionic complexes were reported by Mountford *et al.* using lanthanide metals in the ring-opening of poly(lactide) and poly(ε-caprolactone).[45,46] As reported, these zwitterionic complexes have the tendency to form macrocyclic structures. Group 4 metal bisphenolate complexes of titanium and zirconium were studied by Gendler in the ROP of lactide displaying a 10-fold higher activity of the zirconium complexes relative to the titanium complexes.[47] Other examples of poly(phenolate) complexes are the rare earth silylamido complexes investigated in the ring-opening of lactide by Ma *et al.* and the germanium trisphenolate complexes of Chmura.[48,49]

The most widely known and investigated metal catalyst in the ring-opening polymerization of cyclic esters is tin(II) 2-ethylhexanoate or stannous octoate; not in the least due to the fact that poly(lactides) synthesized by this particular catalyst are approved by the Food and Drug Administration (FDA). The mechanism of the ring-opening by $Sn(Oct)_2$ is subject to discussion as well as the nature of the species in its role as catalyst or initiator. The most supported theory is that $Sn(Oct)_2$ reacts with protic agents as concomitant water or an additional co-initiating alcohol present to afford the factual active covalent tin(II) alkoxide species, as expressed in equations 1-1 and 1-2 by Kowalski.[18,20,50]

$$Sn(Oct)_2 + ROH \leftrightarrows OctSnOR + OctH \qquad\qquad\qquad (1\text{-}1)$$

$$OctSnOR + ROH \leftrightarrows Sn(OR)_2 + OctH \qquad\qquad\qquad (1\text{-}2)$$
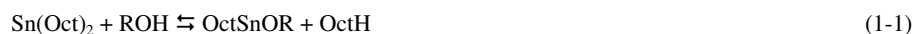
The polymerization would then actually proceed via a coordination-insertion between the Sn-OR bond.[51-54] Other metal alkoxide species are aluminum alkoxides in particular the aluminum trialkoxides ($Al(OR)_3$). An example is aluminum tri-isopropoxide which by a coordination-insertion mechanism polymerizes lactide but is significantly less active than $Sn(Oct)_2$.

Nevertheless, unlike the tin-catalyzed reaction, the polymerization is characterized by a very low amount of transesterification side reactions.[55] As aluminum is suspected to cause Alzheimer, it is less often used than the competing tin(II) species, although the use of tin species in the field of medicine is also still questionable. Generally, the disadvantages of metal-based catalysts are the toxicity, the complex syntheses and the expenses of the materials.

1.2.1.2 Enzymes

The word enzyme was firstly adopted by Wilhelm Kühne in 1878 to describe the catalyst in the process of fermentation of sucrose. Enzymes are built up from amino acids and fulfill in nature the role of catalyst in many different metabolic reactions. Classification of enzymes is done according to the type of reaction they catalyze. A few enzymes are known to catalyze polymerizations of which lipase is probably the most famous. Lipases are enzymes belonging to the class of hydrolases and are capable of the hydrolysis of fatty acid esters. The use of lipases in the ring-opening of lactones was first reported in 1993 by Knani[56] and Uyama.[57] Next to ring-opening polymerizations, lipases can also catalyze polycondensation reactions. Most successful in terms of molecular weight and reaction rate are the ring-opening polymerizations of lactones. Different sizes of lactone-rings varying from β-butyrolactone to ω-pentadecalactone have been opened and polymerized using lipases. The ring-opening polymerization of lactides, however, has not been as successful. Some intensively investigated lactones are given in Figure 1-5.
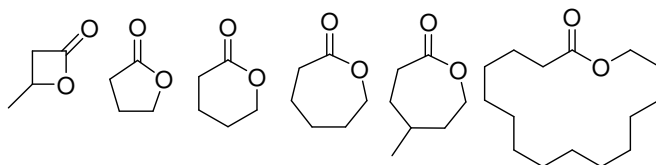
Figure 1-5. Different sized lactones, a) β-butyrolactone, b) γ-butyrolactone, c) δ-valerolactone, d) ε-caprolactone, e) 4-methyl-ε-caprolactone f) ω-pentadecalactone.

Most research has been conducted in the field of polymer chemistry on *Candida antarctica* or Novozyme 435 named after the Danish firm that commercialized this lipase. Enzymes have several advantages over their metal analogues; enzymes are non toxic, can operate under mild reaction conditions (pH, pressure, temperature) and still display a great selectivity. Moreover, the use of organic solvents can be avoided, although many enzymes exhibit activity in these media.

The catalytic activity of an enzyme in ring-opening polymerization reactions derives from the primary alcohol of a serine moiety.

The nucleophilic attack of this alcohol on the ester substrate of the lactone, results in a ring-opening followed by formation of an acyl-enzyme intermediate. The next initiation step is induced by water present or by an additional alcohol regenerating the free lipase. Finally, the addition of units to a polymer chain is accomplished by the nucleophilic attack on the intermediate by an earlier ring-opened product. The mechanism of eROP is given in Scheme 1-1.[58-61]

Acyl-Enzyme Intermediate
(Enzyme-activated monomer)

Initiation:

EM + H$_2$O $\longrightarrow$ H$-$O(CH$_2$)$_m$C$-$OH + Lip.$-$OH

Propagation

EM + H[O(CH$_2$)$_m$C]$_n$OH $\longrightarrow$ H[O(CH$_2$)$_m$C]$_{n+1}$OH + Lip.$-$OH
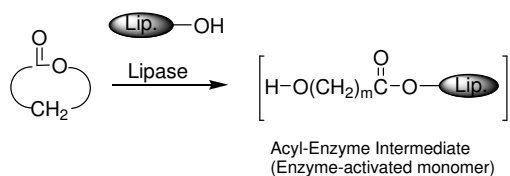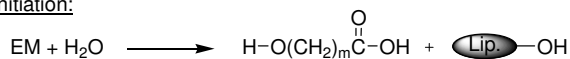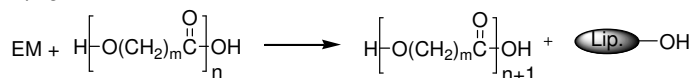
Scheme 1-1. Postulated mechanism of enzymatic ring-opening polymerization (eROP) of cyclic esters.[60]

Comparison of the enzymatic ring-opening with the chemical ring-opening was performed for different ring sizes of lactones. Van der Mee thoroughly investigated the eROP of different sized lactones from the 6 to the 13 membered ring and the 16 membered ring.[62] The easy polymerizability of ω-pentadecalactone by lipase already suggested that ring strain is not the driving force here. In chemical ring-opening polymerizations it was found by Duda *et al.* that a liquid-state polymerization of smaller ring lactones is driven by the negative change of enthalpy. Contrarily, the polymerization of larger rings is driven by a positive change in entropy.[63] Currently, the only metal-based catalyst known to ring open PDL in a controlled way is yttrium isopropoxide.[64] Overall it can be concluded that bigger ring sized lactones are difficult to polymerize using metal-based catalysts. The capability of enzymes to attack the ester bonds of non ring-strained lactones also explains the facile transesterification observed during eROP of lactones.

1.2.1.3 Organic catalysts

The first example of a living polymerization using organic catalysts in the polymerization of cyclic esters was reported by Nederberg *et al.* in 2001 using 4-N,N-(dimethylamino pyridine) and 4-pyrrolidinopyridine as catalysts.[65]

Later that year, Connor *et al.* reported on the ring-opening of lactide, *ε*-caprolactone and *β*-butyrolactone by N-heterocyclic carbenes.[66] The ROP of lactide using a diaryl carbene proceeded at room temperature within a few seconds. The living character of the polymerization is apparent from the linear relation between molar mass and conversion and from the narrow molar mass distribution (PDI < 1.2). Remarkable is the formation of purely macrocyclic structures without the presence of an initiator attributed to a zwitterionic mechanism.[67] Recently, it was reported that phosphazenes quantitatively polymerize lactide in 10s at room temperature. [68,69] A good overview of the diverse organic catalysts used in ROP is published by Kamber *et al.*[70] The common nominator is their nucleophilic character and their attack on the carbon atom of the polar carbonyl bond, inducing a break of the acyl bond. The advantage of this type of catalysts is the absence of (toxic) metals. The most important organic catalysts in the ring-opening polymerization of lactide and the proposed mechanism are displayed in Scheme 1-2.
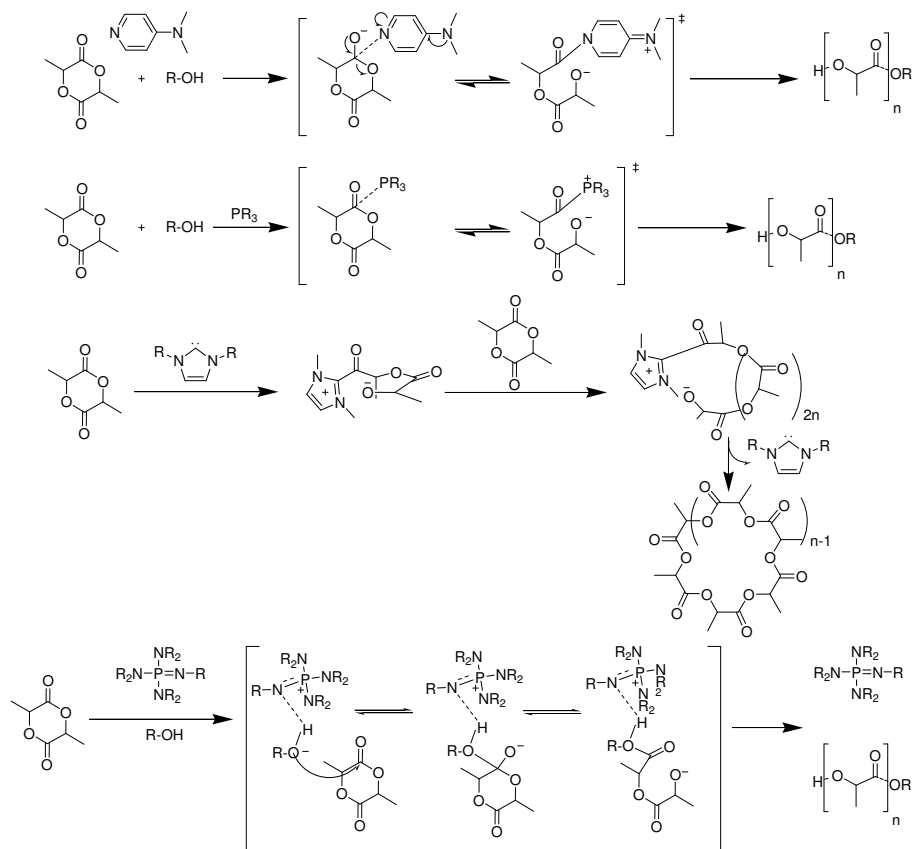
Scheme 1-2. Postulated mechanisms for the diverse reactions of the organocatalytic ROP of lactide.

In summary, ring-opening can proceed in various ways, by various catalysts in a controlled and less controlled manner with metal catalysts and without, in different solvents, at different temperatures and times. Table 1-1 provides a very general and selected overview of the activity of different catalytic systems for the ring-opening polymerization of lactide.

Table 1-1. Selected overview of results in ROP of lactide with different catalysts.

Catalyst	M/I	T (^{o}C)	t (h)	M_n (g·mol^{-1})	PDI
Sn(Oct)$_2$[71]	100/1	120	24	23,760	n.d.
Porphyrin Aluminum alkoxide[72]	100/1	100	96	16,400	1.12
Salen Aluminum Ethyl[35]	100/1	70	26	8,000	1.2
(BDI-1)Zn^{i}OPr[38]	200/1	20	0.33	37,900	1.10
Amino-alkoxy-bis(phenolate)Yttrium[42]	100/1	20	0.08	14,400	1.06
Carbene[67]	100/1	25	0.008	15,000	1.16
Phosphazene[68]	100/1	20	0.003	25,800	1.23
Candida antarctica	-	-	-	-	-
Pseudomonas cepacia[73,74] (10 wt% lipase)	-	80-130	days	<245,455	1.1-1.3

1.3 Properties of lactones and lactides

Poly(lactide) slowly became of commercial interest in the past decades in a time that environmental pollution was an uprising political issue. Nowadays, as the existence of the green house effect is no longer deniable, the use of poly(lactide) has gained momentum in packaging technology. The polymer can be made from a renewable resource, namely lactic acid which is derived from cornstarch. When tossed away, the plastic will degrade into natural products, thereby closing the environmental cycle. Unfortunately, major drawbacks of employing poly(lactide) for commercial purposes are its low glass transition temperature (~55 ^{o}C) and brittleness. Apart from its physical properties, other issues are obstructing the use of poly(lactide) as replacement for petrochemically produced polymers. Thinkable, the cultivation of corn on such a large scale can also demand its environmental toll. Moreover, the morality of using food for these kinds of purposes, while there is still hunger in this world, is questionable.[75,76]

Research has been focusing on enhancement of the thermal- and mechanical properties by making composite materials, by blending, copolymerizing and by slightly changing its chemical structure. Several lactides with other substituents than methyl on the 2,5 positions of the glycolide ring have been synthesized, as shown in Figure 1-6.
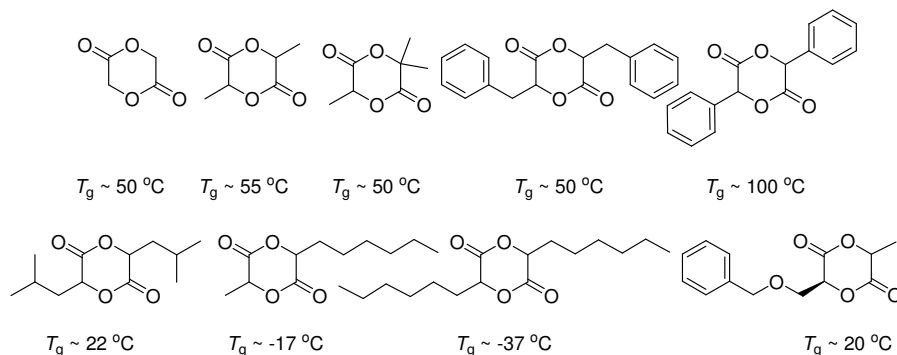
Figure 1-6. Different polymerized lactides.[77-81]

Chemical modification has the disadvantage that additional reactions are required which is not desirable for large scale manufacturing. Although the physical properties of modified polymers can be better, blending can be a cheaper alternative. Poly(lactide) blends of its stereo-isomers have been investigated. Both optically pure poly(L-lactide) and poly(D-lactide) are semi-crystalline. The material however remained brittle upon blending the polymers of these stereo-isomers.[82] An exceptional property of poly(lactide) is its stereocomplex formation of PLLA with PDLA increasing its melting temperature to 230 °C. This enhances thermal stability but not its mechanical performance.[83] Blends with different polymers have also been studied and the most reported one is the blend of poly(lactide) with poly(ε-caprolactone).[84] A problem in blending of different type of polymers is phase separation, ultimately leaving copolymerization as the last option to decrease crystallinity and brittleness by breaking up chain regularity. A well-known copolymer of lactide, is PLGA, poly(lactide-*co*-glycolide) which is intensively studied for controlled drug delivery. PLGA is amorphous, can degrade by hydrolysis and be broken down to carbon dioxide and water within the human body. Unfortunately, higher glycolide content means a poorer solubility and a worse processability. Marketed drug delivery products of both PLA as well as PLGA are:

- Atridox®, periodontal disease, poly(lactide).
- Zoladex®, prostate cancer, poly(lactide).
- Lupron depot®, prostate cancer, microspheres of 75:25 lactide/glycolide.
- Nutropin depot®, growth deficiencies, poly(lactide-*co*-glycolide).
- Trelstar depot®, prostate cancer, poly(lactide-*co*-glycolide).

Degradation of the material is an important aspect as well in the environment as in the human body. Polyesters degrade by bulk erosion through simple hydrolysis of the ester bonds. Degradation times in the human body vary from 18-24 months for the homopolymer poly(L-lactide) to 2-4 months for

poly(glycolide). The degradation for copolymers occurs faster than for the homopolymer poly(lactide) and is related to the glycolide content; a higher glycolide content means a faster degradation. Accordingly, the degradation rate can be tailored by the amount of glycolide.[85]

The pool of different lactones is much bigger than of the lactides. The most widely investigated polylactone is poly(ε-caprolactone). Poly(ε-caprolactone) is also semi-crystalline and has a glass transition of ~ −60 ^{o}C, *i.e.* at room temperature the amorphous phase is in its rubber state, and a melting point of ~ 60 ^{o}C. Poly(ε-caprolactone) possesses a low tensile modulus but a high elongation at break whereas for lactide this is more or less reversed. Therefore depending on the ratio of ε-caprolactone to lactide, their copolymers diverge from weaker elastomers to tougher thermoplastics.[86] An example of an implantable device constituted of poly(ε-caprolactone) is Capronor^{TM}, a 1-year contraceptive. Poly(β-hydroxybutyrate) is a less well-known polyester for biomedical applications. Interesting is the fact that this polymer is produced by a bacterium *Alcaligenes eutrophus (Ralstonia metallidurans)* upon fermentation of sugars. The commercialized product Biopol is a registered trademark of Metabolix. This polyester is brittle and highly crystalline with as result that research has been directed to its copolymerization with hydroxyvaleric acid in analogy to lactide and glycolide.[87] Finally, poly(ω-pentadecalactone), the so-called bio equivalent to polyethylene, is a polymer that can with difficulty be synthesized by chemical ring-opening. PPDL has a glass transition of –20 ^{o}C and a melting point of 95 ^{o}C. The elasticity modulus was reported to be indeed similar to that of low density polyethylene.[88] A summary of the most important physical properties of polymers discussed here is given in Table 1-2.

Table 1-2. Thermal- and mechanical properties of different polyester films.

Polyester	T_g (^{o}C)	T_m (^{o}C)	Tensile Modulus MPa	Tensile Strength MPa	Elongation Yield (%)	Elongation Break (%)
PET[89]	73	245	2800	55-75	-	-
PGA[89]a	35	225	6500	375	-	20
PLA[87]	60	130	1000-3000	30-50	~4	~7
PHB[87]	15	175	2500	36	2.2	2.5
PHV[87]	-11	105	-	-	-	-
P(HB-co-22% HV)[87]	-5	137	620	16	8.5	36
PCL[87]	-60	60	400	16	7	80
PDL[88]	-20	95	370	14.5	12	-

a Dexon fibre

In this Chapter, the first decades of the aforementioned new era of polyester research were described in a nutshell. It can be concluded that many pathways exist to synthesize aliphatic polyesters with different properties but that only a few of these materials have been qualified as being suitable for large scale production.

1.4 Aim and outline of this thesis

Many papers have dealt with ring-opening polymerizations of lactones and lactides. Realistically, the major part of these articles reports on the synthesis and standard characterization techniques of the homopolymers obtained. However, in the quest of finding new polymeric materials and to obtain detailed information on their physical properties, advances in analytical tools are required as well as new insights into established fundaments and models on which polymer chemistry is based. The analysis of polymers and especially polymers with multiple monomer residues is a challenge due to their often complex microstructure. Important items are the chain length distribution, sequence distribution and composition of multiple component polymers, but for most their mutual dependence. In this thesis attempts are being presented on the synthesis of new polyesters but also on the development of a method to determine in a single measurement the most important chemical parameters that influence the physical properties of the material.

Chapter 2 discusses all the aspects related to the measurements and interpretation of MALDI-ToF-MS. This highly important analytical tool can give the relation between chain length distribution and chemical composition distribution for copolymer materials. These distributions depend on the polymerization pathway and on the reactivity of the monomers used. In **Chapter 3** the simulated distributions of a first order Markov chain by both the Monte Carlo technique and an analytical formula are fitted to the chemical composition distributions obtained by MALDI-ToF-MS. In this way, propagation probabilities and reactivity ratios can accurately be obtained.

Chapter 4 and **Chapter 5** deal with two different classes of aliphatic polyesters. The different synthetic routes of poly(lactide-*co*-glycolide) and its microstructure are described in **Chapter 4**. The ring-opening polymerization of oxiranes and anhydrides to form polyesters using salen and porphyrin metal catalysts is reported in **Chapter 5**.

Finally, **Chapter 6** reviews the applicability of these materials in a drug delivery device that employs the glass transition as an on and off switch for pulsatile drug administration. Furthermore, the relation between glass transition and topology is emphasized in the context of the data obtained by MALDI-ToF-MS.

References

[1]   M. Nichols, The Graduate, **1967** (United Artists).

[2]   The Economist, 28th June, p 71, **2008**.

[3]   a) http://www.whatispolyester.com/history.html,

        b) http://www.ecvm.org/code/page.cfm?id_page=107,

        c) http://inventors.about.com/library/inventors/blpolyester.htm,

        d) A.J. East*, Encyclopedia of Polymer Science and Technology, Polyesters, Thermoplastic, 7,* p504-528 John Wiley & Sons, Inc., **2002**,

        e) World Plastics Production, Plastics*Europe*, WG Market Research & Statistics.

[4]   A.-C. Albertsson, I.K. Varma, *Advances in Polymer Science, Degradable Aliphatic Polyesters*, *Aliphatic Polyesters: Synthesis, Properties and Applications, 157*, p 1-40, *Springer Berlin,* **2002**.

[5]   T. Aida, K. Sanuki, S. Inoue, *Macromolecules* **1985**, *18*, 1049.

[6]   T. Aida, S. Inoue, *J. Am. Chem. Soc.* **1985**, *107*, 1358.

[7]   R.C. Jeske, A.M. DiCiccio, G.W. Coates, *J. Am. Chem. Soc.* **2007**, *129*, 11330.

[8]   W.J. Bailey, *Polym. J.* **1985**, *17*, 85.

[9]   W.J. Bailey, Z. Ni, S.R. Wu, *J. Polym. Sci., Part A: Polym. Chem.* **1982**, *20*, 3021.

[10]   D.P. Garner, *J. Polym. Sci., Part A: Polym. Chem.* **1982**, *20*, 2979.

[11]   D. Takeuchi, Y. Sakaguchi, K. Osakada, *J. Polym. Sci., Part A: Polym. Chem.* **2002**, *40*, 4530.

[12]   E. Drent, E. Kragtwijk, (Shell Internationale Research Maatschappij BV, Neth.) E. Eur. Pat. Appl. 577206, **1994**.

[13]   M. Allmendinger, R. Eberhardt, G. Luinstra, B. Rieger, *J. Am. Chem. Soc.* **2002**, 124 (20), 5646.

[14]   K. Ito, Y. Hashizuka, Y. Yamashita, *Macromolecules* **1977**, *10*, 821.

[15]   K. Ito, Y. Yamashita, *Macromolecules* **1978**, *11*, 68.

[16]   H.R. Kricheldorf, I. Kreiser, *Makromol. Chem.* **1987**, *188*, 1861.

[17]   D. Bourissou, B. Martin-Vaca, A. Dumitrescu, M. Graullier, F. Lacombe, *Macromolecules* **2005**, *38*, 9993.

[18]   O. Dechy-Cabaret, B. Martin-Vaca, D. Bourissou, *Chem. Rev.* **2004**, *104*, 6147.

[19]   J. Wu, T.-L. Yu, C.-T. Chen, C.-C. Lin, *Coord. Chem. Rev.* **2006**, *250*, 602.

[20]   Ph. Lecomte, R. Jérôme, *Encyclopedia of Polymer Science and Technology, 11,* p547-566, John Wiley & Sons, Inc., **2002**.

[21]   T. Aida, S. Inoue, *Acc. Chem. Res.* **1996**, *29*, 39.

[22]   S. Inoue, H. Koinuma, T. Tsuruta, *J. Polym. Sci., Part B: Polym. Lett.* **1969**, *7*, 287.

[23]   T. Aida, S. Inoue, *Macromolecules* **1982**, *15*, 682.

[24]   P. Pfeiffer, E. Breith, E. Lubbe, T. Tsumaki, *Ann. der Chemie, Justus Liebigs* **1933**, *503*, 84.

[25]   E.N. Jacobsen, W. Zhang, A.R. Muci, J.R. Ecker, L. Deng, *J. Am. Chem. Soc.* **1991**, *113*, 7063.

[26]   D.J. Darensbourg, *Chem. Rev.* **2007**, *107*, 2388.

[27]   D.J. Darensbourg, R.M. Mackiewicz, A.L. Phelps, D.R. Billodeaux, *Acc. Chem. Res.* **2004**, *37*, 836.

[28]   C.T. Cohen, T. Chu, G.W. Coates, *J. Am. Chem. Soc.* **2005**, *127*, 10869

[29]   C.T. Cohen, C.M. Thomas, K.L. Peretti, E.B. Lobkovsky, G.W. Coates, *Dalton Trans.* **2006**, 237.

[30]   N. Spassky, M. Wisniewski, C. Pluta, A. Le Borgne, *Macromol. Chem. Phys.* **1996**, *197*, 2627.

[31]   Z. Zhong, P.J. Dijkstra, J. Feijen, *Angew. Chem. Int. Ed.* **2002**, *41*, 4510.

[32]   Z. Zhong, P.J. Dijkstra, J. Feijen, *J. Am. Chem. Soc.* **2003**, *125*, 11291.

[33]   H. Du, X. Pang, H. Yu, X. Zhuang, X. Chen, D. Cui, X. Wang, X. Jing, *Macromolecules* **2007**, *40*, 1904.

[34]   N. Nomura, R. Ishii, M. Akakura, K. Aoi, *J. Am. Chem. Soc.* **2002**, *124*, 5938.

[35]   N. Nomura, R. Ishii, Y. Yamamoto, T. Kondo, *Chem. Eur. J.* **2007**, *13*, 4433.

[36]   M. Cheng, E.B. Lobkovsky, G.W. Coates, *J. Am. Chem. Soc.* **1998**, *120*, 11018.

[37]   M. Cheng, D.R. Moore, J.J. Reczek, B.M. Chamberlain, E.B. Lobkovsky, G.W. Coates, *J. Am. Chem. Soc.* **2001**, *123*, 8738.

[38]   M. Cheng, A.B. Attygalle, E.B. Lobkovsky, G.W. Coates, *J. Am. Chem. Soc.* **1999**, *121*, 11583.

[39]   L.R. Rieth, D.R. Moore, E.B. Lobkovsky, G.W. Coates, *J. Am. Chem. Soc.* **2002**, *124*, 15239.

[40]   M.H. Chisholm, J.C. Gallucci, K. Phomphrai, *Inorg. Chem.* **2004**, *43*, 6717.

[41]   M.H. Chisholm, J.C. Gallucci, K. Phomphrai, *Chem. Comm.* **2003**, 48.

[42]   A. Amgoune, C.M. Thomas, J.-F. Carpentier, *Macromol. Rapid Commun.* **2007**, *28*, 693.

[43]   A. Amgoune, C.M. Thomas, S. Ilinca, T. Roisnel, J.-F. Carpentier, *Angew. Chem. Int. Ed.* **2006**, *45*, 2782.

[44]   C.-X. Cai, A. Amgoune, C.W. Lehmann, J.-F. Carpentier, *Chem. Comm.*, **2004**, 3, 330.

[45]   H.E. Dyer, S. Huijser, A.D. Schwarz, C. Wang, R. Duchateau, P. Mountford, *Dalton Trans.* **2008**, *1*, 32.

[46]   F. Bonnet, A.R.C. Cowley, P. Mountford, *Inorg. Chem.* **2005**, *44*, 9046.

[47]   S. Gendler, S. Segal, I. Goldberg, Z. Goldschmidt, M. Kol, *Inorg. Chem.* **2006**, *45*, 4783.

[48]   A.J. Chmura, C.J. Chuck, M.G. Davidson, M.D. Jones, M.D. Lunn, S.D. Bull, M.F. Mahon, *Angew. Chem. Int. Ed.* **2007**, *46*, 2280.

[49]   H. Ma, J. Okuda, *Macromolecules* **2005**, *38*, 2665.

[50]   A. Kowalski, A. Duda, S. Penczek, *Macromolecules* **2000**, *33*, 7359.

[51]   G. Schwach, J. Coudane, R. Engel, M. Vert, *J. Polym. Sci., Part A: Polym. Chem.* **1997**, *35*, 3431.

[52]   M. Vert, G. Schwach, R. Engel, J. Coudane, *J. Controlled Release* **1998**, *53*, 85.

[53]   H.R. Kricheldorf, I. Kreiser-Saunders, A. Stricker, *Macromolecules* **2000**, *33*, 702.

[54]   S. Penczek, A. Duda, A. Kowalski, J. Libiszowski, K. Majerska, T. Biela, *Macromol. Symp.* **2000**, *157*, 61.

[55]   P. Dubois, C. Jacobs, R. Jerome, P. Teyssie, *Macromolecules*, **1991**, *24*, 2266.

[56]   D. Knani, A.L. Gutman, D.H. Kohn, *J. Polym. Sci., Part A: Polym. Chem.* **1993**, *31*, 1221.

[57]   H. Uyama, S. Kobayashi, *Chem. Lett.* **1993**, 22, 1149.

[58]   R.A. Gross, A. Kumar, B. Kalra, *Chem. Rev.* **2001**, *101*, 2097.

[59]   I.K. Varma, A.-C. Albertsson, R. Rajkhowa, R.K. Srivastava, *Prog. Polym. Sci.* **2005**, *30*, 949.

[60]   S. Kobayashi, H. Uyama, S. Kimura, *Chem. Rev.* **2001**, *101*, 3793.

[61]   S. Matsumura, *Macromol. Biosci.* **2002**, *2*, 105.

[62]   L. van der Mee, F. Helmich, R. de Bruijn, J.A.J.M. Vekemans, A.R.A. Palmans, E.W. Meijer, *Macromolecules* **2006**, *39*, 5021.

[63]   A. Duda, A. Kowalski, S. Penczek, H. Uyama, S. Kobayashi, *Macromolecules* **2002**, *35*, 4266.

[64]   Z. Zhong, P.J. Dijkstra, J. Feijen, *Macromol. Chem. Phys.* **2000**, *201*, 1329.

[65]   F. Nederberg, E.F. Connor, M. Möller, T. Glauser, J.L. Hedrick, *Angew. Chem. Int. Ed.* **2001**, *40*, 2712.

[66]   E.F. Connor, G.W. Nyce, M. Myers, A. Möck, J.L. Hedrick, *J. Am. Chem. Soc.* **2002**, *124*, 914.

[67]   D.A. Culkin, W. Jeong, S. Csihony, E.D. Gomez, N.P. Balsara, J.L. Hedrick, R.M. Waymouth, *Angew. Chem. Int. Ed.* **2007**, *46*, 2627.

[68]   L. Zhang, F. Nederberg, J.M. Messman, R.C. Pratt, J.L. Hedrick, C.G. Wade, *J. Am. Chem. Soc.* **2007**, *129*, 12610.

[69]   L. Zhang, F. Nederberg, R.C. Pratt, R.M. Waymouth, J.L. Hedrick, C.G. Wade, *Macromolecules* **2007**, *40*, 4154.

[70]   N.E. Kamber, W. Jeong, R.M. Waymouth, R.C. Pratt, B.G.G. Lohmeijer, J.L. Hedrick, *Chem. Rev.* **2007**, *107*, 5813.

[71]   H.R. Kricheldorf, I. Kreiser-Saunders, C. Boettcher, *Polymer* **1995**, *36*, 1253.

[72]   L. Trofimoff, T. Aida, S. Inoue, *Chem. Lett.* **1987**, 991.

[73]   S. Matsumura, K. Mabuchi, K. Toshima, *Macromol. Rapid Commun.* **1997**, *18*, 477.

[74]   S. Matsumura, K. Mabuchi, K. Toshima, *Macromol. Symp.* **1998**, *130*, 285.

[75]   E. Royte, *Smithsonian magazine*, August **2006**.

[76]   V. Carneiro, E. Hwu, M. Tinius, *Synergy*, Clemson University.

[77]   G.L. Baker, E.B. Vogel, M.R. Smith, III, *Polym. Rev.* **2008**, *48*, 64.

[78]   M. Leemhuis, C.F. van Nostrum, J.A.W. Kruijtzer, Z.Y. Zhong, M.R. ten Breteler, P.J. Dijkstra, J. Feijen, W.E. Hennink, *Macromolecules* **2006**, *39*, 3500.

[79]   M. Leemhuis, J.H. van Steenis, M.J. van Uxem, C.F. van Nostrum, W.E. Hennink, *Eur. J. Org. Chem.* **2003**, 3344.

[80]   T. Trimaille, M. Moeller, R. Gurny, *J. Polym. Sci., Part A: Polym. Chem.* **2004**, *42*, 4379.

[81]   M. Yin, G.L. Baker, *Macromolecules* **1999**, *32*, 7711.

[82]   J.R., Sarasua, A. López Arraiza, P. Balerdi, I. Maiza, *Polym. Eng. Sci.* **2005**, *45*, 745.

[83]   Y. Ikada, K. Jamshidi, H. Tsuji, S.H. Hyon, *Macromolecules* **1987**, *20*, 904.

[84]   N. López-Rodriguez, A. López-Arraiza, E. Meaurio, J.R. Sarasua, *Polym. Eng. Sci.* **2006**, *46*, 1299.

[85]   M. Chasin, R. Langer, *Biodegradable Polymers as Drug Delivery Systems*, Marcel Dekker Inc, New York, p1-41, **1990**.

[86]   M. Hiljanen-Vainio, T. Karjalainen, J. Seppälä, *J. Appl. Polym. Sci.* **1996**, *59*, 1281.

[87]   I. Engelberg, J. Kohn, *Biomaterials* **1991**, 12, 292.

[88]   M.L. Focarete, M. Scandola, A. Kumar, R.A. Gross, *J. Polym. Sci., Part B: Polym. Phys.* **2001**, 39, 1721.

[89]   A properties database http://www.polymersdatabase.com.

2

MALDI-ToF-MS to analyze copolymer microstructures.

Abstract. *In the quest for new materials, analysis cannot stand still. Desirably, the ultimate analytical tool for characterization of polymers should be able to display in a single measurement conversion, composition, molar mass distribution, microstructure and kinetic data in a simple, fast and reliable way. MALDI-ToF-MS is one of the most important tools to analyze polymers. Apart from the confirmation that the desired polymer has indeed been synthesized, MALDI-ToF-MS can give insight into composition, total chain length distribution and even on microstructure. Although MALDI-ToF-MS measurements are relatively simple and fast, understanding of the spectra and its underlying information can be tedious and discouraging, especially in the case of polymers with more than one monomer residue. In this chapter we want to provide the reader in a structured way, with the most important aspects of this analytical technique.*[*]

---

[*] This chapter requires special thanks to Dr. B.B.P. Staal and Dr. R.X.E. Willemse.

2.1 Introduction on MALDI-ToF-MS

Matrix Assisted Laser Desorption Ionization Time of Flight Mass Spectrometry made its introduction in 1988 in the analysis of biomacromolecules as peptides and proteins. Only in 1992, the analysis of synthetic polymers was reported. Although the technique was received skeptically due to its known mass discrimination, nowadays MALDI-ToF-MS has earned recognition in the polymer analysis field. The mechanism of separation of charged molecules by this tool is based on the difference in time of flight. A schematic of a typical mass spectrometer is given in Figure 2-1. The MALDI-ToF-MS process starts with a homogeneous mixture of the polymer, an organic matrix and a salt in solvent. This mixture is deposited on a target plate and upon evaporation of the solvent a co-crystallization of matrix and sample can be observed. Next, the target plate is inserted into the machine and subjected to high vacuum. Irradiation by an ultraviolet laser of the sample produces ions which are brought into the gaseous phase by the 'explosion' of the matrix molecules. Typically, the salt is responsible for ionization and the matrix, an organic substance, is responsible for desorption. The discovery of matrices has mainly been realized by trial and error since the role in relation to the chemical structure was not fully understood. However, Meier performed a thorough statistical research on different matrices and proposed in 2007 several new matrices, but galvinoxyl was awarded as most promising.[1]
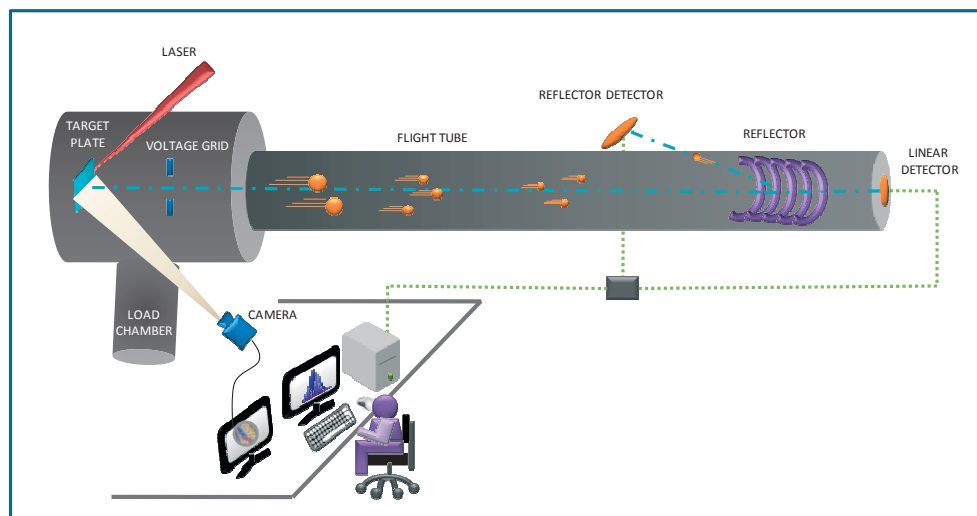
Figure 2-1. Principle and schematic overview of a MALDI-ToF-MS based on the Applied Biosystems Voyager DE-STR.

After ablation, the ionized molecules are delayed by 300-800 ns before acceleration by a high potential of 15-35 kV. This potential is applied to the target plate holder as well as a voltage grid. The grid has a slightly lower potential thereby extracting the ionized molecules into the flight tube with different velocities depending on the mass to charge ratio.[4]
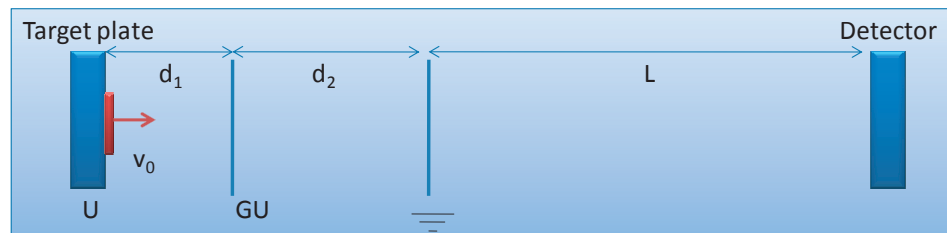
Figure 2-2. Acceleration of particles in between the target plate and the grid. Potentials of U and GU are applied (G < 1), d_1 = distance between target plate and voltage grid, d_2= distance between voltage grid and ground grid, 0 = ground grid, L = length of flight tube.[9]

The time the ions drift over the length of the flight tube now rests on these velocities. The *m/z* ratio is given by:

$$\frac{m}{z} = e\Delta V \frac{2(t-t_0)^2}{L^2} \tag{2-1}$$

in which *m* represents the mass of the ion, *z·e* the charge, ΔV the electric potential difference, L the length of the tube, t_0 the time the laser pulse hits the target and t the time of flight.[10]

The MALDI apparatus used for the measurements reported in this thesis has two different modes of operation, *namely* the linear and the reflector mode. In the linear mode the ionized molecules 'fly' directly towards a detector, whereas in the reflector mode the ions are firstly reflected before detection. The reflection by an electrostatic mirror increases the pathway of the ions and therefore the resolution. Commonly, the detection of a MALDI-ToF-MS is accomplished by a Microchannel Plate (MCP). A Microchannel Plate exists of millions of fused lead glass capillaries (diameter in the micrometer range) in an array. Every single capillary operates as an independent secondary-electron multiplier. Secondary electrons liberated upon ion impact are themselves detected by photo multiplication. In essence, the detector counts the number of ions that enter at the same time and thus having the same mass, making the distribution recorded by MALDI-ToF-MS a number average molar-mass distribution.[2-8,10]

2.2 Isotope distributions

In the Polymer Chemistry group at the University of Technology Eindhoven, a software program is being developed to fast and easily solve the MALDI-ToF-MS spectra for copolymers. Dr. R.X.E. Willemse and Dr. B.B.P. Staal initiated this project and in this chapter we will describe the current status of the project.[10,11] The only data required as input for the program are *i)* a recorded spectrum opened in the Applied Biosystems Voyager Data Explorer software®, *ii)* the chemical formulas of the monomer residues and *iii)* the expected end groups. The calculations performed by the programs are based on the following ideas and algorithms. We used in this study the atomic weights of the elements and their relative abundances of their isotopes reported by NERMAG which are based on data compiled by SAIC from IUPAC.[12] The calculation of the isotopic distribution of a given molecule was reported by Yergey and recently by Snider.[13-15] The polynomials are given in Equations 2-2 to 2-4 and describe the isotope distribution of a single molecule:[13]

$$(a_1 + a_2 + a_3 + \cdots)^m (b_1 + b_2 + b_3 + \cdots)^n (c_1 + c_2 + c_3 + \cdots)^o \ldots \qquad (2\text{-}2)$$

where a, b and c are the different isotopes of the elements in the molecule and the exponents m, n and o are the numbers of occurrence of the atoms in the molecule. So for the following structure $C_{10}H_{14}O_4$ Equation 2-1 will look like:

$$\left(^{12}C + {}^{13}C\right)^{10} \left(^{1}H + {}^{2}H\right)^{14} \left(^{16}O + {}^{17}O + {}^{18}O\right)^4 = (2)^{10}(2)^{14}(3)^4 = 1.4 \cdot 10^9$$

Abundances of the isotope distribution of the atoms in a molecule are calculated by:

$$A = \frac{n!}{(a)!(b)!(c)!\ldots} (r_1)^a (r_2)^b (r_3)^c \ldots \ldots \qquad (2\text{-}3)$$

in which n is the total number of atoms of the element in the molecule, a, b and c etc. are the number distributions of the atom for the isotopes, and r_1, r_2, r_3 etc. are the relative abundances of each isotope. The equation for example for $^{12}C_8{}^{13}C_2$ for the previously mentioned molecule will look like:

$$A = \frac{(10)!}{(8)!(2)!} (0.9889)^8 (0.0111)^2 = 0.005070812$$

Table 2-1 shows the relative abundances of all the atoms in the molecule for the first six permutations. The ^{17}O has been left out of consideration for sake of simplicity.

Table 2-1. Relative abundances for the first five isotopes of $C_{10}H_{14}O_4$.

^{12}C	^{13}C	A_C
10	0	0.894383480
9	1	0.100390905
8	2	0.005070812
7	3	0.000151781
6	4	2.98144E-06

^1H	^2H	A_H
14	0	0.997762328
13	1	0.002095636
12	2	2.04357E-06
11	3	1.22634E-09
10	4	5.05946E-13

^{16}O	^{18}O	A_O
4	0	0.990434505
3	1	0.007942538
2	2	2.38849E-05
1	3	3.19232E-08
0	4	1.6E-11

The abundances of the molecule are calculated by the product of the abundances of the separate atoms. For example the abundance of $^{12}C_{10}{}^1H_{14}{}^{16}O_4$ equals:

$$A_{tot} = A_C \cdot A_H \cdot A_O = 0.883846066 \qquad (2\text{-}4)$$

Likewise, the abundance of $^{12}C_9{}^{13}C_1{}^1H_{14}{}^{16}O_4$ can be calculated in the same way and equals:

$$A_{tot} = A_C \cdot A_H \cdot A_O = 0.099208124$$

Of course a certain threshold has to be built in to reduce the number of calculations and the required computer calculation time. This threshold is often set to a certain number of isotopes in the distribution. It should be noted that the most abundant peak is not necessarily the peak calculated by the masses of the most abundant isotopes of the atoms, *i.e.* the monoisotopic mass.

Most MALDI-ToF-MS apparatus have accompanying software that can calculate isotope distributions for a single combination of both monomers and a certain end group. The calculated isotopes are now plotted for the required combination plus end group chosen and visually it can now be determined if the isotope distributions match. A perfect match with a single isotope pattern of the recorded spectrum does not necessarily mean that the proposed structure is the right one.

Accidentally, that very isotope pattern might match but the other distributions in for example the low or high molecular weight area of the spectrum for other combinations of both monomers and the same end group might not. An example is given in Figure 2-3. Let's say a polymer recorded with the true end groups X and Y, is being simulated with end groups P and Q. The latter combination of end groups gives even for several peaks a match, but at a certain point mathematically cannot form the correct masses anymore given the monomer residues and end group. Therefore it is wise to simulate a few combinations of (co)-monomers and end groups in the lower, middle and upper *m/z* regions of the spectrum to verify whether the calculated isotope patterns match throughout the spectrum.
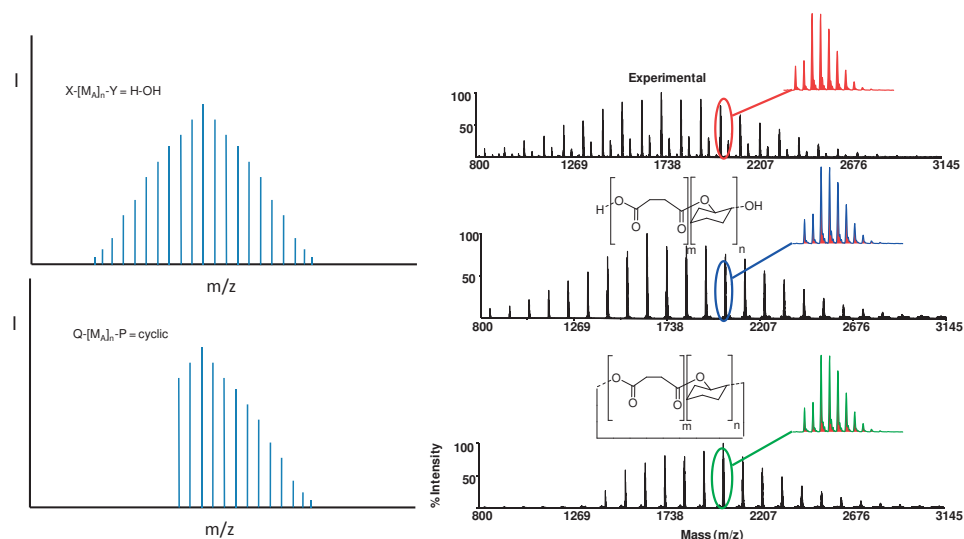
Figure 2-3. An example of misleading matches of isotopes. The cyclic chains cannot explain the peaks in the lower *m/z* region, but give a perfect match for the isotope distributions in the higher *m/z* region. On the other hand simulated distributions for H-OH terminated chains give a match for the whole spectrum. *(N.B. The other low intensity distributions shown in the experimental derive from another end group which will not be treated here.)*

Unique for the in-house developed software, is the possibility to simulate an entire spectrum preventing the misleading matches depicted in Figure 2-3.

2.2.1 Isotope distributions for homopolymers doped with different salts

In the spectrum of a homopolymer, the difference between consecutive isotope distributions is in fact the mass of the repeating unit. Therefore the peak-to-peak distance can directly be used to identify a certain polymeric species. Hopping from peak to peak equals an increase in the degree of polymerization.

The *m/z* belonging to a certain peak equals the molar mass of polymer chains with a certain degree of polymerization after subtraction of the mass of the cation of the dopent and multiplication by the charge of the cation. The choice of the salt is an important parameter and is partially depending on the type of polymer to measure. Generally, alkali metal salts are being used and copper or silver. Silver is commonly applied only for polystyrene and its copolymers. The isotope patterns for a homopolymer for different cations are given in Figure 2-4.
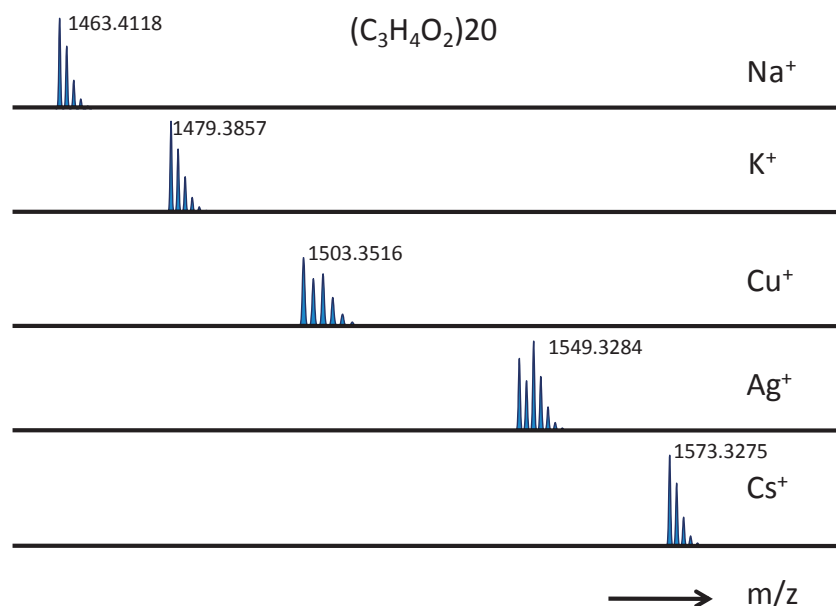
Figure 2-4. Cyclic poly(lactide) simulated isotope patterns for different ionization salts.

The monotonous decrease of the isotope patterns for all the alkali cations is due to the fact that they have only higher isotopes in very low abundances or none at all. The pattern for silver looks different and is characterized by two high peaks which are a result of the fact that silver has two isotopes with almost equal abundance (Table 2-2). Also Cu^+ has an additional isotope with a relatively high abundance. Of course when the oxidation state of the copper cation equals 2, the *m/z* becomes half the value than for oxidation state 1, while simultaneously the differences between the isotopes halves.

Table 2-2. Isotopes of different metals used in the cationization salts.

Li		Na		K		Cs		Cu		Ag	
^{6}Li	0.0742	^{23}Na	1	^{39}K	0.9320	^{133}Cs	1	^{63}Cu	0.6917	^{107}Ag	0.5184
^{7}Li	0.9258			^{40}K	0.00012			^{65}Cu	0.3083	^{109}Ag	0.4816
				^{41}K	0.0673						

The dependence of MALDI-ToF-MS on the nature of the cation chosen is reported in just a few studies.[16,17] The conformation of the chain by coordination to the metal is reported by Gidden *et al.* for PS, PET and PEG.[18-20] Simply put, the bigger the ion, the larger the coordination.

Several papers report on MALDI-ToF-MS experiments in which no additional doping agent is applied. This is possible for polar polymers that are ionized by cations deriving from the glassware, solvent or other impurities. Adducts of sodium and/or potassium are often found in the spectra of polyesters. Nevertheless, to increase the ionization, it is wise to add an additional salt. Another case in which no additional cationization salt is required is for pre-charged polymers. An example of a pre-charged polymer is described in Chapter 5.

There are polymers that cannot be ionized by conventional methods and as result no spectrum can be recorded. Polyolefins, *e.g.* polyethylene and polypropylene, form the best example. In general polymers that do not possess any polar moieties, aromaticity or bond unsaturation are incapable of gas-phase metal cationization. Modification of these polymers' end groups prior to the mass spectrometry measurements can help to analyze them by these kinds of analytical techniques after all. Bauer and Wallace reported a relatively successful study on pre-charged polyethylene by covalently bonded charges.[21,22] *(N.B. Ionization can occur on backbone as well as on end group.)*

2.2.2 Isotope distributions for copolymers

Typically, the difference between isotope distributions (peak-to-peak distance) in a spectrum of a copolymer is the difference in mass between monomer residues. The isotope distributions deriving from chains with the same total chain length are themselves again part of a distribution. An example of a copolymer with a difference of 14 g·mol^{-1} between the monomer residues is given in Figure 2-5. An overlap of the blue and red colored distributions can be observed which logically is entitled as *isotope overlap*. It is clear that if such an overlap becomes significant, it will dramatically complicate the elucidation of the spectrum. Examples of monomer residues with a difference of 14 g·mol^{-1} being dealt with in this thesis are the pairs, lactic acid/glycolic acid, δ-valerolactone/ε-caprolactone, ε-caprolactone/4-methyl-ε-caprolactone, MMA/EMA, MA/EA, VAc/MMA, VAc/EA and BA/EMA.

Figure 2-5. Two chain length distributions (chain length 10 and 11) with the corresponding isotope distributions for a comonomer pair with a molar mass difference of 14 g·mol^{-1}.

The MALDI-ToF-MS spectrum of a copolymer synthesized from a comonomer pair with a mass difference of only 4 g·mol^{-1} appears more open and more like a homopolymer. However, when taking a closer look to the peaks, one can see an isotope distribution built up from several overlapping isotope distributions. Whereas in the previous case the distributions of different chain lengths overlapped, in the present situation different combinations of comonomer residues *for the same chain length,* overlap. Styrene/MMA and styrene/EA are examples of monomers that have a 4 g·mol^{-1} difference in mass.
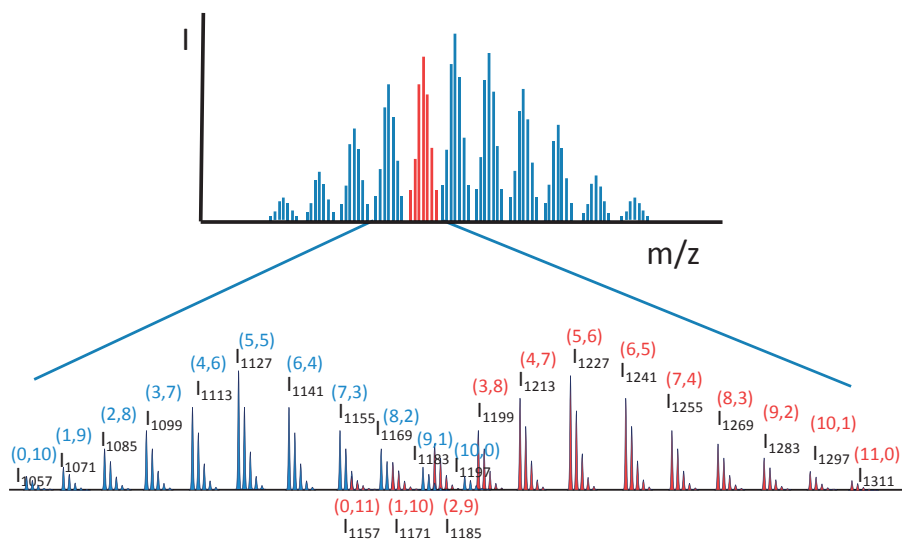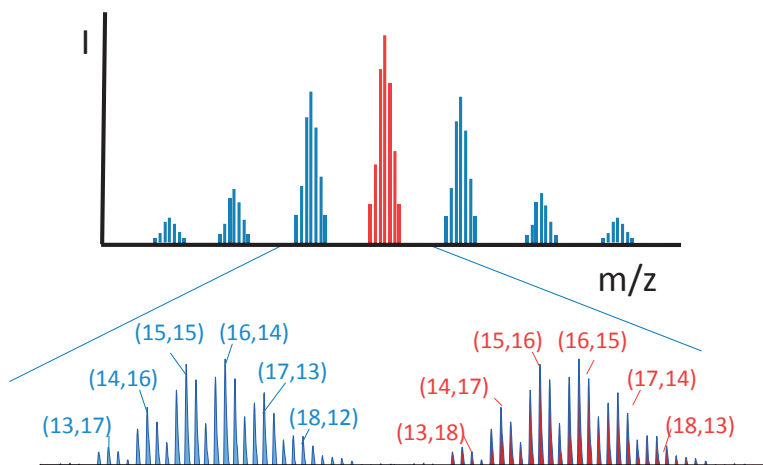

Figure 2-6. Two chain length distributions (chain length 30 and 31) with the corresponding isotope distributions for a comonomer pair with a molar mass difference of 4 g·mol^{-1}.

The extent of isotope overlap does not only depend on the difference between the monomer residues but also on the absolute masses of the residues. The chance on overlap and or multiple peak assignment will be discussed in paragraph 2.5.1.

Comonomer pairs for which the distribution of the separate chain lengths is more difficult to elucidate, are those pairs of which the difference between the monomer residues is not the smallest difference in mass that can be found. In such a case, it is often the difference between the monomer residue highest in mass and a multiple of the other monomer residue. To explain such a situation we take the example of the oxazolines (2-ethyl-2-oxazoline (EtOx) and 2-nonyl-2-oxazoline (NonOx)) discussed in more detail in paragraph 2.4, that have a difference of 98.18 g·mol^{-1}. However, the difference between 2 EtOx and 1 NonOx equals 0.96 g·mol^{-1} resulting in an overlap of chains for which 1 NonOx is replaced by 2 EtOx (Figure 2-7).
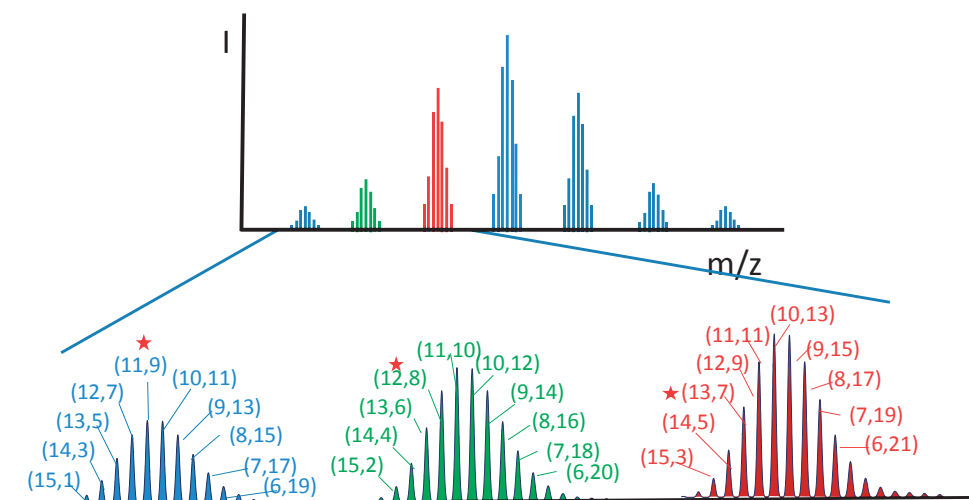
Figure 2-7. Three isotope distributions for a comonomer pair of which the direct mass difference between the monomer residues is bigger than the difference between a multiple of the lightest monomer residue with the heaviest monomer residue. The star represents the distributions for the same chain length.

The chain length distributions are in fact smeared out over the entire mass range covered by the molar mass distribution. In the next paragraph, the correlation between the distribution of monomers within a certain chain length and the distribution of total chain lengths is described.

2.3 Deconvolution of MALDI-ToF-MS spectra

The previous paragraph clearly demonstrated that MALDI-ToF-MS spectra for copolymers are considerably more difficult to interpret than the spectra of homopolymers. Appointing combinations of monomer residues to each isotope distribution in the spectrum is difficult but moreover time consuming. The in-house developed software automatized this procedure with as result, a relatively simple matrix. In this paragraph the method to derive this matrix and additional information that can be obtained from it, is described. MALDI-ToF-MS spectra can be deconvoluted by employing the following equation:

$$m_{cal} = n_1 Mw_1 + m_2 Mw_2 + E_I + E_{II} + M^+ \qquad (2\text{-}5)$$

E_I and E_{II} represent the molar masses of the end groups at opposite sides of the chain, $n_1 Mw_1$ and $m_2 Mw_2$ represent the number and molar mass of the monomer residues of monomer M_1 and M_2 respectively, and M^+ the mass of the cation. A complete matrix with $n_{1,i}$ rows and $m_{2,j}$ columns can be constructed for a given end group using Equation 2-5. Assignment of the peaks in the spectrum to a certain position in the matrix can be done employing the following inequality:

$$\left| m_{\exp} - m_{cal} \right| \leq \frac{\Delta m}{2} \qquad (2\text{-}6)$$

in which m_{exp} represents the experimental mass, m_{cal} the calculated mass and Δm the accuracy (1-2 g mol^{-1}). By calculating the natural abundance isotope distributions for each position in the matrix and rescaling it to the corresponding highest-intensity mass-peak, a full spectrum can now be simulated.
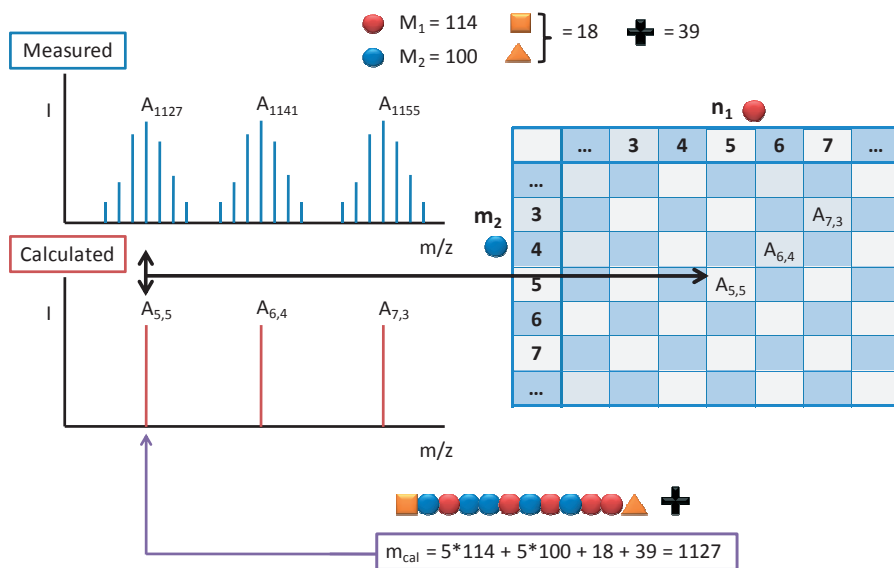
Figure 2-8. Filling out the matrix by the area underneath the peaks.

Next, the matrix can be represented as a 2D contour plot or as 3D graph with monomer residues and intensity on the x,y and z-axis respectively. Most favorable is often the contour plot because it is visually easier to subtract data from it. Once the matrix is obtained, the total chain length distribution and the chemical composition distribution can be obtained. The chemical composition distributions for the chain lengths covered by the total chain length distribution can be obtained by diagonally walking through the matrix from $(0,m_{2,n})$ to $(n_{1,n},0)$ after normalization using the sum of intensities within this chain length (Figure 2-9).
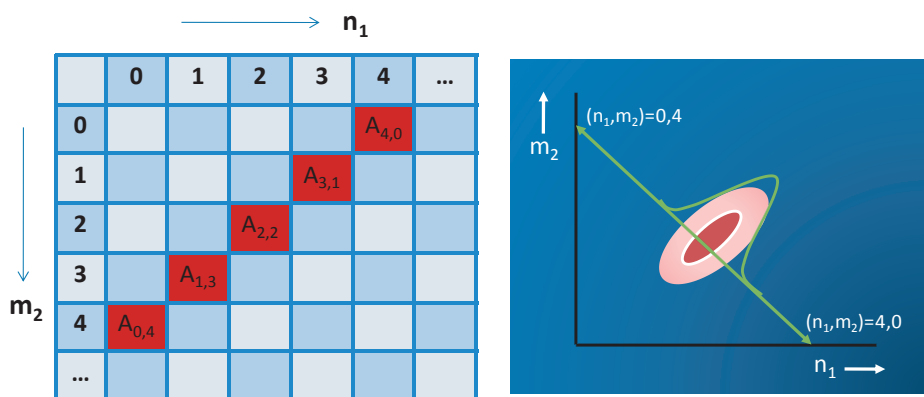
Figure 2-9. Chemical composition distribution (CCD) can be determined for each chain length.

Summing all the intensities of the individual chains and normalizing them affords the total chain length distribution. This means that one sums the intensity of the red colored cells for chain length n in the matrix given in Figure 2-9, and divides this by the sum of the entire matrix. This process is captured in Figure 2-10.

$$\Sigma(A_{4,0}...A_{0,4})/\Sigma(A_{total\ matrix})$$
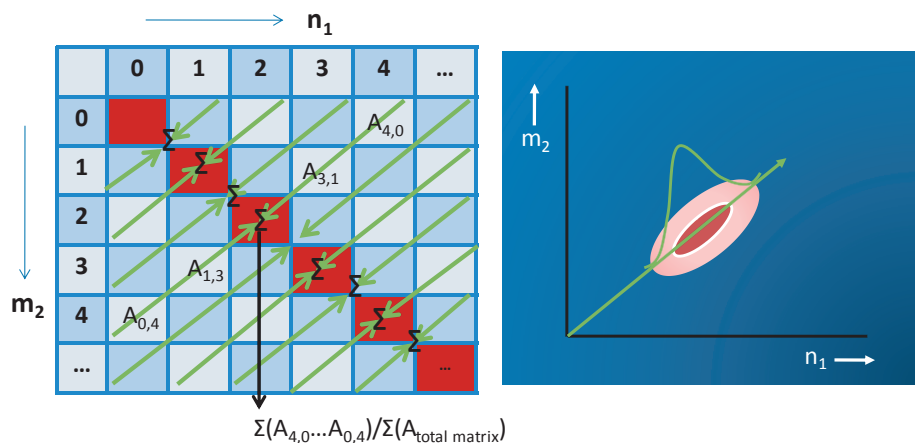
Figure 2-10. Total chain length distribution (CLD).

In case of a block copolymer, the projections on the ordinate and abscissa equal the individual block length distributions. In other words, the block length distributions equal the marginal distributions of this joint probability distribution and in fact are equal to the PDIs of the polymerizations performed. This is depicted in Figure 2-11.
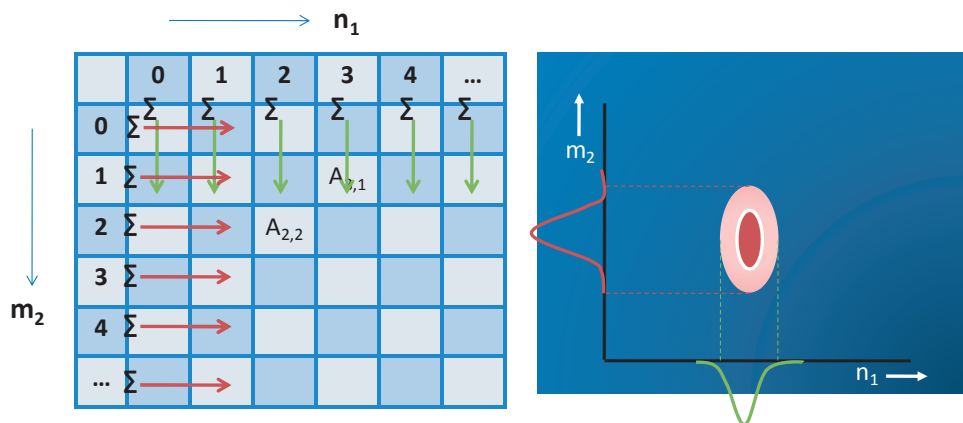
Figure 2-11. Block length distributions (BLD) for a di-block copolymer.

In order to have a good isotope resolution, fitting of isotopes by employing equation 2-6 to obtain the distributions depicted in Figures 2-9 to 2-11 is done on a spectrum recorded in the reflector mode.

Although, in some cases the isotope distributions simulated with sufficient resolution for a spectrum recorded in linear mode give an identical match to the isotope distributions recorded in the reflector mode, it is not advisable to use this mode for these purposes.

2.4 Topology determination

Knowing the exact polymer fine structure is of fundamental importance to predict the polymer's physical properties. To determine the fine structure or the topology of the polymer, we have to commit ourselves to a statistical analysis of the data. However, often simply the shape and position of the contour plot can already reveal the most likely microstructure such as, alternating, random, gradient, block.
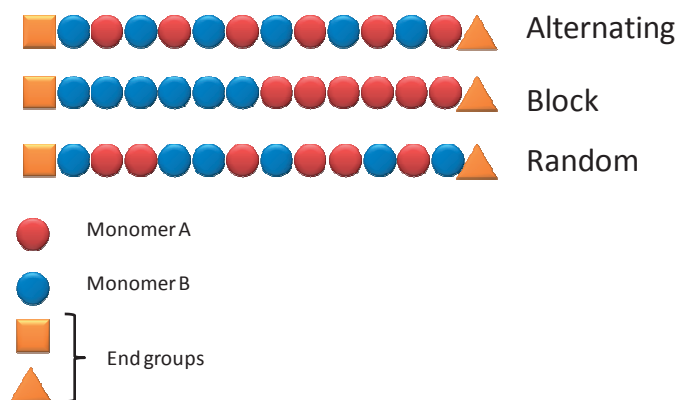
Figure 2-12. Possible copolymer topologies.

A line drawn through the optimum of the contour plot is a measure for the average chemical composition (Figure 2-10). Roughly, if this line crosses the origin and the slope remains constant the copolymer can be classified as random. In the special case that the line is one combination of comonomers wide, we are dealing with a perfectly alternating copolymer. When the line is curved but still crosses the origin, the plot represents a gradient copolymer. That is a copolymer which in the beginning of growth is more random but starts to become enriched in one of the monomers for higher conversions. An example of such a system has been reported by Staal for the comonomer pair styrene / butadiene.[10] The gradient type of topology will not be treated here extensively. Finally, if the line does not cross the origin and the contour plot has a circular or oval shape, we are dealing with a block copolymer.[10]

To determine the topology of the polymers formed, we use a slightly extended mathematical analysis of the MALDI-ToF-MS spectra of the studies reported by Wilczek-Vera[23-25] for block copolymers. The extension towards random and alternating copolymers was first reported by Staal and Willemse.[10,11] Unfortunately, the earlier ideas that from the shape and position of the contour plot alone, the topology of a polymer can be determined without knowledge of the polymer's synthesis history had to be discarded when a nearly perfect random (Bernoulli) copolymer was synthesized by means of ring-opening polymerization. In the special case that both reactivity ratios (see Chapter 3 for more information on reactivity ratios) are close to 1 for a living polymerization, the shape of the contour plot of the random copolymer is circular and very similar to the contour plot of a perfect block copolymer. The plot on the left in Figure 2-13 derives from a block copolymer of isoprene and styrene and the plot on the right from a copolymer synthesized by ring-opening polymerization of 4-methyl-ε-caprolactone and ε-caprolactone.
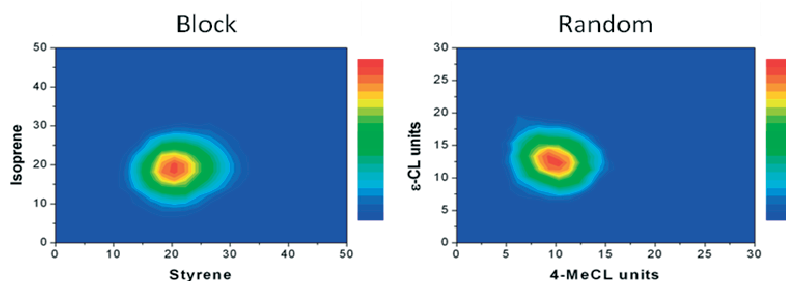
Figure 2-13. Contour plots, *Left:* block copolymer of isoprene and styrene.[28] *Right:* random copolymer of ε-caprolactone and 4-methyl-ε-caprolactone (nearly Bernoulli).

To test whether a random copolymer, built of monomers with a reactivity ratio close to 1, would give the same contour plot as the block copolymer synthesized by sequential addition of the same comonomer pair, the microwave assisted living cationic polymerization of 2-ethyl-2-oxazoline and 2-nonyl-2-oxazoline was performed.

The corresponding block copolymer was synthesized by firstly converting EtOx and then adding NonOx.[26,27] The plots derived from the MALDI spectra of both polymers (Figure 2-15) are depicted in Figure 2-14.
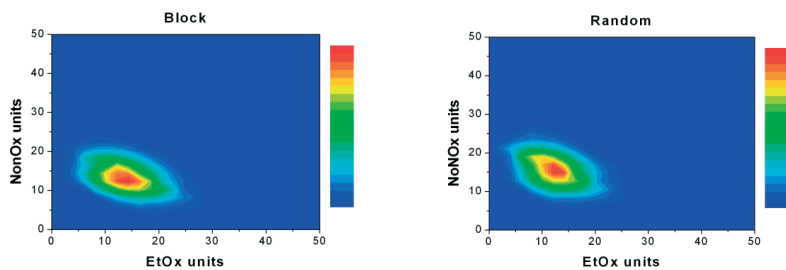
Figure 2-14. Contour plots, *Left:* block copolymer and *Right:* random copolymer of 2-ethyl-2-oxazoline and 2-nonyl-2-oxazoline.
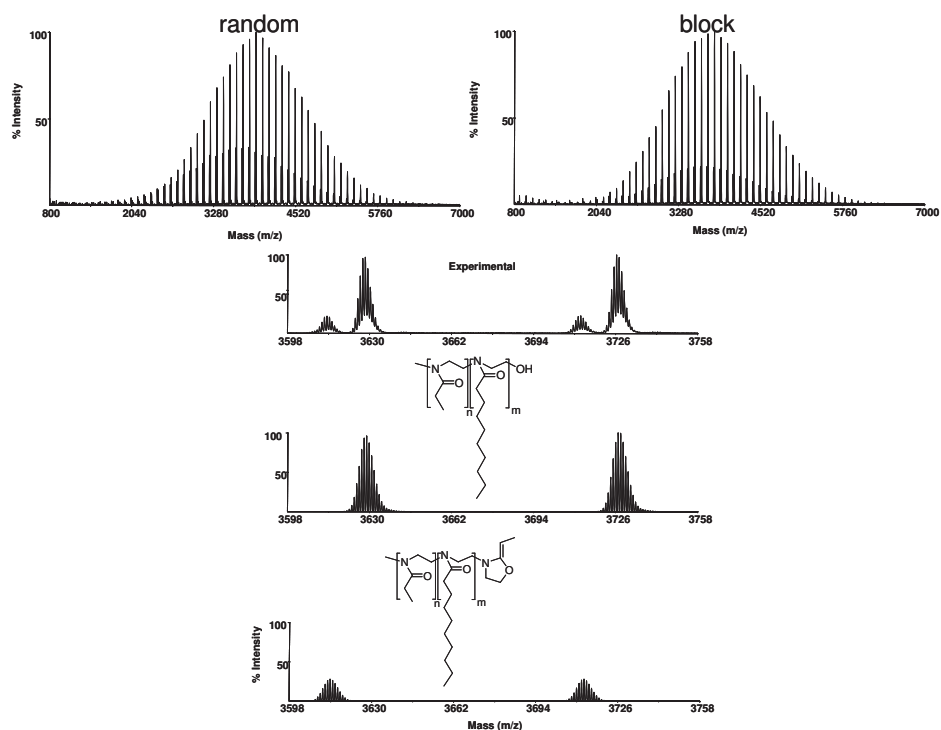
Figure 2-15. MALDI-ToF-MS spectra of block and random copolymer of 2-ethyl-2-oxazoline and 2-nonyl-2-oxazoline. The recorded and simulated spectra.

As can be seen, in these oxazoline copolymerizations the plots are indeed almost identical. This finding actually complicates the determination of the polymer's topology by looking at the shape and position or even the CCDs of the plot. An unknown copolymer pair giving a plot as described in Figures 2-13 and 2-14 can both be perfectly random and block. Fortunately not many one pot syntheses for block copolymers are known; thus one might faster conclude the more likely random topology. Nevertheless, an option to check the topology is by recording a few samples over time. The growth of a block copolymer moves the plot either vertically or horizontally (unless both blocks grow simultaneously), while the plot for a random copolymer moves along the diagonal (see appendix on CD-R). This phenomenon is described in Chapter 5 for poly(ester-*co*-carbonate)s. The shape of the contour plot is determined by the chemical composition distribution but also by the total chain length distribution. The total chain length distribution depends mainly on the type of polymerization, whereas the chemical composition distribution depends mainly on the reactivity ratios of the monomers. An example of different total chain length distributions is given in Figure 2-16. The distribution on the left is calculated for a free radical copolymerization, the distribution on the right for a ring-opening polymerization.
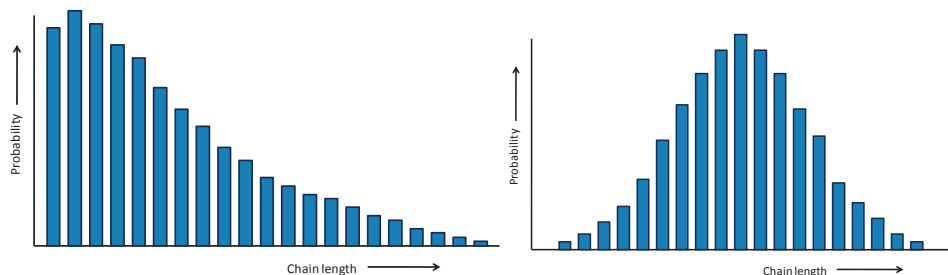
Figure 2-16. Total chain length distributions, Schulz-Flory-type (free radical and step growth) and Poisson-type for living polymerizations.

A schematic overview of contour plots expected for different types of polymerization is presented in Figure 2-17. The Poisson type of distribution can be expected for all types of living polymerizations and therefore the more elliptic to circular plots will be obtained.
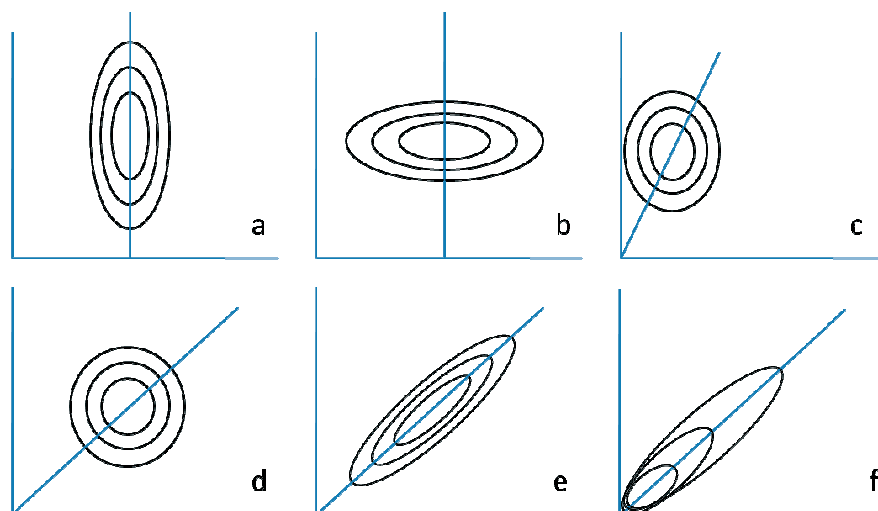
Figure 2-17. Schematics of contour plots a) + b) Typical for di-block copolymers with one block length longer than the other, c) typical for a living system with a higher reactivity ratio for one of the monomers, d) block copolymer with equal block lengths or a Bernoulli random $r_1 = 1$ $r_2 = 1$ (50% composition), e) living polymerization with both reactivity ratios smaller than one, f) typical for free radical and step growth reactions.

As far as our knowledge reaches, the first two plots **a** and **b** can only be created in case of block copolymers. Block copolymers are frequently synthesized sequentially and therefore do not need to have the same PDI with as result an elliptic plot. Willemse showed this for a block copolymer synthesized anionically of styrene and isoprene. The styrene block distribution is of the Poisson type while the isoprene block (2nd block) distribution at the beginning of growth fits to a Gaussian distribution.[28] Plot **c** is typical for a binomial chemical composition distribution along with a Poisson- or Gaussian-like total chain length distribution with one of the reactivity ratios of the comonomers higher than the other. Evidently, this plot could also be positioned against the abscissa when the reactivity ratios are opposite. In fact this type of plot complicates the distinction from the plot of a pure block copolymer since visually both of these plots are circular to elliptic. This also holds for plot **d** which is typical for a block copolymer with a 50 mol% composition but also of a living polymerization in which both monomers have a reactivity ratio of 1 (as shown in Figure 2-13). The next example highlights the importance of knowing the feed composition to interpret the MALDI-ToF-MS spectrum of a binomial copolymer. The plot of a copolymer synthesized from a starting composition of 50 mol% and reactivity ratios of $r_1 = 4$ and $r_2 = 0.25$ and the plot of a copolymer synthesized from a starting composition of 80 mol% and reactivity ratios of $r_1=1$ and $r_2=1$ are virtually identical. The simulated CCDs for both situations are given in Figure 2-18.
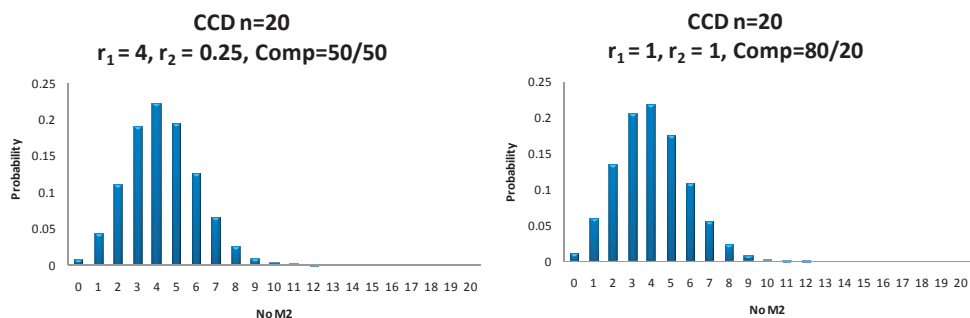
Figure 2-18. Comparison of the simulated CCD of chain length 20 for a comonomer pair with feed composition 50/50 and $r_1 = 4$, $r_2 = 0.25$ and for a comonomer pair with feed composition 80/20 and $r_1 = 1$, $r_2 = 1$.

Next, plot **e** of Figure 2-17 is typical for a living system with both reactivity ratios smaller than one. Finally, plot **f** is typical for free radical reactions (will be discussed in Chapter 3) and for step growth reactions in which two carboxylic acids are reacted with one diol or vice versa and where two hydroxyacids are copolymerized. Of course when a single diol is reacted with a single di-acid, the plot will only be a line since the polymer is perfectly alternating. Two examples of polycondensation reactions are given in Figure 2-19. The plot on the left is a reaction of adipate with two different diols, the plot on the right is the reaction of a single diol with a single diester. Willemse showed similar plots for the polymerizations of 1,4-butanediol with adipic acid and isophthalic acid or glutaric acid.[29]
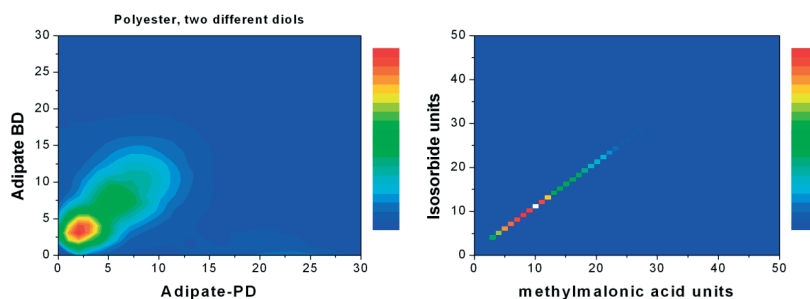
Figure 2-19. Contour plots, *Left:* dimethyl adipate polymerized with 1,3-propanediol and 2,3-butanediol. *Right:* isosorbide polymerized with dimethyl methylmalonate. (both by polycondensation) *(The MALDI-ToF-MS spectra are given in the Appendix on the CD-R.)*

The aforementioned difference in total chain length distribution (Schulz-Flory versus Poisson) becomes clearer when we compare the contour plots of a living with a non-living polymerization. Figure 2-20 shows the contour plots of a free radical polymerization and an atom transfer radical polymerization of styrene and methyl methacrylate.

It was reported that the reactivity ratios for the comonomer pair styrene/MMA in ATRP are in good agreement with those found for conventional free radical polymerization.[30] As can be seen, the width of the CCD is mainly determined by the reactivity ratios which are the same for both systems, but the CLD is different since there is no termination in ATRP.
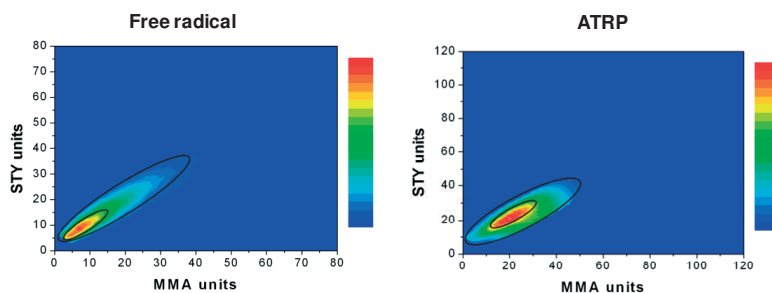
Figure 2-20. Contour plots, *Left:* Copolymer of styrene and methyl methacrylate synthesized by free radical. *Right:* Copolymer of styrene and methyl methacrylate synthesized by ATRP.

Throughout this thesis, most of the schematic contour plots given in this chapter can be found back for truly existing copolymers. From the discussion above it is clear that the contour plots can provide significant information about the topology of the copolymers, although there are special cases for which assignment of the topology becomes difficult without knowing the experimental details of the polymerization. A more accurate way to determine the topology is by determination of reactivity ratios as mentioned earlier and will be described in Chapter 3.

2.5 Disadvantages and pitfalls of MALDI-ToF-MS

This paragraph will deal with some disadvantages and known limitations using the fingerprint method and MALDI-ToF-MS, which are summarized below:

- Multiple peak assignment.
- Isotope overlap.
- Isotope interference.
- Fragmentation.
- End group discrimination.
- Mass discrimination.

These problems have been discussed by Staal[10] and Willemse[11], but for sake of clarity and completeness they will be summarized here and where possible accompanied with true examples.

2.5.1 Multiple peak assignment and isotope overlap

Isotope overlap is very common for polymers with more than one monomer residue and occurs when peaks from one isotope distribution overlap with peaks from another isotope distribution (Figure 2-5 to 2-7). This is only problematic if one of the peaks of the first distribution overlaps with the most abundant peak of the second distribution when building up the matrix. A good example of isotope overlap is given in Chapter 4, Figure 4-2. Isotope interference occurs when the difference between the most abundant peaks of the distributions is smaller than the resolution of the MALDI-ToF-MS measurement. This is in reality an extreme case of overlap. Staal and coworkers have proposed solutions for these problems.[10]

Multiple peak assignment occurs when more combinations of both monomer residues can be appointed to the same mass. This phenomenon was addressed by Wilczek-Vera[25] and expressed in the following equation:

$$\frac{\Delta n_1}{\Delta m_2} = \frac{M_2}{M_1} = \frac{26}{25} \approx \frac{104.15}{100.12} \qquad (2\text{-}7)$$

with as example styrene (104.15 g·mol^{-1}) and methyl methacrylate (100.12 g·mol^{-1}). A chain built up with 40 styrene and 40 methyl methacrylate residues has almost the same mass as a chain with 65 styrene and 14 methyl methacrylate residues and is even closer to a chain with 15 styrene and 66 methyl methacrylate residues. This multiple peak assignment finds expression in the formation of ghost plots as shown in Figure 2-21. In order to appoint the real plot, knowledge on composition is required either by NMR or by having an idea on the reactivity ratios and the feed. Additionally, other ghost plots can be obtained when there is a distribution of a copolymer chain ended with end group I, that can mathematically also explain peaks of another distribution of that copolymer terminated by end group II.
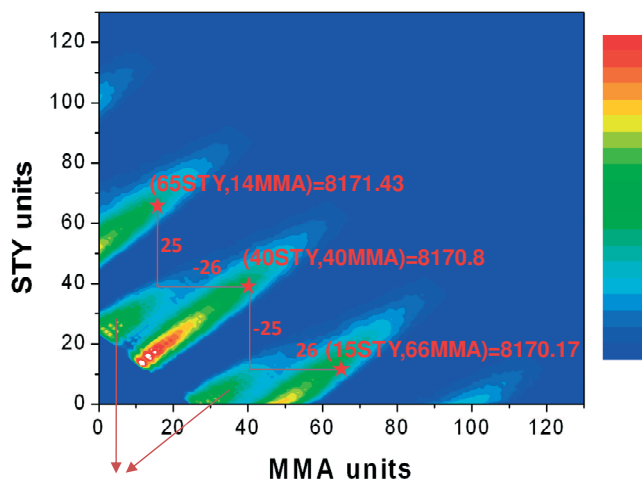
Ghost plots, other end group.

Figure 2-21. Examples of ghost plots originating from the fact that peaks in the spectrum can be appointed to multiple combinations of monomer residues and of ghost plots originating from the fact that peaks belonging to a distribution of species terminated by XY can mathematically be explained by another polymer species terminated by PQ.

2.5.1.1 Choice of the salt

The exchange of an acidic proton for a cation of the added ionization salt can be problematic when it causes for example isotope overlap. A good example is the spectrum of poly(lactide-*co*-glycolide). If the acidic proton of the carboxylic acid end group is exchanged for a potassium ion, the end group mass (K-OH) becomes approximately 56 g·mol^{-1}. This mass is close to the repeating unit glycolyl (appr. 58 g·mol^{-1}). A cyclic chain with an additional glycolyl unit is only 2 g·mol^{-1} higher in mass than a K-OH terminated chain with one glycolyl unit less. This problem and the way to solve it will be explained in more detail in Chapter 4. The exchange of the proton for a cation of the dopent is in some cases also beneficial, *e.g.* in the case of poly(cyclohexene succinate). Ring-opening of oxiranes and carboxylic anhydrides generally results in hydroxyl and carboxylic acid end-capped linear chains (referred to as an H-OH *A* end group), in hydroxyl terminated linear chains (referred to as H-OH *B*) but also in carboxylic acid terminated linear chains (referred to as H-OH *C*), see Table 2-3. Additionally, cyclic polymer structures can be formed by end-to-end condensation or intramolecular transesterification. Normally, the three linear structures can be distinguished based on their detected mass. Here, this is not possible because of the reaction of cyclohexene oxide with itself to form ether functionalities in the polymer chain. The extra cyclohexene oxide unit can for example be situated in the middle of the backbone rather than at the end of the chain.

Fortunately, the fact that the acidic protons of the carboxylic acid end groups are readily exchanged for a cation of the cationization salt helped to detect the diacid terminated structures (H-OH C) when both acidic protons were replaced by the cation of the added salt. Using potassium trifluoroacetate as ionization salt the exchange of the acidic protons indeed took place, yielding two extra distributions with either one or two COOK end groups. This prompted us to do further research into the roles of different salts. Next to KTFA, KI, NaTFA, NaI and CsTFA were tested. The most striking difference was observed between KTFA and KI as shown in Figure 2-22.
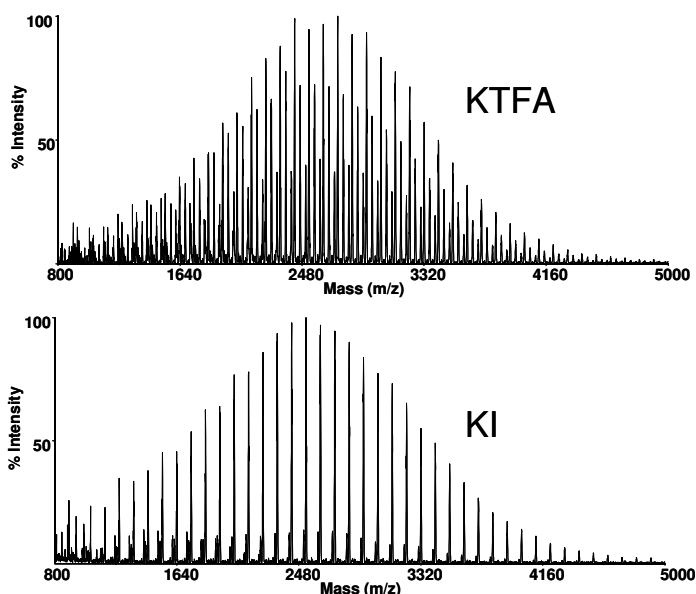
Figure 2-22. MALDI-ToF-MS spectrum (recorded with K^{+}) of poly(cyclohexene succinate) synthesized in bulk.

The transfer of the protons did not take place using KI. In principle now only one distribution should be detected if no cyclic structures are present. Pollution of KI by NaI afforded nevertheless another low intensity distribution. Using different salts can be very beneficial to determine the end groups. In this example, measurements with NaTFA helped in establishing the correct end group. A shift of −16 m/z, the difference in mass between potassium and sodium, of the most abundant isotope distributions in the spectra recorded with sodium in respect to the spectra recorded with potassium, pointed in the direction of an H-OH end group or cyclic structures.[†]

[†] Despite the fact that potassium has two isotopes and sodium none, comparison is still possible since potassium and sodium give similar isotope patterns for a single polymer chain.

A $\Delta m/z$ of 32 derives from the transfer of two potassium atoms for two sodium atoms, which is only possible when one acidic proton is replaced. Finally, if both acidic protons are replaced of a diacid terminated chain, a $\Delta m/z$ of 48 is found (Figure 2-23).
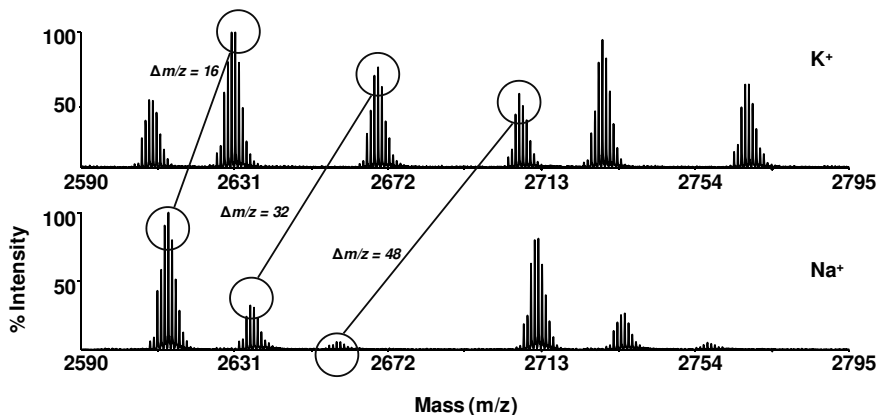
Figure 2-23. Comparison of an enlargement of the MALDI-ToF-MS spectra measured with sodium and potassium. The shift established in m/z between the spectra of the different peaks is depending on the number of acidic protons exchanged for a cation of the doping agent.

Table 2-3. Possible structures of the poly(cyclohexene succinate)
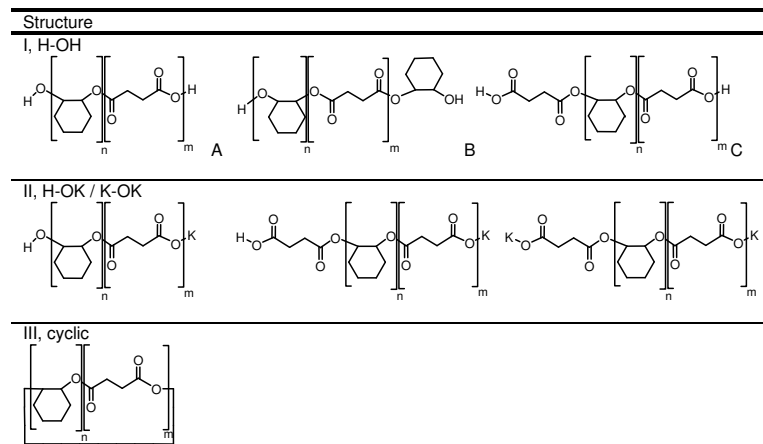
2.5.2 Discrimination and fragmentation

Mass discrimination and end group discrimination are generally the result of a difference in ionization efficiency during the MALDI-ToF-MS measurement. Mass discrimination is said to occur already for samples with a polydispersity higher than 1.2. Schriemer and Li thoroughly studied mass discrimination effects.[31,32] They reported two studies, one on sample preparation and one on instrumental issues. It was found that M_n values are depending on the sample preparation and are a function of the ratio polymer : matrix : cation. The influence of instrumental settings on mass discrimination is mainly related to detector design and detector saturation. Another study on mass discrimination was performed by Staal, who investigated the effect of different matrices on a blend of six narrow polystyrene standards. He found that DCTB was superior to other matrices by showing the least discrimination.[10] The discrimination can be a problem for the contour plot as shown graphically in the Appendix on the CD-R.

Puglisi *et al.* reported a difference in ionization efficiency for hydroxy terminated and carboxylic acid terminated PBT in their research on Ny6/PBT blends.[33] We have observed a dramatic difference in the ionization efficiency of hydroxy terminated aliphatic polyesters compared to their acid terminated counter parts.[34] Therefore MALDI-ToF-MS can't be employed for quantitative analysis for differently terminated chains. Other techniques like NMR, end group titration and or LCCC (provided it has the correct detection) have to be applied for this purpose.

Although MALDI-ToF-MS is a so-called soft ionization technique, fragmentation occurs in some situations. Probably, the best known example is the cleavage of the bromine functionality at the chain end of polymer chains synthesized by ATRP. The loss of the terminal halide occurs easier in case of acrylates than in case of styrene polymers as could be concluded from our own experience. Another example is the chains terminated by a dithioester moiety deriving from a RAFT agent.[35]

2.6 MALDI-ToF-MS in relation to SEC

The relation between size exclusion chromatography and MALDI-ToF-MS is important to comprehend in order to be able to compare the results obtained by both techniques. In fact the comparison can give immediate insight into (mass) discrimination by MALDI. A MALDI spectrum shows a number molar mass distribution after summation of each peak for a given mass followed by normalization.[‡]

[‡] Summation of the peaks can only be done in the mass domain. Transformation of the intensity signal from the time to the mass domain is necessary to correctly integrate the areas underneath the peaks.[10]

Generally in a SEC chromatogram representing the average weight molar mass distribution, the differential weight fraction (*dw/d logM*) is plotted versus the logarithm of the molar mass (*log M*).[36,37] The equations needed to convert a MALDI-ToF-MS spectrum in order to make a proper comparison with a size exclusion chromatogram are the following:

$$w(logM) = w(M)\frac{dM}{d\log M} \tag{2-8}$$

$$w(M) = n(M)M \tag{2-9}$$

$$w(logM) = n(M)M^2 ln10 \tag{2-10}$$

Examples of an overlay with and without discrimination are given in Figure 2-24. To increase the visual comparison the ordinate is normalized. It can be concluded that the plot on the left clearly demonstrates discrimination of the bimodality observed by SEC, whereas in the plot on the right this is not the case.
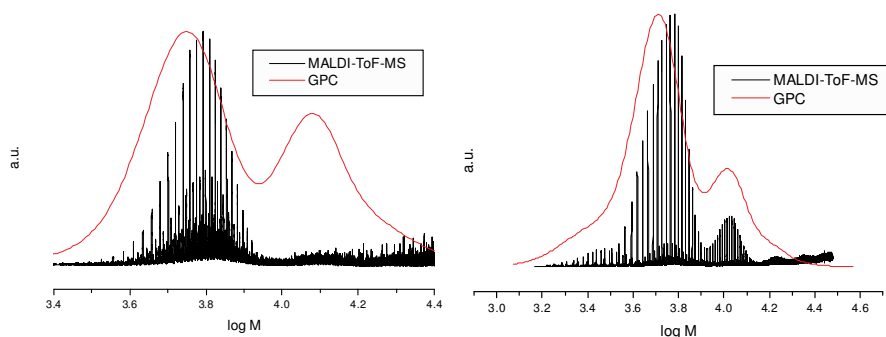
Figure 2-24. Overlay of a MALDI-ToF-MS spectrum with a SEC chromatogram.

2.6.1 Overestimation by SEC

The significant overestimation on molar mass by size exclusion chromatography using polystyrene standards for polyesters is well-known.[38] Different methods to determine absolute average molar masses are developed such as universal analysis using the polymer's known Mark-Houwink parameters for correction, triple detector set-ups including RI-light scattering -viscosity and by combination of SEC-MALDI-ToF-MS. Here, the latter method was employed for poly(lactide) and poly(ε-caprolactone). We made two calibration curves by fractionation according to molar mass, reinjection of these fractions in the normal SEC set-up and by measuring MALDI-ToF-MS on these fractions.

Plotting the Mpeaks of the narrow distributions obtained from SEC against the Mpeaks derived from MALDI for the different fractions results in the desired calibration curve. In Figure 2-25 it can be seen that on average the molar mass determined by SEC for poly(lactide) and for poly(ε-caprolactone) using PS standards is indeed overestimated by a factor of approximately 2.[39,40]
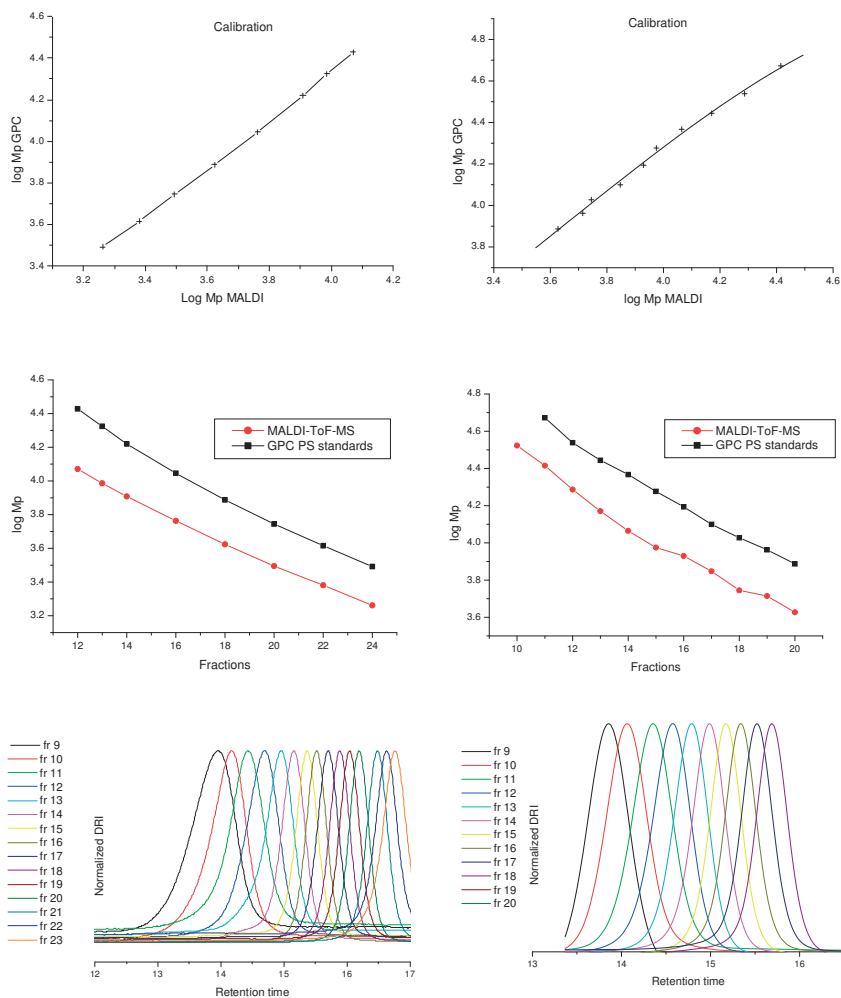
Figure 2-25. Calibration curve for poly(lactide) (left) and for poly(ε-caprolactone) (right), log M_{peak} for both MALDI and SEC against fraction number, and size exclusion chromatograms for the re-injected fractions.

2.7 MALDI-ToF-MS and LCCC

An important item in the synthesis of polyesters is the quantification of the known formation of cyclic structures. Insight into the amount of cyclics might help to understand a polymer's physical properties like for example glass transition temperatures and melting points. Liquid chromatography under critical conditions is the most well-known analytical tool that separates polymers on basis of their chain termini rather than on molecular weight. A problem with this technique is the construction of a proper calibration line since the detectors often used do not display a linear relation between areas underneath the peaks in the chromatogram and quantity. Another technique like pyrolysis GC-MS can be applied to quantify the separated fractions by LCCC. In any case, standard samples with a known amount of cyclic chains are required, therefore, facing exactly the initial issue. However, with the developments of N-heterocyclic carbenes as catalysts in the polymerization of lactides, a door has been opened to obtain well-defined standards for calibration due to the possibility of synthesizing purely cyclics by a zwitterionic mechanism as reported by Waymouth *et al.*[41] (Chapter 1, Scheme 1-2). For this purpose four samples (two plus two) were synthesized using in one case MeOH as initiator and in the other case no initiator. The MALDI-ToF-MS spectra (Figure 2-26) of the products confirmed what was expected, methoxy terminated and cyclic chains respectively. Moreover, a difference of 144 *m/z* (equal to the mass of one lactydyl unit) was detected between two consecutive distributions. This indicates a kinetically controlled reaction and the absence of inter- and more importantly intramolecular transesterification reactions which is a requirement for obtaining the linear calibration standard.
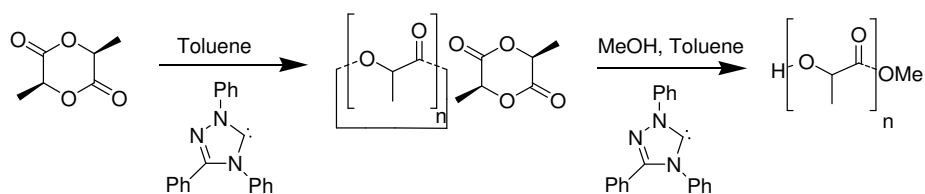
Scheme 2-1. Polymerization of D-lactide with and without initiator using a carbene as catalyst.
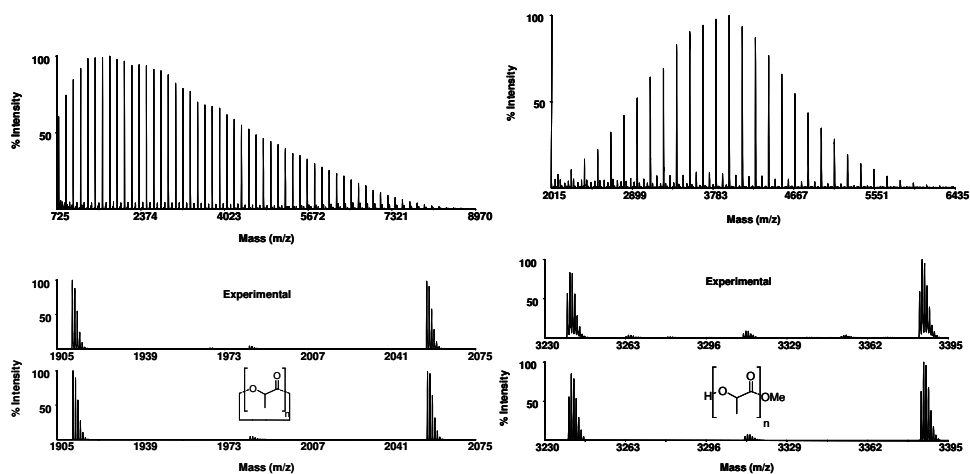
Figure 2-26. MALDI-ToF-MS spectra of cyclic (reaction without additional initiator) and linear (reaction with MeOH as initiator) poly(D-lactide) obtained by solution polymerization with an N-heterocyclic carbene as catalyst.

All four samples (two samples without initiator (to deliberately form cyclics) and two samples with MeOH as initiator) were analyzed by LCCC after an intensive fine tuning of the operating conditions. The evaporative light scattering detection chromatograms are depicted in Figures 2-27 and 2-28. (The difference between the two samples is the molar mass.)
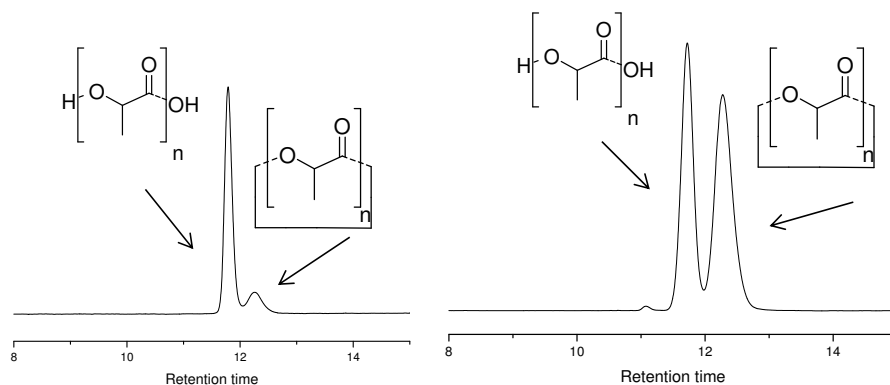
Figure 2-27. LCCC chromatograms of poly(D-lactide) synthesized by the triazolilydene carbene *without* the presence of an initiator. Chemical structures depict species detected by MALDI-ToF-MS of fractions accumulated according to retention time of peaks. *Left:* M_n =6004 g·mol^{-1}, *PDI* = 1.3. *Right:* M_n =9639 g·mol^{-1}, *PDI* = 1.3
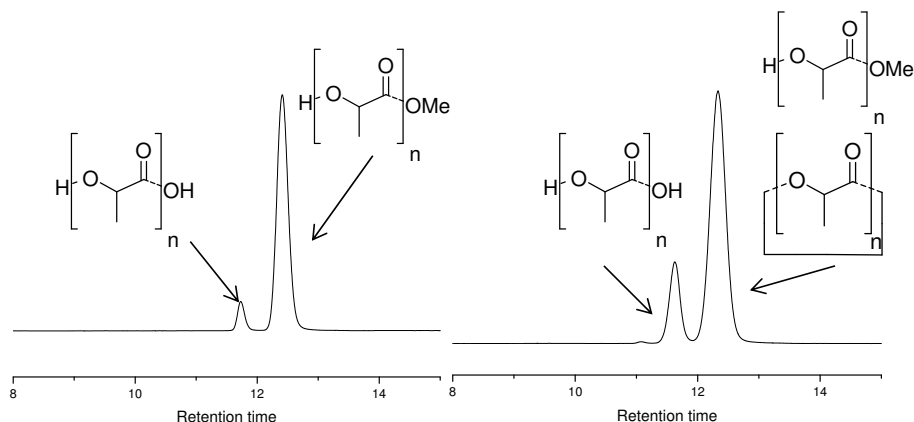
Figure 2-28. LCCC chromatograms of poly(D-lactide) synthesized with triazolilydene carbene in the presence of MeOH as initiator. Chemical structures depict species detected by MALDI-ToF-MS of fractions accumulated according to retention time of peaks. *Left: M_n =6024 g·mol^{-1}, PDI = 1.2. Right: M_n =9692 g·mol^{-1}, PDI = 1.2.*

Fractions were collected according to the elution time of the peaks for all four samples (two samples of poly(lactide) synthesized in the presence of an initiator and two samples of poly(lactide) synthesized in the absence of an additional initiator). These fractions were analyzed by MALDI-ToF-MS from which it could be concluded that the peak on the left in the chromatograms for all samples derived mainly from the H-OH terminated chains. The peak on the right in the chromatogram of poly(lactide), synthesized *with* initiator but for the lower molecular weight, evolved from purely methoxy terminated polymer chains. In the higher molecular weight sample, also cyclics were found in the spectra of fractions from both peaks, but the signal was more profound for the peak on the right. In the other case, for poly(lactide) synthesized *without* initiator, the peak on the right consisted of purely cyclic structures, but the peak was higher in intensity for the higher molecular weight sample.

In order to collect more evidence that the conditions operated with were indeed critical, other poly(lactides) were synthesized by the conventional way using stannous octoate. These samples were also subjected to liquid chromatography under critical conditions. Three different samples were measured, only changing in type of initiator. The chromatograms are given in Figure 2-29. For poly(lactide) synthesized by Sn(Oct)$_2$ and benzylalcohol as initiator, the LCCC fractions were collected to verify if the chain termini were different for each peak. MALDI-ToF-MS analysis of the fractions showed that firstly the H-OH terminated chains eluted, secondly the benzylalcohol and thirdly, the cyclics (Figure 2-29). The order of elution of the polymers separated on end group was identical to the order detected for poly(ε-caprolactone) as recently reported by De Geus *et al.*[42]
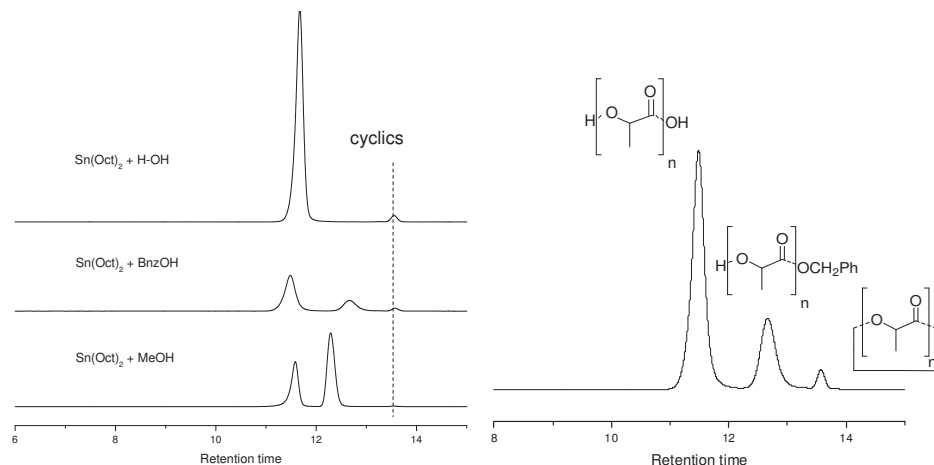
Figure 2-29. *Left:* Chromatograms of poly(lactide) synthesized by Sn(Oct)$_2$ without additional initiator, with benzylalcohol as initiator and with methanol as initiator. *Right:* Chromatogram of poly(lactide) synthesized by Sn(Oct)$_2$ with benzylalcohol as initiator and the structures as determined by MALDI-ToF-MS.

A comparison of the chromatograms of these samples with the samples of poly(lactide) synthesized by employing carbene, learns that the MeO-H terminated polymer chains elute at a similar retention time, just as the H-OH terminated chains, but that the cyclics of poly(lactide) synthesized by Sn(Oct)$_2$ elute later than the cyclics of poly(lactide) synthesized by carbene (Figure 2-30).
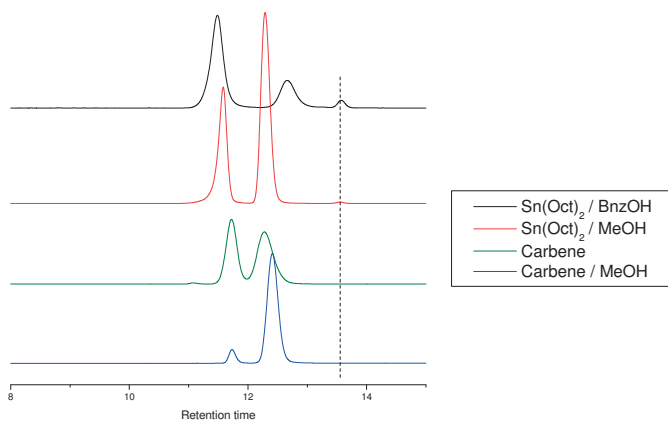
Figure 2-30. Overview of chromatograms of poly(lactide) synthesized by Sn(Oct)$_2$ and carbene.

This is impossible when truly separating on type of end group, which implies that the conditions are not critical or that the cyclic structures synthesized by carbene are in fact linear but "cyclisize" during the MALDI-ToF-MS measurements. Although the latter scenario is more plausible since the chromatograms are well resolved, further research is necessary to gather more evidence for the possible cyclization during MALDI analysis.

2.8 Experimental Section

Reagents. All chemicals were purchased from Aldrich unless stated otherwise. Henkel kindly provided 2-nonyl-2-oxazoline. Methyl tosylate as well as the 2-oxazolines were distilled prior to use. Acetonitrile was obtained from Biosolve, dried on molecular sieves and stored under an Argon atmosphere. Styrene was purchased from Merck and purified by passing over an inhibitor remover column. Methyl methacrylate was distilled under vacuum. Lactide was a gift from Purac. Toluene was dried over an alumina column and stored on molecular sieves under argon. 1,3,4-triphenyl-4,5-dihydro-1*H*-1,2-triazol-5-ylidene carbene was purchased from Acros. 2,3-butanediol was purchased from Fluka.

Synthesis polycondensation. Dimethyl adipate, 1,3-propanediol and 2,3-butanediol in a ratio of 2.0:1.0:3.0 respectively were added into a four-neck flask equipped with a nitrogen inlet, a thermal couple, a mechanical stirrer, a reflux condenser and a Dean Stark trap. After removing the air by applying vacuum-argon for 3 times, the reactor was heated to 220 ^{o}C. Finally Titanium (IV) butoxide (4 wt% of DMAd) was added. After 5h remaining monomer was removed under vacuum.

Synthesis oxazolines. The polymerizations were performed in acetonitrile at 140 ^{o}C in capped vials in a single mode microwave reactor. The vials were dried in an oven and filled under Argon atmosphere. The reactions were terminated by quenching with water. For the random copolymer, the crimp lid vial was charged with 2-ethyl-2-oxazoline (99.13 µL, 1 mmol), 2-nonyl-2-oxazoline (197.23 µL, 1 mmol) and 0.7 mL acetonitrile. Methyl tosylate was added as initiator in a monomer to initiator ratio of 34. The mixture was reacted for 680 s in the microwave reactor. For the block copolymer, the crimp lid vial was charged with only 2-ethyl-2-oxazoline (99.13 µL, 1 mmol) and 0.7 mL acetonitrile. Methyl tosylate was now added as initiator in a monomer to initiator ratio of 17 (after addition of the second monomer [M]/[I]=34/1 again). The mixture was allowed to react for 542 s in the microwave reactor before adding the second monomer 2-nonyl-2-oxazoline. After addition of the second monomer, the mixture was reacted an additional 608 s.

Synthesis ATRP. Styrene (2.5 g, 24 mmol), methyl methacrylate (2.4 g, 24 mmol), N,N,N',N',N''-pentamethyl diethylene triamine (PMDETA) (35 mg, 0.19 mmol) and Cu^{I}Br (22 mg, 0.17 mmol) were mixed into a Schlenk tube together with toluene (5 mL). The mixture was deoxygenated by Argon flushing during 30 min. Next, the Schlenk tube was immersed into an oil bath preheated at 80 ^{o}C and the initiator ethyl α-bromoisobutyrate (EBIB) (33 mg, 0.17 mmol) was added. After an hour, every 15 min. a sample for MALDI-ToF-MS analysis was withdrawn.

Synthesis poly(lactide). Lactide (2.0 g, 13.9 mmol), 1,3,4-triphenyl-4,5-dihydro-1*H*-1,2-triazol-5-ylidene carbene (41.3 mg, 0.14 mmol), methanol (5.6 µL, 0.14 mmol) (only in case of linear polymer chains) and 4 mL toluene were charged in the glovebox in a 5 mL crimp lid vial along with a magnetic stirring bar. The vial was removed from the glovebox and put into an aluminum heating block. The mixture was stirred for 3h at 100 ^{o}C. Samples of the crude mixture were taken and used for LCCC measurements after evaporation of the solvent toluene.

SEC fractionation. SEC analyses were performed on a system consisting of a two-column set 300 x 7.5 mm (PLgel Mixed-E 3 µm Polymer Laboratories) with a guard column 50 x 7.5 mm (PLgel 3 µm Polymer Laboratories), an isocratic pump (Waters P590, flow rate of 1.0 mL·min^{-1}) and a UV detector (Spectra Physics LinearTM UV-VIS 200, 254 nm). THF was used as the solvent. A fraction collector (Millipore) was used to collect 32 fractions per run with the time per fraction set to 0.27 min. In total 10 runs were accumulated from a sample with a concentration 10 mg·mL^{-1}.

LCCC. LCCC experiments were conducted on an Agilent 1100 equipped with a column oven set to 5 ^{o}C, a diode-array detector (DAD) and an external Alltech ELSD detector. The mobile phase, 17 w/w% ultra pure water and 83 w/w% THF, was premixed and pumped with a flow rate of 0.5 mL·min^{-1}. Four reversed phase Zorbax eclips XDB-C8-columns in series (150 x 4.6 mm) were used to achieve critical separation. An injection volume of 5 µL sample of a concentration of 8 mg·mL^{-1} dissolved in eluent was applied in case of fractionation. Fractions of fifteen runs were accumulated to be analyzed by MALDI-ToF-MS.

MALDI-ToF-MS. MALDI-ToF-MS analysis was performed on a Voyager DE-STR from Applied Biosystems equipped with a 337 nm nitrogen laser. An accelerating voltage of 25 kV was applied. Mass spectra of 1000 shots were accumulated. The polymer samples were dissolved in THF at a concentration of 1 mg·mL^{-1}. The cationization agent used was potassium trifluoroacetate (Fluka, >99%) dissolved in THF at a concentration of 5 mg·mL^{-1}. The matrix used was trans-2-[3-(4-tert-butylphenyl)-2-methyl-2-propenylidene]malononitrile (DCTB) (Fluka) and was dissolved in THF at a concentration of 40 mg·mL^{-1}. Solutions of matrix, salt and polymer were mixed in a volume ratio of 4:1:4, respectively. The mixed solution was hand-spotted on a stainless steel MALDI target and left to dry. The spectra were recorded in the reflector mode as well as in the linear mode.

References

[1]   M.A.R. Meier, N. Adams, U.S. Schubert, *Anal. Chem.* **2007**, *79*, 863.

[2]   M.W.F. Nielen, *Mass Spectrom. Rev.* **1999**, *18*, 309.

[3]   J.H. Scrivens, A. T. Jackson, *Int. J. Mass Spectrom.* **2000**, *200*, 261.

[4]   G. Montaudo, F. Samperi, M.S. Montaudo, *Prog. Polym. Sci.* **2006**, *31*, 277.

[5]   S.D. Hanton, *Chem. Rev.* **2001**, *101*, 527.

[6]   H.J. Räder, W. Schrepp, *Acta Polym.* **1998**, *49*, 272.

[7]   R. Murgasova, D.M. Hercules, *Int. J. Mass Spectrom.* **2003**, *226*, 151.

[8]   S.F. Macha, P.A. Limbach, *Curr. Opin. Solid State Mater. Sci.* **2002**, *6*, 213.

[9]   P. Juhasz, M.L. Vestal, S.A. Martin, *J. Am. Soc. Mass Spectrom.* **1997**, 8, 209.

[10]   B.B.P. Staal, *PhD thesis*, University of Technology Eindhoven, **2005**, ISBN 90-386-2826-9, http://alexandria.tue.nl/extra2/200510540.pdf.

[11]   R.X.E. Willemse, *PhD thesis*, University of Technology Eindhoven, **2005**, ISBN 90-386-2816-1, http://alexandria.tue.nl/extra2/200510293.pdf.

[12]   Isotope tables NERMAG.

[13]   J.A. Yergey, *Int. J. Mass Spectrom. Ion Phys.* **1983**, *52*, 337.

[14]   J.A. Yergey, *Anal. Chem.* **1983**, *55*, 353.

[15]   R.K. Snider, *J. Am. Soc. Mass. Spectrom.* **2007**, *18*, 1511.

[16]   S. Kéki, L.S. Szilagyi, G. Deak, M. Zsuga, *J. Mass Spectrom.* **2002**, *37*, 1074.

[17]   J.H. Scrivens, A.T. Jackson, H.T. Yates, M.R. Green, G. Critchley, J. Brown, R.H. Bateman, M.T. Bowers, J. Gidden, *Int. J. Mass Spectrom. Ion Processes* **1997**, *165/166*, 363.

[18]   J. Gidden, T. Wyttenbach, A.T. Jackson, J.H. Scrivens, M.T. Bowers, *J. Am. Chem. Soc.* **2000**, *122*, 4692.

[19]   J. Gidden, T. Wyttenbach, J.J. Batka, P. Weis, M.T. Bowers, A.T. Jackson, J.H. Scrivens, *J. Am. Soc. Mass Spectrom.* **1999**, *10*, 883.

[20]   J. Gidden, M.T. Bowers, A.T. Jackson, J.H. Scrivens, *J. Am. Soc. Mass Spectrom.* **2002**, *13*, 499.

[21]   B.J. Bauer, W.E. Wallace, B.M. Fanconi, C.M. Guttman, *Polymer* **2001**, *42*, 9949.

[22]   W.E. Wallace, W.R. Blair, *Int. J. Mass Spectrom.* **2007**, *263*, 82.

[23]   G. Wilczek-Vera, P.O. Danis, A. Eisenberg, *Macromolecules* **1996**, *29*, 4036.

[24]   G. Wilczek-Vera, Y. Yu, K. Waddell, P.O. Danis, A. Eisenberg, *Macromolecules* **1999**, *32*, 2180.

[25]   G. Wilczek-Vera, Y. Yu, K. Waddell, P.O. Danis, A. Eisenberg, *Rapid Commun. Mass Spectrom.* **1999**, *13*, 764.

[26]   F. Wiesbrock, R. Hoogenboom, M. Leenen, S.F.G.M. van Nispen, M. van der Loop, C.H. Abeln, A.M.J. van den Berg, U.S. Schubert, *Macromolecules* **2005**, *38*, 7957.

[27]   R. Hoogenboom, *PhD thesis*, University of Technology Eindhoven, **2005**, ISBN 90-386-2837-4, http://alexandria.tue.nl/extra2/200513223.pdf.

[28] R.X.E. Willemse, B.B.P. Staal, E.H.D. Donkers, A.M. Van Herk, *Macromolecules* **2004**, *37*, 5717.

[29] R.X.E. Willemse, W. Ming, A.M. v. Herk, *Macromolecules* **2005**, *38*, 6876.

[30] M.A. Semsarzadeh, M. Abdollahi, *Polymer* **2008**, 49, 3060.

[31] D.C. Schriemer, L. Li, *Anal. Chem.* **1997**, *69*, 4169.

[32] D.C. Schriemer, L. Li, *Anal. Chem.* **1997**, *69*, 4176.

[33] C. Puglisi, F. Samperi, R. Alicata, G. Montaudo, *Macromolecules* **2002**, *35*, 3000.

[34] B.A.J. Noordover, V.G. van Staalduinen, R. Duchateau, C.E. Koning, R.A.T.M. van Benthem, M. Mak, A. Heise, A.E. Frissen, J. van Haveren, *Biomacromolecules* **2006**, *7*, 3406.

[35] C. Barner-Kowollik, T.P. Davis, M.H. Stenzel, *Polymer* **2004**, *45*, 7791.

[36] H.C.M. Byrd, C.N. McEwen, *Anal. Chem.* **2000**, *72*, 4568.

[37] T.H. Mourey, A.J. Hoteling, S.T. Balke, K.G. Owens, *J. Appl. Polym. Sci.* **2005**, *97*, 627.

[38] M.S. Montaudo, C. Puglisi, F. Samperi, G. Montaudo, *Macromolecules* **1998**, *31*, 3839.

[39] D. Tillier, H. Lefebvre, M. Tessier, J.-C. Blais, A. Fradet, *Macromol. Chem. Phys.* **2004**, *205*, 581.

[40] H. Pasch, K. Rode, *J. Chromatogr., A* **1995**, *699*, 21.

[41] D.A. Culkin, W. Jeong, S. Csihony, E.D. Gomez, N.P. Balsara, J.L. Hedrick, R.M. Waymouth, *Angew. Chem. Int. Ed.* **2007**, *46*, 2627.

[42] M. de Geus, R. Peters, C.E. Koning, A. Heise, *Biomacromolecules*, **2008**, *9*, 752.

Reactivity ratios from a single MALDI-ToF-MS spectrum.

Abstract. *The microstructure (random, block or alternating) of a copolymer reflects on the physical properties of the polymeric material. Therefore it is of great importance to be able to fast and easy determine a copolymer's fine structure. In order to classify the topology of the copolymer, knowledge of the reactivity ratios or their product is required. Conventional ways to determine these ratios demand in most cases tedious laboratory work. Here, a novel method is described to derive these ratios from a single MALDI-ToF-MS spectrum by employing either a Monte Carlo approach to numerically simulate a first order Markov chain or the analytical form of the first order Markov chain. A single MALDI-ToF-MS spectrum proved to give very good estimates of the reactivity ratios of comonomers from copolymer's synthesized by free radical polymerization of styrene and (meth)acrylates or by ring-opening polymerization of lactones and lactides.[§]*

3.1 Introduction

One of the ultimate challenges in polymer chemistry is the ability to control the physical properties of a copolymer by tailoring its microstructure. Knowing the reactivity ratios of the comonomers allows predicting and tuning of the copolymer's microstructure, both with respect to composition and topology. These ratios can be classified as indicated in Table 3-1.

Table 3-1. Classification of reactivity ratios and microstructure.

Ratios	Topology
$r_1 = 1/r_2$, $r_2 = 1/r_1$ ($r_1r_2 = 1$)	Random copolymer
$r_1 \ll 1$, $r_2 \ll 1$ ($r_1r_2 \to 0$)	Tends to alternating copolymer
$r_1 \gg 1$, $r_2 < 1$ ($r_1r_2 < 1$)	Tends to homopolymer of M_1
$r_1 \gg 1$, $r_2 \gg 1$	Tends to a blocky copolymer

The classical method to ascertain reactivity ratios is by determining the comonomer composition of a range of polymers prepared with different feed compositions. A fast and reliable method that can circumvent this tedious and time-consuming laboratory work is therefore highly desired. Various methods to determine reactivity ratios have been reported which deal with either the differential or the integral form of the Mayo-Lewis equation.[1] Nevertheless, most methods have the disadvantage that still quite some reactions have to be performed with different feed compositions. Moreover, comparison of ratios obtained by diverse methods often shows a relatively large variety due to a statistical error, for example as the result of linearization. Choosing the right statistical method is therefore crucial for the reliability of the outcome.[2]

Table 3-2. Different methods to determine reactivity ratios.

Method	Abbreviation	Reference	Publication year
Mayo Lewis	ML	[1]	1944
Fineman-Ross	FR	[3]	1950
Tidwell-Mortimer	TM	[4]	1965
Jaacks		[5]	1972
Kelen-Tüdös	KT	[6]	1975
Extended Kelen-Tüdös	ex-KT	[7]	1976
Barson-Fenn	BF	[8]	1989
Error-in-variables model	EVM	[9]	1991
Mao-Huglin	MH	[10]	1993

Since a copolymer is a statistical mixture of individual molecules, a copolymer sample obtained from a single experiment in principle contains all the information required to retrieve the reactivity ratios. Still, examples of methods that only require a single experiment are limited. Jaacks introduced a method in which the ratios are determined from a single experiment when one of the two monomers is in large excess.[5] This method is limited to systems in which the reactivity ratios do not have an extreme difference in value.[11] Rudin reported on the use of a single NMR spectrum by using the sequence distribution as determined from the measured diads or triads.[12] However, to obtain a highly resolved spectrum, long measuring times are required and assigning the peaks is not straightforward. Matrix assisted laser desorption/ionization time-of-flight mass spectrometry (MALDI-ToF-MS) is a fast and accurate technique to determine copolymer compositions, is very useful to elucidate the copolymers topology and to study mechanistic aspects of various copolymerization systems.[13,14] Since MALDI-ToF-MS gives information on individual polymer chains, access to homo-propagation and cross-propagation probabilities becomes available.[15] These probabilities provide the reactivity ratios by simulation of a first order Markov chain by using for example the Monte Carlo method. The first to apply MALDI-ToF-MS to determine reactivity ratios of comonomers were Suddaby and Willemse but they still required data from different reactions.[16,17]

In this chapter we will report on a reliable method to determine reactivity ratios based on a *single* MALDI-ToF-MS spectrum of the copolymers. The reactivity ratios have been determined for three different types of copolymerizations *i.e.* free radical polymerization, ring-opening polymerization of cyclic esters and ring-opening polymerization of oxiranes and anhydrides. The reactivity ratios were obtained by simulating a first order Markov chain by using both the Monte Carlo approach and an analytical mathematic solution.

3.2 Terminal model ~ first order Markov chain

The simplest copolymer model represents a first order Markov chain in which the propagation depends on the terminal unit of the growing polymer chain, *i.e.* the distribution of monomer residues along an individual chain can be described by a first order Markov chain by means of the Mayo-Lewis (terminal) model.[18,19] In free radical polymerizations, the penultimate model, which represents a second order Markov chain, is a better model for some systems but falls out of the scope of this study. Here, we use the terminal model for copolymers in which we can distinguish the following four probabilities:

$$\sim M_1^* + M_1 \xrightarrow{k_{11}} \sim M_1 M_1^* \qquad P_{11} = \frac{r_1([M_1]/[M_2])}{r_1([M_1]/[M_2])+1}$$

$$\sim M_1^* + M_2 \xrightarrow{k_{12}} \sim M_1 M_2^* \qquad P_{12} = \frac{1}{r_1([M_1]/[M_2])+1}$$

$$\sim M_2^* + M_2 \xrightarrow{k_{22}} \sim M_2 M_2^* \qquad P_{22} = \frac{r_2([M_2]/[M_1])}{r_2([M_2]/[M_1])+1}$$

$$\sim M_2^* + M_1 \xrightarrow{k_{21}} \sim M_2 M_1^* \qquad P_{21} = \frac{1}{r_2([M_2]/[M_1])+1}$$

$$r_1 = \frac{k_{11}}{k_{12}} = \frac{A_{11}\exp\left(-\frac{E_{11}}{RT}\right)}{A_{12}\exp\left(-\frac{E_{12}}{RT}\right)}, \; r_2 = \frac{k_{22}}{k_{21}} = \frac{A_{22}\exp\left(-\frac{E_{22}}{RT}\right)}{A_{21}\exp\left(-\frac{E_{21}}{RT}\right)}$$
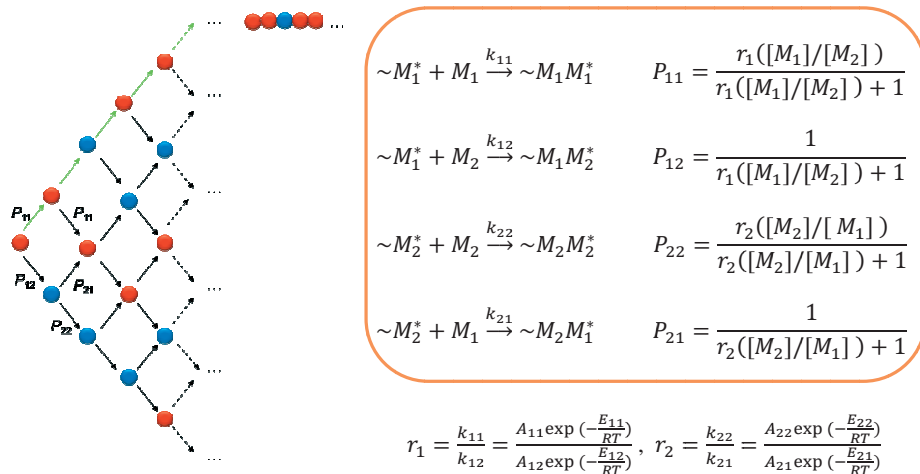
(in which: M_1 and M_2 refer to different monomers, P_{ii} and P_{ij} refer to the homo-propagation and cross-propagation probabilities respectively and r_1 and r_2 to the reactivity ratios of respectively monomer M_1 and M_2.)

In fact, the chemical composition distributions obtained by deconvolution of a MALDI-ToF-MS spectrum as described in Chapter 2 (Figure 2-9), can be fitted to this model if the probability density function of the first order Markov chain based on the propagation probabilities for a given chain length can be determined theoretically. Initially, in order to calculate the probability density function of a first order Markov chain, the numerical Monte Carlo method was employed and will be discussed in paragraph 3.2.1. This method accurately simulated the required chain, yet as time learned, the method was relatively slow. Therefore an analytical solution in closed form as it exists for the zero-order Markov chain, better known as binomial distribution, would be highly desirable to circumvent long and tedious Monte Carlo computations. In the nick of time, the analytical solution was obtained with help of the Mathematical Department of our university and will be discussed in paragraph 3.2.2.

3.2.1 Monte Carlo method

The Monte Carlo method can be used to numerically simulate a single, first order Markov chain with as input the propagation probabilities and the chain length by employing the software package MatLab 7.4.0 (2007a).[20] The distribution of comonomers along a polymer chain is modeled by a simple stochastic process generating 0's and 1's according to the following transition matrix:

from/to	0	1
0	P_{11}	$1-P_{11} (=P_{12})$
1	$1-P_{22} (=P_{21})$	P_{22}

Applying this transition matrix 'n' time results in a distribution of 0's and 1's, resembling the chemical composition distribution as obtained from the MALDI-ToF-MS spectrum. The Monte Carlo simulation starts with a binomial distribution ($P_{11} + P_{22} = 1$) corresponding to a completely random copolymer as initial estimate and is then fitted to the recorded MALDI-ToF-MS distribution making use of the least sum of squares method. The sum of squares was calculated by taking the absolute difference between the fitted and the observed values. The best fit of the model is found when the sum of squares has its least value *i.e.* P_{11} and P_{22} are fitted until the sum of squares converges to a minimum. [21]
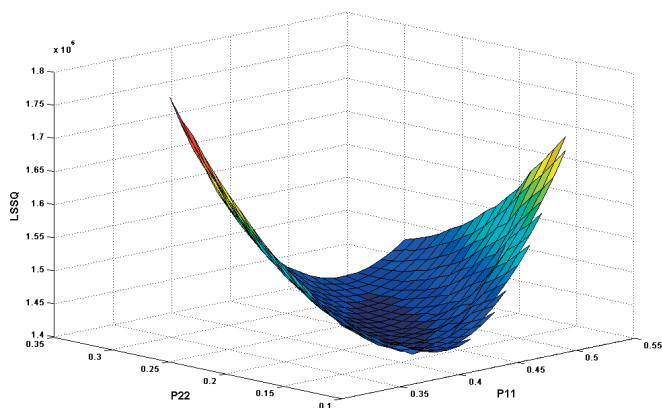
Figure 3-1. LSSQ as a function of P_{11} and P_{22} for a certain chain length.

Other methods than the least sum of squares were applied in our fitting procedure, *e.g.* the maximum likelihood and the absolute difference. However, the correctness of these individual methods was subject to a mathematical discussion. The final decision on the choice of fitting method was rather based on familiarity than on scientific grounds.

Benchmark tests were performed to determine the number of time, 'd', a single chain requires to be simulated by MC to obtain an acceptable absolute error. These tests were performed for a Bernoullian distribution since the analytical expression for the probability density function is known, enabling direct comparison with the chemical composition distribution determined by MC. Evidently, the computer's processor time *increases* but the absolute error *decreases* with increasing sample size as shown in Figure 3-2. In the case of a quad core processor the time required to simulate a chain $3.2 \cdot 10^6$ times is 5 s with an accuracy that allows for three digits.
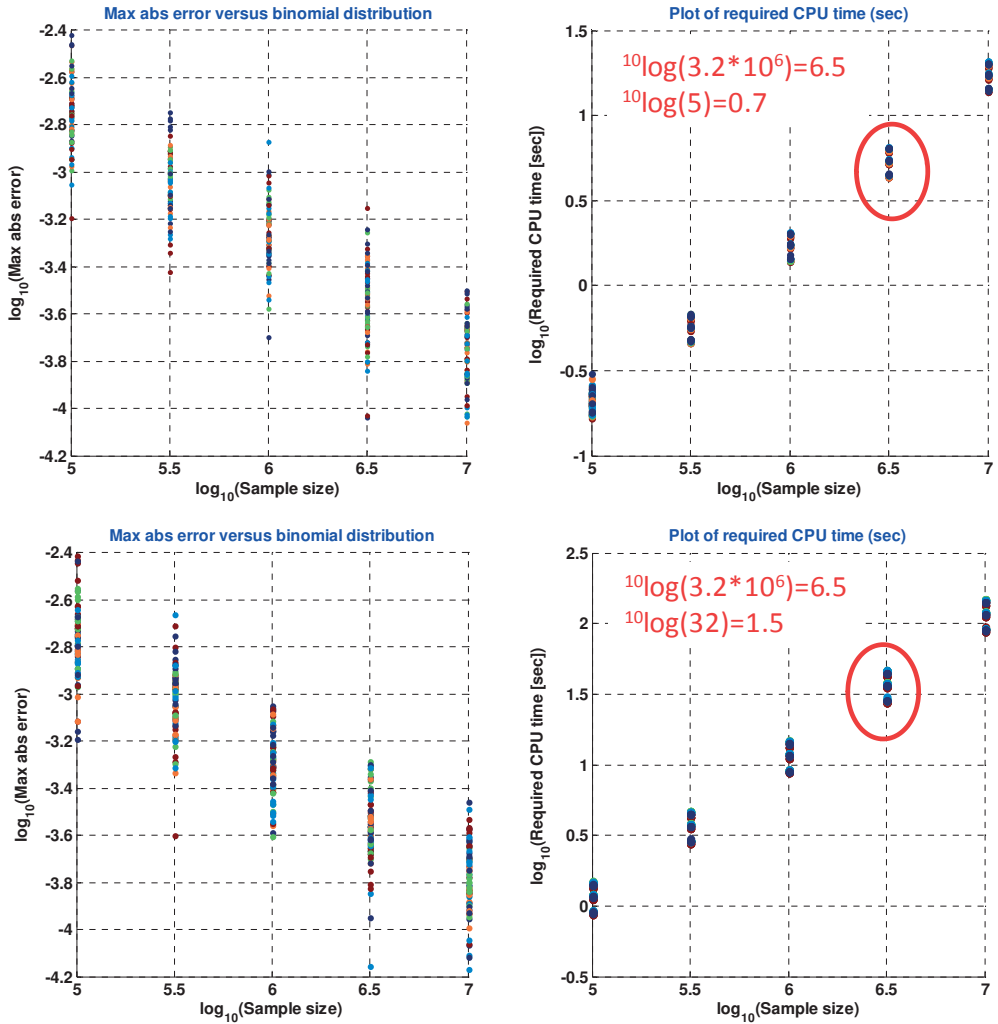
Figure 3-2. a) Benchmark LIME PC, 4 CPUs parallel, 3 GHz processor, 8 Gb RAM. b) Benchmark Dell PC, 1 CPU, 3GHz processor, 1 Gb RAM.

The method described here is captured in a flow chart, given in Figure 3-3. Important to mention is that the probability of the first unit is based on the feed composition.
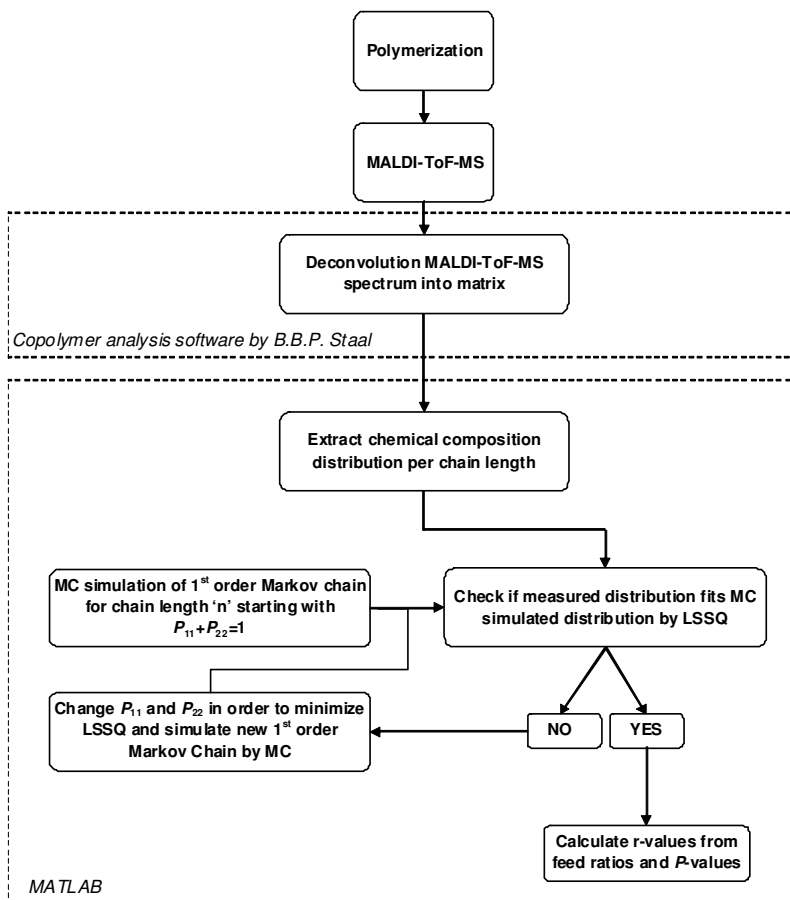
Figure 3-3. Flowchart of procedure to determine reactivity ratios by MALDI-ToF-MS.

3.2.2 The analytical solution

An expression in analytical form of a first order Markov chain can be considered a luxury as the derivation requires an extensive use of linear algebra and is certainly not straightforward. Van der Hofstad reported the derivation of the analytical solution in an internal note given on the CD-R in the back of this thesis.[**] In order to compute the probability mass function of a first order Markov chain, Van der Hofstad makes use of the Fourier theory.[22]

[**] Prof. Dr. R. van der Hofstad of the University of Technology Eindhoven, Department of Mathematics and Computer Science.

The main advantage of using Fourier transforms is their ability to relatively simple compute analytical formulas which otherwise are difficult to obtain. Tobita[23] performed a similar derivation, but made use of a probability generating function instead, which results in multiple differentiations in contrast to a single integral obtained by the method of Van der Hofstad. A summary of Van der Hofstad's derivation will be given here.[22]

A polymer chain is modeled by a Markov chain $\{X_n\}_{n=0}^{\infty}$ with state space $\{1,2\}$ and its defined Markov transition matrix:

$$P = \begin{pmatrix} P_{11} & 1 - P_{11} \\ 1 - P_{22} & P_{22} \end{pmatrix} \tag{3-1}$$

in which:

$$P_{ij} = P(X_{m+1} = j | X_m = i) \tag{3-2}$$

is a so-called transition probability, *i.e.* P_{ij} is the probability that the polymer chain moves from the current state s_i in the next step to state s_j. Now we want to compute for a polymer chain of length n+1, the probability mass function for the number of units of monomer 1 with $a \in \{1,2\}$:

$$f(m) = P_a^{(n)}(m) = \mathbb{P}_a(N_1(n) = m) \tag{3-3}$$

with $N_1(n)$ the sum of the number of monomer one in the chain:

$$N_1(n) = \sum_{i=0}^{n} \mathbb{1}_{(X_i=1)} \tag{3-4}$$

INTERMEZZO As mentioned before, Van der Hofstad makes use of the Fourier theory. Let $f : \mathbb{N} \to \mathbb{R}$, then its Fourier transform is given by:

$$\hat{f}(k) = \sum_{x=0}^{\infty} e^{ikm} f(m)$$

where i denotes the imaginary unit $i^2 = -1$. The power of Fourier transforms is that they allow for analytical computations that may otherwise be hard. For example, from the Fourier transform, $\hat{f}(k)$, the function f can be retrieved in a unique way using the Fourier inversion formula:

$$f(m) = \int_{-\pi}^{\pi} e^{-ikm} \hat{f}(k) \frac{dk}{2\pi}$$

Thus, in a certain sense, computing the Fourier transform of a function is equivalent to the computation of the function itself.[22]

We now describe such an application in order to compute the probability mass function of $N_1(n)$ using Fourier theory and linear algebra. We denote, for $k \in [-\pi, \pi]$, the characteristic function of $N_1(n)$, or the Fourier transform of its probability mass function, by

$$\hat{f}_a^{(n)}(k) = \sum_{m=0}^{n} e^{ikm} \mathbb{P}_a(N_1(n) = m) \tag{3-5}$$

Then, by the Fourier inversion theorem, we have that, for $m \in \{0, \dots, n\}$,

$$\mathbb{P}_a(N_1(n) = m) = \int_{-\pi}^{\pi} \hat{f}_a^{(n)}(k) e^{-ikm} \frac{dk}{2\pi} \tag{3-6}$$

in which:

$$\hat{f}_a^{(n)} = P_{a_1} \hat{f}_1^{(n-1)}(k) + P_{a_2} e^{ik} \hat{f}_2^{(n-1)}(k) = \hat{P}(k) \hat{f}^{(n-1)}(k) \tag{3-7}$$

where $\hat{f}^{(n-1)}(k)$ is a column vector $(\hat{f}_1^{(n-1)}(k), \hat{f}_2^{(n-1)}(k))^T$ (3-8) and $\hat{P}(k)$ a matrix:

$$\hat{P}(k) = \begin{pmatrix} P_{11} & (1 - P_{11})e^{ik} \\ 1 - P_{22} & P_{22}e^{ik} \end{pmatrix} \tag{3-9}$$

By iteration of 3-7 and the fact that $\hat{f}^{(0)}(k) = (1, e^{ik})^T$ we finally obtain:

$$\hat{f}_a^{(n)} = \hat{P}(k)^n \begin{pmatrix} 1 \\ e^{ik} \end{pmatrix}$$

(3-10)

Albeit a complex matrix, the software package MatLab 7.4.0[20] has no problem computing with it. A software application based on this mathematical package including the above mentioned calculations and a fitting procedure to the recorded CCD by MALDI-ToF-MS has been programmed by G.D. Mooiweer.[††] The input required is a matrix as described in Chapter 2, depicted in Figure 2-8. The interface of this program is given in Figure 3-4.
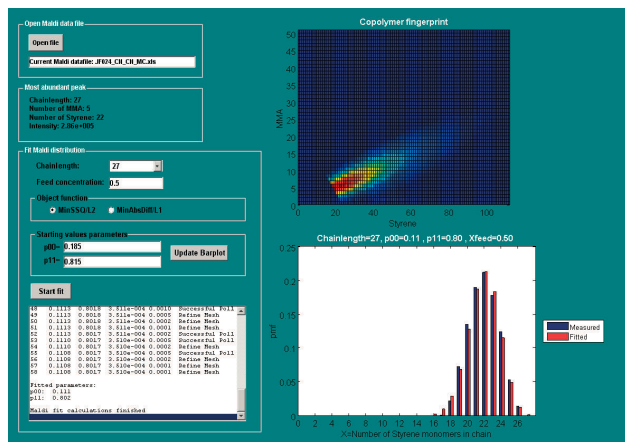
Figure 3-4. Interface of Markov analysis software developed by G.D. Mooiweer.

3.3 Free radical copolymerizations

Most reactivity ratios of comonomers reported are for copolymers formed via a free radical polymerization. The *Polymer Handbook*[24] reports a vast number of reactivity ratios for many comonomer pairs. Probably the most reported reactivity ratios are for the free radical copolymerization of styrene / methyl methacrylate (STY/MMA) and therefore this copolymer was included in our study. Next, we explored the copolymer of vinyl acetate and (meth)acrylates since the reactivity of these (meth)acrylates is much higher than of vinyl acetate, enabling us to explore our method's limits. Furthermore, copolymers of various (meth)acrylates and copolymers of (meth)acrylates and styrene obtained via free radical polymerization were studied. The polymerizations were performed at 60 or 70 °C using AIBN as initiator and 1-dodecanethiol as chain transfer agent. The spectra were analyzed using the method explained in Chapter 2.

[††] Ir. G.D. Mooiweer, guest lecturer of the University of Technology Eindhoven and Senior Consultant of the LIME institute.

The matrices thus obtained were plotted in a 2D surface contour plot and the results are depicted in Figure 3-5. The contour plots in Figure 3-5 are characteristic for free radical copolymerizations at low conversion ($\sim < 10\%$) for which the polydispersity is relatively high.
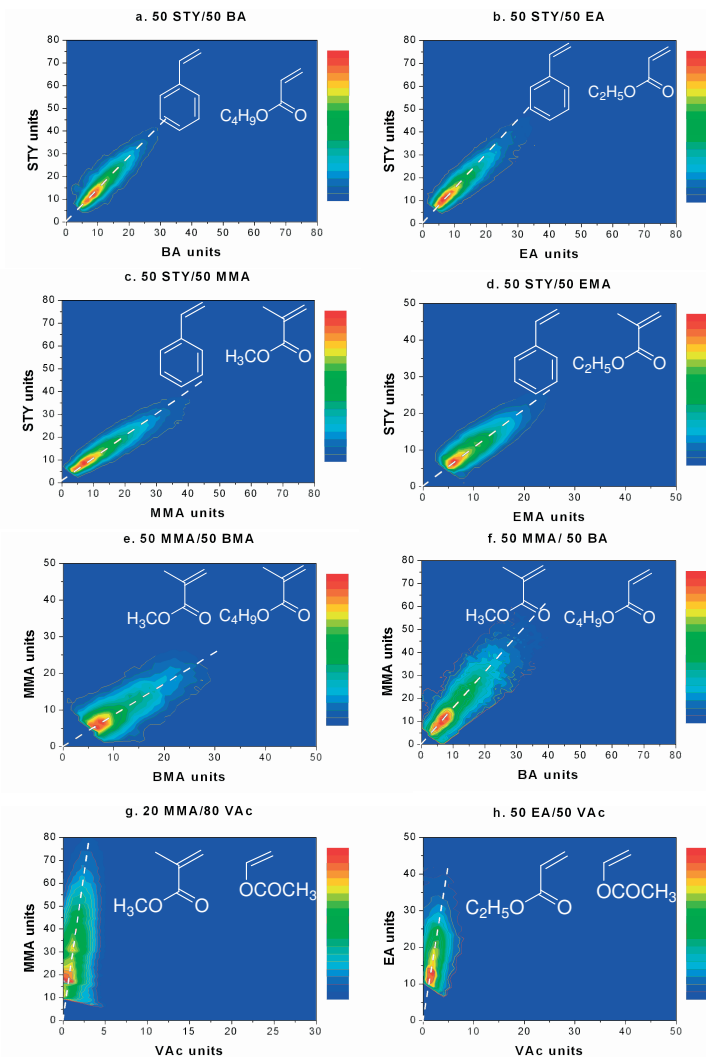
Figure 3-5. Contour plots of the deconvoluted MALDI-ToF-MS spectra of copolymers prepared via free radical polymerization: a) styrene/butyl acrylate, b) styrene/ethyl acrylate, c) styrene/methyl methacrylate, d) styrene/ethyl methacrylate, e) methyl methacrylate/butyl methacrylate, f) methyl methacrylate/butyl acrylate, g) methyl methacrylate/vinyl acetate, h) ethyl acrylate/vinyl acetate. The applied feed compositions for all comonomer pairs are 50 mol%/ 50 mol%; except for the comonomer pair MMA/VAc in which a feed composition is applied of 20 mol% / 80 mol% respectively.

The contour plots of the MMA/VAc and EA/VAc comonomer pairs lie steep and against the ordinate, clearly illustrating the much higher reactivity for MMA and EA compared to VAc. The combination of acrylates, methacrylates and styrene (Figure 3-5) resulted in more random to alternating copolymers, with a slightly higher reactivity for styrene compared to the acrylates and methacrylates. The copolymers of styrene and (meth)acrylates have a more narrow distribution than the copolymers synthesized from (meth)acrylates only, a correlation also expressed in the Stockmayer equation by the product of reactivity ratios $r_1 \cdot r_2$. The Stockmayer equation gives the relation between chemical composition and chain length for long chain lengths.[37] Direct comparison with our chemical compositions therefore is not advisable as our distributions deviate from a Gaussian and our chains are up to approximately 50 units long. Nevertheless, the influence on the width of the chemical composition distribution by an increase in reactivity ratios was also observed here (Figure 3-7a). To appoint discrete values for the reactivity ratios, the most abundant chain length is used, although it was found that in most cases negligible variations in the ratio were observed for less abundant chain lengths.[21] The obtained reactivity ratios for the comonomers in the different copolymers are given in Table 3-3 together with corresponding literature values reported for classical methods. Comparison of our results with these literature values evidently demonstrates the ability of our method to produce reasonably good point estimates, with the major advantage that our method is simple and very fast. The deviations observed can at least partly be explained by variations in the conditions applied during different studies.

Table 3-3. Reactivity ratios of free radical copolymerizations determined by MALDI-ToF-MS (gray background) compared to literature values.

T (^{o}C)	r_{STY}	r_{BA}	r_{STY}	r_{EA}
50	0.73	0.33[25]	0.79	0.15[26]
70	**0.79**	**0.21**	**0.85**	**0.20**
80			0.80	0.48[27]
T (^{o}C)	r_{STY}	r_{MMA}	r_{STY}	r_{EMA}
50			0.67	0.26[24]
55			0.62	0.35[28]
60	0.53	0.45[29]		
70			0.65	0.29[24]
70	**0.55**	**0.39**	**0.68**	**0.40**
T (^{o}C)	r_{MMA}	r_{BMA}	r_{MMA}	r_{BA}
50	0.91	1.09[30]		
60	0.79	1.27[31]	1.77	0.29[33]
70	0.96	1.04[32]		
70	**0.81**	**1.28**	**1.78**	**0.66**
T (^{o}C)	r_{MMA}	r_{VAc}	r_{EA}	r_{VAc}
30	28.60	0.04[34]		
60	20.0	0.015[35]	4.68	0.03[36]
60	**23.0**	**0.03**	**6.27**	**0.07**

The fact that the shapes of the contour plots in Figure 3-5 are symmetric indicates that there is little composition drift between different chain lengths, which was indeed confirmed by analysis of the composition for various chain lengths (Figure 3.6).[21]
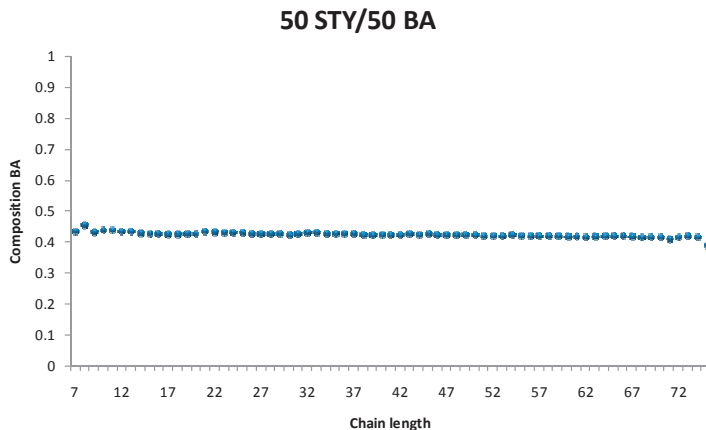
Figure 3-6. a) Composition versus chain length for the copolymer of styrene and butyl acrylate.
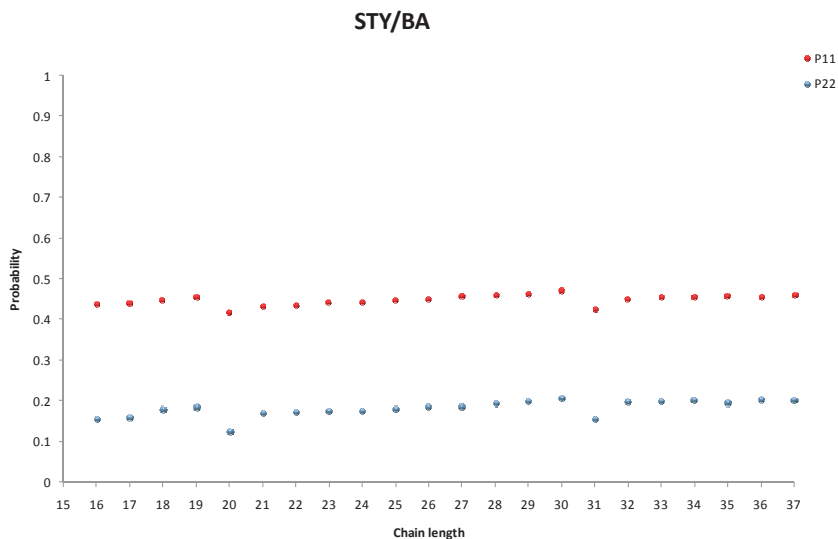
Figure 3-6. b) Homo-probabilities, P_{11} and P_{22} versus chain length for the copolymer of styrene and butyl acrylate.

Several of the recorded chemical composition distributions and the fitted distributions by employing the Monte Carlo method followed by a LSSQ fit are shown in Figure 3-7 for different systems. The chemical composition distributions for other systems are given in the Appendix.
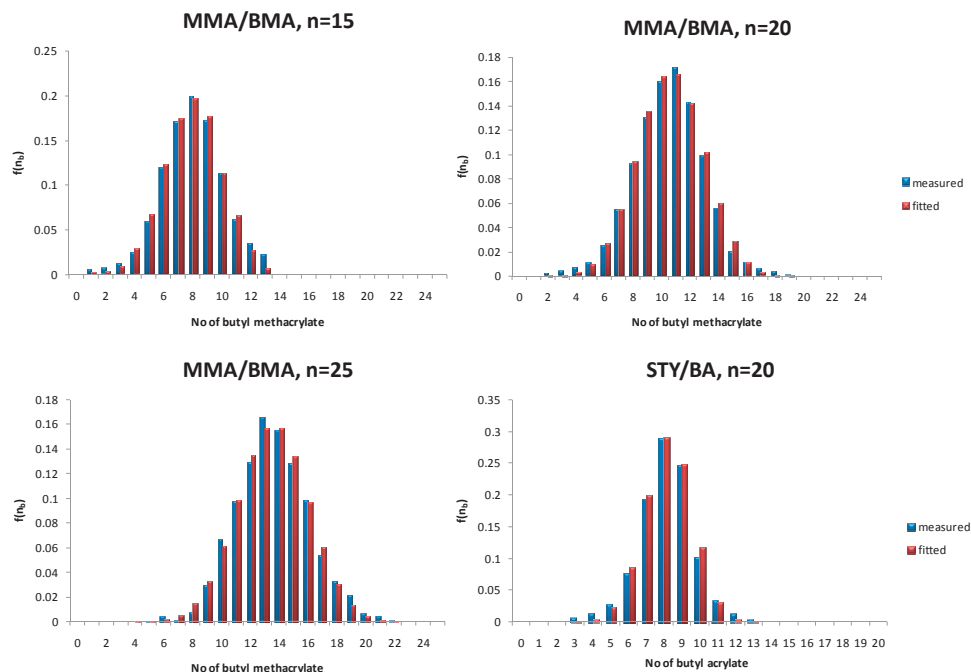
Figure 3-7a. Chemical composition distributions recorded (—) and fitted by using the Monte Carlo method followed by minimizing the SSQ (—) for chain lengths 15, 20 and 25 for the copolymer synthesized by methyl methacrylate and butyl methacrylate. Chemical composition distributions recorded and fitted for the system styrene/butyl acrylate of the most abundant chain length.

3.4 Ring-opening copolymerizations

Typical examples of copolymers obtained by ring-opening polymerization are copolymers of lactides and lactones or for example the combination of epoxides and anhydrides. Lactides and lactones have recently gained increasing interest due to their biocompatibility and biodegradability, which make them suitable for in vivo medical devices. The exact microstructure and chemical composition of such copolymers is a highly important parameter due to its reflectance on the physical properties. Reliable reactivity ratios for the various comonomers of this class of copolymers would be highly desirable to pre-define the copolymer's composition. The number of reactivity ratios for these systems reported in literature is, however, limited. A probable reason might be that transesterification, which often occurs as a competing side reaction, dramatically complicates the determination of the reactivity ratios. Hence, to obtain reliable reactivity ratios it is of importance to record MALDI-ToF-MS spectra in the beginning of the reaction at low conversion when transesterification is absent or limited.

The lactide monomer can give insight into the amount of transesterification by formation of isolated -OCH(Me)C(=O)- sequences, which cannot be formed by propagation.[13,14] The presence of such sequences obviously reveals the ability of the catalyst to transesterify at the temperature applied. Another indication of transesterification is the formation of cyclic structures, which are also easily detectable by MALDI-ToF-MS.

For this study we prepared several copolymers. To minimize the influence of the catalyst (*e.g.* steric hindrance) on the reactivity ratios, Sn(Oct)$_2$ was used as catalyst. The comonomer pairs used were ε-caprolactone / 4-methyl-ε-caprolactone, ε-caprolactone / 1,5-dioxepan-2-one, ε-caprolactone / trimethylene carbonate, 1,5-dioxepan-2-one / δ-valerolactone, 1,5-dioxepan-2-one / lactide and finally ε-caprolactone / lactide. The contour plots obtained from the deconvoluted spectra are given in Figure 3-8. The point estimates of the reactivity ratios obtained by our Monte Carlo simulation method and the values reported in literature for the diverse comonomer pairs are given in Table 3-4.
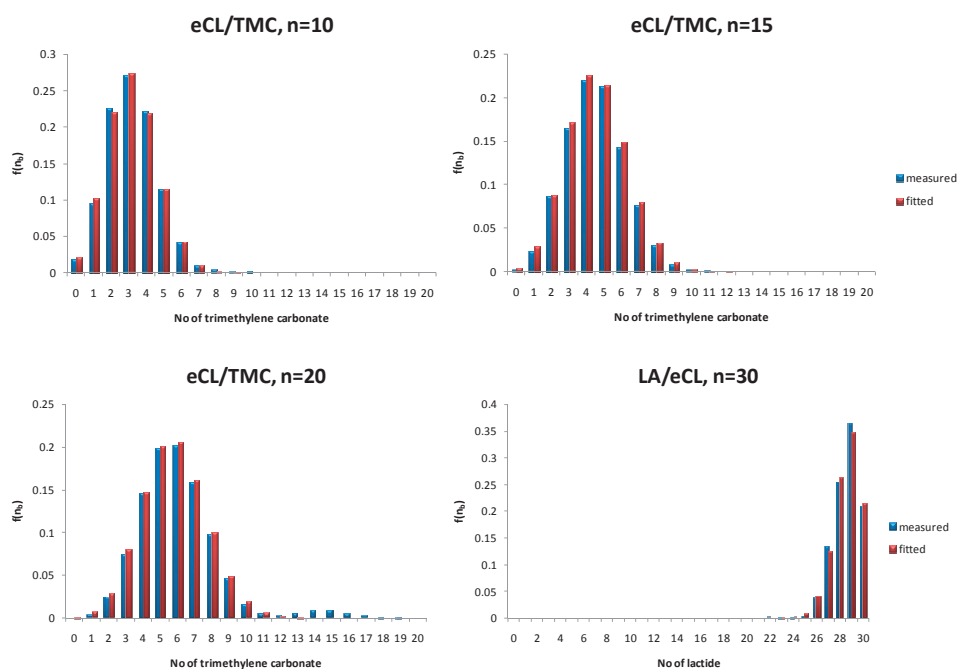
Figure 3-7b. Chemical composition distributions recorded (—) and fitted by using the Monte Carlo method followed by minimizing the SSQ (—) for chain lengths 10, 15 and 20 for the copolymer synthesized by ε-caprolactone and trimethylene carbonate. Chemical composition distributions recorded and fitted for the system lactide/ε-caprolactone of the most abundant chain length.
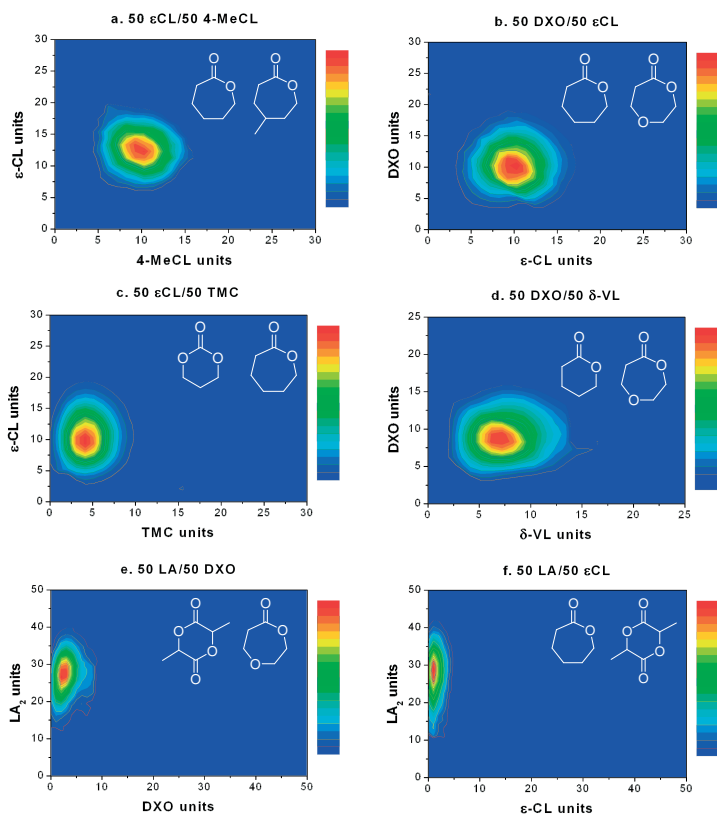
Figure 3-8. Contour plots of the deconvoluted MALDI-ToF-MS spectra of copolymers prepared via ring-opening polymerization: a) *ε*-caprolactone/4-methyl-*ε*-caprolactone, b) *ε*-caprolactone/1,5-dioxepan-2-one, c) *ε*-caprolactone/trimethylene carbonate, d) *δ*-valerolactone/1,5-dioxepan-2-one, e) lactide/1,5-dioxepan-2-one, f) lactide/*ε*-caprolactone. The applied feed compositions for all comonomer pairs are 50 mol%/ 50 mol%.

Table 3-4. Reactivity ratios of ring-opening copolymerizations determined by MALDI-ToF-MS (gray background) compared to literature values.

T(°C)	r_{CL}	r_{MeCL}	r_{DXO}	r_{CL}	r_{CL}	r_{TMC}
25	1.5	0.6[38]				
60			1.3	0.9[40]		
100					2.41	0.20[43]
100					2.70	0.38[43]
110			1.6	0.6[41]		
110					**2.13**	**0.39**
130	**1.1**	**0.8**	**1.22**	**0.68**		
T(°C)	r_{DXO}	r_{VL}	r_{LA}	r_{DXO}	r_{LA}	r_{CL}
70					17.9	0.58[38]
80					57.1	0.39[44]
90					14.4	0.36[45]
110	2.3	0.5[39]			42.0	0.36[44]
115			10	0.1[42]		
130					34.7	0.24[44]
130	**1.6**	**0.8**	**7.95**	**0.10**	**18.8**	**0.04**
150					44	0.28[46]

As can be seen, the shape of the plots for the ring-opening copolymerizations is very different compared to the plots of the copolymers synthesized by free radical polymerizations. This is the result of a difference in total chain length distribution due to the copolymerization mechanism. The total chain length in case of free radical polymerization has a Schultz-Flory type of distribution that is analogous to a step growth reaction while the ring-opening polymerization exhibits a Poisson-like distribution in analogy to living polymerizations, *i.e.* a more cigar-like plot in case of free radical polymerization and a more oval to circular plot for ring-opening polymerization. This circular shape complicates the determination of the copolymer's microstructure since the distinction with a block copolymer can no longer be made without knowing the history of synthesis (see Chapter 2). The copolyesters synthesized from ε-caprolactone / 4-methyl-ε-caprolactone and ε-caprolactone / 1,5-dioxepan-2-one are close to a perfectly random system $\sim r_1 \cdot r_2 = 1$. Vion *et al.*[38] reported r-values of a similar system in which ε-caprolactone was reacted with another isomer of the methyl-substituted ε-caprolactone (ε-methyl-ε-caprolactone) and their findings are in good agreement with ours. Trimethylene carbonate has a lower reactivity compared to ε-caprolactone resulting in long sequences of subsequent ester functionalities. Using the Fineman-Ross and Kelen-Tüdös approach, Albertsson and Eklund found similar values for the reactivity ratios of these comonomers using the same catalyst.[43] The polymerizations of lactide with 1,5-dioxepan-2-one or ε-caprolactone tend to make lactide homopolymer. Although, the reactivity ratios for ε-caprolactone and lactide reported in literature are widely scattered, in agreement with our observation most of them show a much higher reactivity of lactide. The fact that no [-OCH(Me)C(=O)-] fragments were formed excludes interference of transesterification reactions.[13,14] Surprisingly, Hiljanen-Vainio *et al.* reported values of $r_{LA} = 1.22$ and $r_{CL} = 0.64$, implying a close to perfectly random microstructure.[47]

However, these values were determined for high conversions. Faÿ *et al.* also reported a much smaller difference in reactivity ratios between lactide and ε-caprolactone using Ti(OBu)$_4$ as catalyst, which also happens to be a well-known transesterifying agent.[48] It is assumed that both deviating values for the reactivity ratios are the result of competing transesterification processes. Transesterification makes the contour plots more cigar shaped like as can be seen in the Figure 3-9 due to a broadening of polydispersity. Calculation of reactivity ratios of these plots would lead to incorrect r-values. Therefore it is crucial to determine the reactivity ratios only using polymerization conditions where transesterification is rather slow and record the spectra at low enough conversion when transesterification is not yet significant.
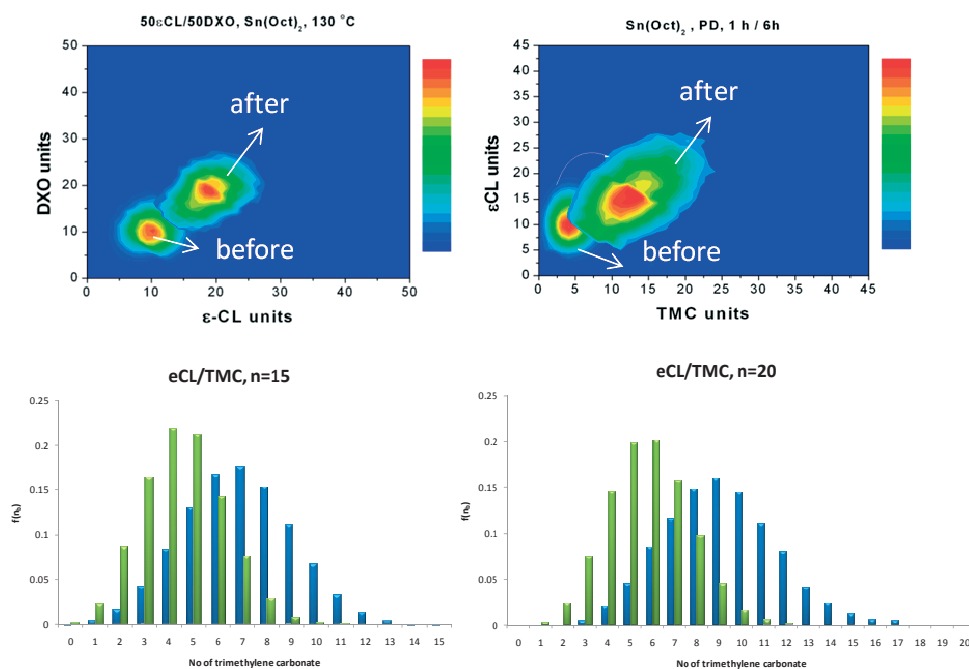
Figure 3-9. Contour plots before (original plot used to calculate r-values) and after transesterification. Transesterification causes a randomization of the polymer which can be observed by comparison of the contour plots before and after transesterification. The chemical composition distribution for chain lengths 15 and 20 of the copolymer synthesized from ε-caprolactone and trimethylene carbonate before (—) and after transesterification (—). A clear shift to a higher TMC content as a result of transesterification can be observed.

Another interesting ring-opening reaction is the reaction between oxiranes (M_1) and anhydrides (M_2).[49] This system illustrates two special situations that can occur for copolymerizations, *i.e. i)* a perfectly alternating incorporation of both monomers ($P_{11} = 0$, $P_{22} = 0$) or *ii)* a subsequent incorporation of exclusively one of the two comonomers ($P_{11} > 0$, $P_{22} = 0$). A purely alternating incorporation of both monomers leads to a polyester. Depending on the oxirane – anhydride combination and the catalyst applied, subsequent incorporations of oxiranes ($P_{11} > 0$) can occur, which results in a poly(ester-*co*-ether). Conversely, sequential incorporation of anhydrides is generally not observed for these systems, which corresponds to an anhydride homo-propagation probability of $P_{22} = 0$. Contour plots of a purely alternating system (cyclopropane anhydride – cyclohexene oxide) and a system in which ether bonds co-exist (succinic anhydride – cyclohexene oxide) are given in Figure 3-10. The perfectly alternating copolymer corresponds to a $P_{11} = 0$ and $P_{22} = 0$, whilst the poly(ester-*co*-ether) corresponds to a $P_{11} > 0$ for the oxirane and a $P_{22} = 0$ for the anhydride. As expected, the contour plot of the alternating copolymer is a line at the diagonal, although the anhydride monomer can exceed the oxirane monomer by one unit as a chain can start and end with an anhydride unit. Since cyclopropane anhydride and cyclohexene oxide afford a perfectly alternating copolymer, the reactivity ratios for these monomers are by definition equal to 0. The contour plot for the poly(ester-*co*-ether) is cut off at the diagonal, which is the cross over point from an excess of the first monomer to an excess of the second monomer. From this plot it is clear that a random poly(ester-*co*-ether) is formed. This will be discussed in more detail in Chapter 5.
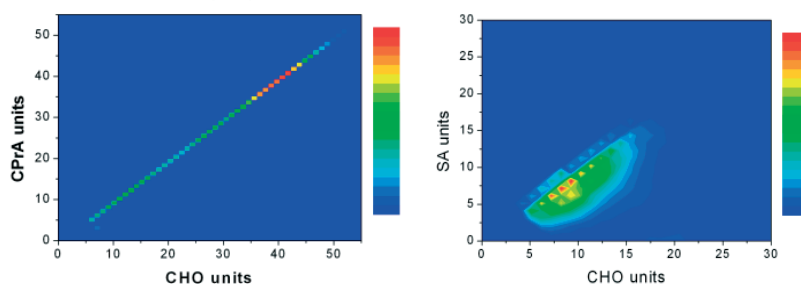
Figure 3-10. Contour plots, *Left:* Cyclohexene oxide copolymerized with 1,3-cyclopropane dicarboxylic acid anhydride resulted in a purely alternating polyester. *Right:* Cyclohexene oxide copolymerized with succinic anhydride resulted in a poly(ester-*co*-ether).

3.5 Comparison of Recorded, Monte Carlo and Analytical chains

An additional prove of the correctness of the computations performed is in any case advisable and desirable. Comparison of the mean and variance calculated directly from the recorded distribution by the mean and variance of the numerically determined Markov chain by Monte Carlo is possible by filling out the values for the homo-propagations in the analytical formulas for the mean and variance of a first order Markov chain. Tobita[23] reported part of the derivation of a first-order Markov chain and was able to express the mean and variance of the probability density function in terms of the propagation probabilities, see equations 3-11 and 3-12. However, the mean reported by Tobita misses an additional term and describes actually the binomial case as can be understood from the equations derived by Bogartz[50], 3-13 and 3-14.

$$\overline{m_n} = \frac{nP_{21}}{P_{12}+P_{21}} \tag{3-11}$$

$$V_m = \frac{P_{12}P_{21}}{(P_{12}+P_{21})^4}\{2(n+1)(P_{12}+P_{21}) - n(P_{12}+P_{21})^2 + 2(1 - P_{12} - P_{21})^{n+1} - 2\} \tag{3-12}$$

$$ETN = Nq_\infty - d(1 - s^N)(1 - s)^{-1} \tag{3-13}$$

$$Var(T_N) = E(T_N)[1 - E(T_N)] + 2P_{22}E(U_{1,N-1}) + 2\{q_\infty[(N-1)E(U_{1,N-2}) - \alpha(2)] - (q_\infty - P_{22})s(1 - s)^{-1}[E(U_{1,N-2}) - q_\infty s(1-s)^{-1}(1 - s^{N-2}) + (N-2)ds^{N-2}]\} \tag{3-14}$$

in which $q_\infty = P_{12}(P_{12} + P_{21})^{-1}$, $s = P_{11} - P_{21}$, $d = q_\infty - q_1$, $q_n = q_\infty - ds^{n-1}$ and N is the length of the polymer chain. Instantly, it becomes clear that the first term Nq_∞ equals the equation given by Tobita. Nevertheless, Tobita's formula appeared for the given cases to be a good approximation as the last term of Bogartz equation for these given systems is small. A comparison study was performed for the chain lengths given in the Appendix. The weighted mean and variance directly calculated from the recorded chain lengths are reported in Table 3-5 along with the mean and variance calculated from equations 3-11, 3-12 and 3-13, 3-14.

Table 3-5. Comparison of mean and variance of recorded CCD with the mean and variance of a true analytical Markov Chain.

Pair		N	Probabilities		Markov Chain Tobita		Markov Chain Bogartz		Recorded	
ROP			P_{11}	P_{22}	Mean	Variance	Mean	Variance	Mean	Variance
CL	MCL	18	0.51	0.40	8.09	3.76	8.00	3.82	8.03	3.39
CL	DXO	20	0.42	0.50	10.74	4.27	10.74	4.27	10.90	4.19
CL	TMC	15	0.69	0.28	4.51	2.98	4.51	2.98	4.34	2.79
VL	DXO	15	0.47	0.57	8.28	4.00	8.28	4.00	8.28	4.23
DXO	LA	20	0.14	0.92	18.30	1.75	18.27	1.77	17.09	2.89
CL	LA	30	0.03	0.95	28.53	1.35	28.54	1.34	28.55	1.29
Free radical										
STY	BA	20	0.41	0.12	8.03	1.84	8.00	1.83	8.11	2.36
STY	EA	20	0.45	0.17	7.97	2.25	7.94	2.25	7.73	2.31
STY	MMA	19	0.37	0.28	8.87	2.37	8.86	2.37	8.71	2.14
STY	EMA	16	0.38	0.32	7.63	2.24	7.63	2.24	7.65	2.25
MMA	BMA	15	0.48	0.55	8.04	3.95	8.04	3.95	7.99	4.73
MMA	BA	20	0.62	0.42	7.91	5.16	7.92	5.16	7.46	4.27
VAc	MMA	18	0.18	0.82	14.76	2.66	14.76	2.66	14.95	2.39
VAc	EA	15	0.08	0.86	13.02	1.54	13.04	1.52	13.04	1.49

The variation in the mean is less than the variation in the variance. Furthermore, the mean and variance calculated for ring-opening are more accurate than for free radical. This can be related to the fact that the intensity recorded for polymers obtained by ring-opening is much higher due to their better ionization efficiency compared to acrylates and copolymers with styrene.

A comparison study of the homo-propagation probabilities obtained by MC and by fitting the analytical solution has been performed on the chain lengths reported in Table 3-6. As expected the analytically computed Markov chain gives very similar to identical values for the propagation probabilities as the Monte Carlo method. However, the analytical method is much faster (2-3 orders of magnitude) than the Monte Carlo simulations and very accurate. With the availability of the analytical solution of the first order Markov chain it is now possible to compute highly accurate reactivity ratios based on the analysis of a large span of chain lengths in a very short time.

Table 3-6. Comparison of homo-propagation probabilities determined by MC and by the analytical solution by fitting to a first order Markov chain.

Pair		N	Probabilities MC		Probabilities Analytical	
ROP			P_{11}	P_{22}	P_{11}	P_{22}
CL	MCL	18	0.51	0.40	0.51	0.40
CL	DXO	20	0.42	0.50	0.41	0.50
CL	TMC	15	0.69	0.28	0.70	0.27
VL	DXO	15	0.47	0.57	0.47	0.57
DXO	LA	20	0.14	0.92	0.07	0.93
CL	LA	30	0.03	0.95	0.1	0.97
Free radical			P_{11}	P_{22}	P_{11}	P_{22}
STY	BA	20	0.41	0.12	0.41	0.12
STY	EA	20	0.45	0.17	0.47	0.15
STY	MMA	19	0.37	0.28	0.37	0.26
STY	EMA	16	0.38	0.32	0.37	0.32
MMA	BMA	15	0.48	0.55	0.48	0.55
MMA	BA	20	0.62	0.42	0.62	0.41
VAc	MMA	18	0.18	0.82	0.19	0.85
VAc	EA	15	0.08	0.86	0.09	0.89

3.6 Confidence intervals for r-values

The r-values determined for all the systems have good point estimates as we have shown but without a standard error and confidence intervals, one cannot give a verdict on the accuracy of this method. The error in the reactivity ratios depends on the accuracy of the balance with which the feed ratios were weighed in, but also on the error in propagation probabilities. The latter is determined by an error in the recording of the actual MALDI-ToF mass spectra but also by an error in fitting of the first order Markov chain. In order to determine confidence intervals, multiple MALDI-ToF-MS spectra of the same polymer on the same spot on the sampling target plate were recorded (for the spectrum of 50 mol% ε-caprolactone / 50 mol% 4-methyl-ε-caprolactone) and subjected to the procedure of determining propagation probabilities by MC. In addition, these fifteen spectra were used to create an approximating distribution f(x, N(x,n-x)) for each number of monomer residue within a certain chain length, which was applied as re-sampling source for statistical bootstrapping.[‡‡]

[‡‡] This bootstrapping is a statistical method and should not be confused with the bootstrap effect reported by Harwood on the apparent reactivity ratios.[51]

The bootstrap method is a re-sampling method capable of determining standard errors of point estimators with an unknown standard error. The number of random sampling from the empirically determined distribution equalled 150 for each number of monomers M_2 in the chemical composition distribution for the most abundant chain length of 23. The areas (intensity) recorded for the fifteen spectra for 8-18 residues of M_2 for chain length 23 are listed in the appendix on the CD-R. These fifteen recorded areas of the numbers of monomer residues M_2 were tested to be normally distributed. The individual bootstrap samples for the number of monomers constituting the chemical composition distribution of chain length 23, were reconstructed to 150 new chemical composition distributions by using the covariance matrix which is given in the appendix. In Figure 3-11, the blue dots represent the probabilities calculated for the fifteen recorded chemical composition distributions for chain length 23 and the red dots represent the 150 propagation probabilities determined by bootstrapping.
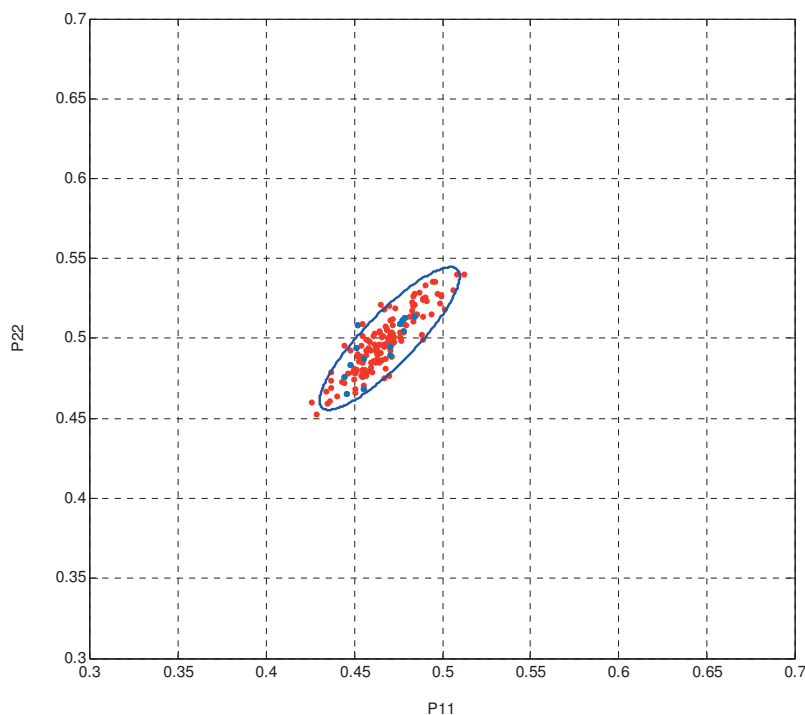

Figure 3-11. 95% Joint confidence interval for the homo-propagation probabilities determined from the most abundant chain length of n=23.

The bootstrap standard errors are given in Table 3-7 along with the lower and upper confidence intervals. As can be seen, an error of less than 5% is obtained.

Table 3-7. Confidence intervals determined by statistical bootstrapping.

		Asymptotic Standard Error	Confidence Interval	
	Estimate		*Lower*	*Upper*
P_{11}	0.47	0.016	0.434	0.499
P_{22}	0.50	0.018	0.461	0.534

3.7 Discussion and Conclusion

The data obtained for the reactivity ratios were surprising in the sense that we were expecting much larger deviations as a result of the neglect of transfer, initiation and termination effects since the chains we are taking into consideration do not surpass a length of more than 50 units. It was expected that chain termination and initiation would be profound in these relatively short chains resulting in r-values diverting from literature reported. However, the r-values in any case of free radical and ring-opening were at least in the same order of magnitude and often even within the joint confidence intervals reported for these r-values. This is in conflict with the long chain theorem which is a prerequisite for the Mayo-Lewis equation.

An intrinsic MALDI-ToF-MS problem is differences in ionization efficiency both in mass as in composition. This requires cautiousness and more research into different feed compositions. A polymer chain richer in one of the monomers can ionize better or worse than another polymer chain with less of that monomer. The ultimate way to test the applicability of the method is to investigate whether the obtained reactivity ratios can indeed be used to pre-define a copolymer's composition. For this study we used the ε-caprolactone/1,5-dioxepan-2-one system. The reactivity values ($r_{DXO} = 1.2$, $r_{CL} = 0.7$) were obtained for a 50 mol%/50 mol% mixture of the two comonomers. Based on these reactivity ratios a feed composition of 30 DXO : 70 eCL should result in a copolymer with a composition of 37 DXO : 63 eCL monomer residues. The actual composition for the most abundant chain length was indeed found to be 37 mol%, which exactly corresponds with the predicted composition. Keeping the abovementioned discussion in mind, one can expect that a strong variation in ionization efficiency with varying composition might result in inaccurate predictions for other compositions of a certain comonomer pair.

With an eye on the instantaneous composition versus conversion, one would expect a great difference in MALDI-ToF-MS spectra taken over time in terms of composition, especially for a system like methyl methacrylate and vinyl acetate (Figure 3-12). However, the spectra recorded at the beginning and end of the polymerization appeared to be identical. This most likely is the result of mass discrimination by using this analytical tool. The chains recorded are the lower molar mass chains,

which are the result of early termination. Fortunately, as mentioned earlier, phenomena like initiation and termination do not seem to have a great influence on the reactivity ratios determined, especially when looking at it from an engineering point of view.
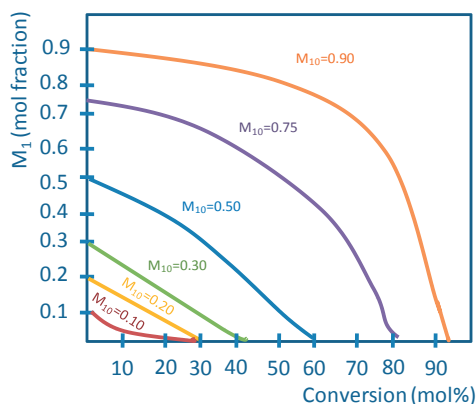
Figure 3-12. The effect of conversion on the change of the instantaneous comonomer composition at various initial feed compositions for the comonomer pair methyl methacrylate / vinyl acetate. M_1 is MMA and M_2 is VAc.[1]

MMA / VAc was the only system where we deviated from an initial feed composition of 50/50. The starting composition used was 80 VAc / 20 MMA, purely chosen from an experimental strategic point of view. The propagation rate coefficient of VAc is higher than for MMA, making the time slot of sampling within a conversion of 10% for this feed composition more difficult, but the probability of finding VAc units higher. As previously mentioned, the MALDI-ToF-MS spectrum taken for different time intervals did not change, which can be a practical advantage of this analytical technique for this particular situation although generally discrimination effects are not desirable. The feed composition of 50/50 for this pair was employed in the synthesis of a regular free radical reaction (*i.e.* without the presence of a chain transfer agent) for which a spectrum only in the linear mode could be obtained. Calculation of the CCDs and their fits resulted in 'spot on' r-values. Notwithstanding that a fit on a peak without isotope distribution is dangerous; apparently even spectra recorded in linear mode in some cases can give insight into this kind of parameters.

The P-values determined as a function of the degree of polymerization only were consistent for the most abundant chains. The least abundant chains in several cases even gave P-values of 0. This has not only to do with the abundance but also with the detection limit of the MALDI equipment. Certain recorded chain length distributions are consisting of only peaks corresponding to combinations that have just enough abundance to be detected (see appendix on CD-R). A fit on these chains will not give the correct probabilities.

Evidently the signal to noise ratio is also more obtrusive for these chains complicating the fitting procedure even more. These effects are more profound for CCDs which are not smeared out over a larger *m/z* range of the spectrum, reminding Figures 2-6 and 2-7, like for example in the case of styrene/MMA. Therefore, we have used the most abundant chains to calculate the reactivity ratios, but one might take into account an individual weighing scheme according to the abundance of the different chain lengths which can be obtained from the total chain length distribution.

The method as presented in this chapter is certainly not considered as the Holy Grail to determine r-values. It was merely an attempt to investigate the possibility to do so. Evidently, a more extensive investigation on the method's limitations is required related to different feed compositions and different propagation rates. More feed compositions for the same comonomer pair have to be examined as well as multiple systems with similar r-values but different propagation rates to establish a better understanding of the relation between CLD and CCD. Nevertheless, we might conclude that a single MALDI-ToF-MS spectrum can be used to obtain not only a good idea about a polymer's total chain length distribution, microstructure and composition, but in addition can give a surprisingly good estimate of reactivity ratios. In this respect MALDI-ToF-MS is a unique analytical tool. This can result in an enormous time profit and minimization of tedious laboratory work. Further research is in progress to fit in a single step the complete matrix and to develop this method to a routine procedure which is not unthinkable considering the development of computer memory over the last decades and the forthcoming ones.

3.8 Experimental Section

Reagents. *Free radical:* Monomers were purified by conventional methods. 2,2'-azobis(isobutyronitrile) (AIBN) was recrystallized from methanol. 1-Dodecanethiol (DDT) was used without further purification and purchased from Aldrich. *Ring-opening:* 1,5-dioxepan-2-one and 4-methyl-ε-caprolactone were prepared according to literature procedures.[52,53] D-Lactide was a gift from Purac. ε-Caprolactone, δ-Valerolactone and Tin (II) 2-ethylhexanoate (Sn(Oct)$_2$) were purchased from Aldrich. The data of the copolymerization of trimethylene carbonate and ε-caprolactone are reported elsewhere.[54]

Synthesis. *Free radical:* A mixture of comonomers (6 mmol) in required molar ratio, initiator AIBN and chain transfer agent DDT (in a molar ratio of 500:10:1 respectively) was reacted in a 1.5 mL crimp lid vial placed into an aluminum heating block at 60 or 70 ^{o}C. Prior to reaction, the mixture was deoxygenated by carefully flushing with Argon for a few minutes. Crude samples were taken with an interval of 30 s to undergo immediate MALDI-ToF-MS analyses. *Ring-opening:* A mixture of comonomers (10 mmol) in required molar ratio and a drop of Sn(Oct)$_2$ was reacted in a 1.5 mL crimp lid vial placed into an aluminum heating block at 130 ^{o}C. Crude samples were taken with an interval of 5 minutes to undergo immediate MALDI-ToF-MS analyses.

MALDI-ToF-MS Analysis. MALDI-ToF-MS analysis was performed on a Voyager DE-STR from Applied Biosystems equipped with a 337 nm nitrogen laser. An accelerating voltage of 25 kV was applied. Mass spectra of 1000 shots were accumulated. The polymer samples were dissolved in THF at a concentration of 1 mg·mL^{-1}. The cationization agent used was potassium trifluoroacetate (Fluka, >99%) dissolved in THF at a concentration of 5 mg·mL^{-1}. The matrix used was trans-2-[3-(4-tert-butylphenyl)-2-methyl-2-propenylidene]malononitrile (DCTB) (Fluka) and was dissolved in THF at a concentration of 40 mg·mL^{-1}. Solutions of matrix, salt and polymer were mixed in a volume ratio of 4:1:4, respectively. The mixed solution was hand-spotted on a stainless steel MALDI target and left to dry. The spectra were recorded in the reflector mode as well as the linear mode.

References

[1]   C. Hagiopol, *Copolymerization*, *'Towards a systematic approach'*, Kluwer Academic, **1999**.

[2]   A.M. van Herk, T. Dröge, *Macromol. Theory Simul.* **1997**, *6*, 1263.

[3]   M. Fineman, S.D. Ross, *J. Polym. Sci., Part A: Polym. Chem.* **1950**, *5*, 259.

[4]   P.W. Tidwell, G.A. Mortimer, *J. Polym. Sci., Part A: Polym. Chem.* **1965**, 3, 369.

[5]   V. Jaacks, *Makromol. Chem.* **1972**, *161*, 161.

[6]   T. Kelen, F. Tüdös, *J. Macromol. Sci. Chem.* **1975**, *A9*, 1.

[7]   F. Tüdös, T. Kelen, T. Földes-Berezsnich, B. Turcsányi, *J. Macromol. Sci. Chem.* **1976**, *A10*, 1513.

[8]   C.A. Barson, D.R. Fenn, *Eur. Polym. J.* **1989**, *25*, 719.

[9]   M. Dubé, R.A. Sanayei, A. Penlidis, K.F. O'Driscoll, P.M. Reilly, *J. Polym. Sci., Part A: Polym. Chem.* **1991**, *29*, 703.

[10]   R. Mao, M.B. Huglin, *Polymer* **1994**, *35*, 3525.

[11]   D.R. Burfield, C.M. Savariar, *J. Polym. Sci., Polym. Lett. Ed.* **1982**, *20*, 515.

[12]   A. Rudin, K.F. O' Driscoll, M.S. Rumack, *Polymer* **1981**, *22*, 740.

[13]   S. Huijser, B.B.P. Staal, J. Huang, R. Duchateau, C.E. Koning, *Angew. Chem. Int. Ed.* **2006**, *45*, 4104.

[14]   S. Huijser, B.B.P. Staal, J. Huang, R. Duchateau, C.E. Koning, *Biomacromolecules* **2006**, *7*, 2465.

[15]   M.S. Montaudo, A. Ballistreri, G. Montaudo, *Macromolecules* **1991**, *24*, 5051.

[16]   K.G. Suddaby, K.H. Hunt, D.M. Haddleton, *Macromolecules* **1996**, *29*, 8642.

[17]   R.X.E. Willemse, A.M. van Herk, *J. Am. Chem. Soc.* **2006**, *128*, 4471.

[18]   F.R. Mayo, F.M. Lewis, *J. Am. Chem. Soc.* **1944**, *66*, 1594.

[19]   F.P. Price, *J. Chem. Phys.* **1962**, *36*, 209.

[20]   Software from www.mathworks.com.

[21]   See CD-R for Appendix.

[22]   R. van der Hofstad, internal communications, 11 November **2008**.

[23]   H. Tobita, *Polymer* **1998**, *39*, 2367.

[24]   J. Brandrup, E.H. Immergut, *Polymer Handbook*, 3d ed., John Wiley&sons, **1989**.

[25]   M. Fernández-García, M. Fernández-Sanz, E.L. Madruga, R. Cuervo-Rodriguez, V. Hernández-Gordo, M.C. Fernández-Monreal, *J. Polym. Sci., Part A: Polym. Chem.* **2000**, *38*, 60.

[26]   A. Fehérvári, T. Földes-Berezsnich, F. Tudos, *J. Macromol. Sci.: Chem.* **1982**, *A18*, 337.

[27]   L.J. Young, *J. Pol. Sci.* **1961**, *54*, 411.

[28]   T.P. Davis, K.F. O' Driscoll, M.C. Piton, M.A. Winnik, *Macromolecules* **1990**, *23*, 2113.

[29]   J.F. Kuo, C.Y. Chen, *J. Appl. Polym. Sci.* **1982**, *27*, 2747.

[30]   B.G. Manders, W. Smulders, A.M. Aerdts, A.M. van Herk, *Macromolecules* **1997**, *30*, 322.

[31] J.C. Bevington, D.O. Harris, *J. Polym. Sci., Polym. Lett. Ed.* **1967**, *5*, 799.

[32] A.S. Brar, G.S. Kapur, *Polymer J. (Tokyo)* **1988**, *20*, 811.

[33] M.A. Dubé, A. Penlidis *Polymer* **1995**, *36*, 587.

[34] J.N. Atherton, A.M. North, *Trans. Faraday Soc.* **1962**, *58*, 2049.

[35] F.R. Mayo, C. Walling, F.M. Lewis, W.F. Hulse, *J. Am. Chem. Soc.* **1948**, *70*, 1523.

[36] A.S. Brar, S. Charan, *J. Polym. Sci., Part A: Polym. Chem.* **1995**, *33*, 109.

[37] W.H. Stockmayer, *J. Chem. Phys.* **1945**, *13*, 199.

[38] J.M. Vion, R. Jérôme, P. Teyssié, M. Aubin, R.E. Prud'homme, *Macromolecules* **1986**, *19*, 1828.

[39] M. Gruvegård, T. Lindberg, A.-C. Albertsson, *J. Macromol. Sci., Pure Appl. Chem.* **1998**, *A35*, 885.

[40] R.K. Srivastava, A.-C. Albertsson, *Biomacromolecules* **2006**, *7*, 2531.

[41] A.-C. Albertsson, M. Gruvegård, *Polymer* **1995**, *36*, 1009.

[42] A.-C. Albertsson, A. Löfgren, *J. Macromol. Sci., Pure Appl. Chem.* **1995**, *A32*, 41.

[43] A.-C. Albertsson, M. Eklund, *J. Polym. Sci., Part A: Polym. Chem.* **1994**, *32*, 265.

[44] D.W. Grijpma, A.J. Pennings, *Polym. Bull. (Berlin)* **1991**, *25*, 335.

[45] J. Contreras, D. Dávila, *Polym. Int.* **2006**, *55*, 1049.

[46] M. Bero, J. Kasperczyk, G. Adamus, *Makromol. Chem.* **1993**, *194*, 907.

[47] M. Hiljanen-Vainio, T. Karjalainen, J. Seppälä, *J. Appl. Polym. Sci.* **1996**, *59*, 1281.

[48] F. Faÿ, E. Renard, V. Langlois, I. Linossier, K. Vallée-Rehel, *Eur. Polym. J.* **2007**, *43*, 4800.

[49] R.C. Jeske, A.M. DiCiccio, G.W. Coates, *J. Am. Chem. Soc.* **2007**, *129*, 11330.

[50] R.S. Bogartz, *Psychometrika* **1966**, *31*, 383.

[51] H.J. Harwood, *Makromol. Chem., Macromol. Symp.* **1987**, *10-11*, 331.

[52] T. Mathisen, K. Masus, A.-C. Albertsson, *Macromolecules* **1989**, *22*, 3842.

[53] M. Trollsås, M.A. Kelly, H. Claesson, R. Siemens, J.L. Hedrick, *Macromolecules* **1999**, *32*, 4917.

[54] G.R.P. Henry, S. Huijser, A. Heise, C.E. Koning, *manuscript in preparation*.

4

Polyesters formed by ring-opening polymerization of lactide and glycolide.

Abstract. *The topology of poly(lactide-co-glycolide), in other words the distribution of lactyl and glycolyl units along the individual chains, was determined by creatively exploiting MALDI-ToF-MS analysis. End groups were determined by calculation of the isotope distributions by in-house developed software and by using the shift in m/z of the polymer chains comparing the MALDI-ToF-MS spectra recorded for two different ionization salts. Ring-opening polymerizations of a molar ratio of 80/20 lactide/glycolide catalyzed by lipase or Sn(Oct)₂ were performed as well as a step growth polymerization of lactic and glycolic acid employing the same molar ratio in the presence of Ti(OBu)₄ as catalyst. We observed a difference in topology for copolymers of glycolide with either L-lactide or D,L-lactide for PLGA synthesized by both metal-based catalysts, tin for ring-opening polymerization and titanium for polycondensation. Moreover, we demonstrated the difference in transesterification of PLGA synthesized according to the diverse pathways by converting a MALDI-ToF-MS spectrum into a so-called fingerprint or contour plot. We discovered three types of fingerprints, a striped fingerprint showing dimer-wise incorporation of one of the lactide monomers, a checkerboard pattern deriving from a dimer-wise incorporation of both monomers and a homogeneous plot as a result of complete transesterification or using the hydroxyacids as monomers.*[§§]

4.1   Introduction

Homo- and copolymers of lactide and glycolide have drawn increasing attention for medical applications due to their good biodegradability and biocompatibility. Especially, the use of poly(lactide-*co*-glycolide) as a matrix for drug delivery devices has grown rapidly over the last decades. For example, controlled drug release by controlled degradation of the polymer matrix is the topic of numerous publications.[1] It is clear that factors affecting the degradation characteristics, such as the copolymer's molar mass, molar mass distribution, its chemical composition and microstructure, are crucial for such applications. Hence, knowledge of the exact topology of PLGA, which can attain a random, block, alternating or gradient structure, is of high importance to govern degradation rates of the polymer matrix within the human body. The topology of the polymer is strongly determined by the applied synthetic route, which can be direct polycondensation of the hydroxyacids or copolymerization of lactide and glycolide (Scheme 4-1).
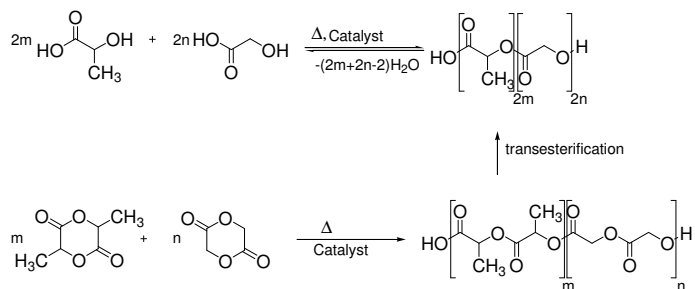
Scheme 4-1. Synthesis of poly(lactide-*co*-glycolide) by polycondensation and by ring-opening.

Ring-opening polymerization can proceed anionically[2], cationically[3] and by a metal-catalyzed coordination/insertion mechanism.[4,5] Especially the latter method is widely employed due to the capability of performing stereospecific polymerizations resulting in high molecular weight polymer.
All these different pathways leave their fingerprint in the topology of the polymer. Generally, microstructures of this particular copolymer are characterized by high resolution ^{13}C-NMR using mainly the carbonyl signals because of their sensitivity to sequence effects.[6-12] However, to obtain a highly resolved spectrum, long measuring times are required as well as powerful NMR machinery. Moreover, the assignment of the peaks is complex and not always straightforward. Albeit challenging, MALDI-ToF-MS might be a suitable and fast tool to disclose the fine structure even of complex copolymers as poly(lactide-*co*-glycolide). In this Chapter we report a comprehensive and comparative study on the composition and topology of PLGA by making use of the method based on MALDI-ToF-MS as described in Chapter 2.[13,14]

In-house developed software not only enables elucidation of individual chain structures, but a full characterization including even the copolymer's chemical composition and topology (random, gradient, block, alternating). Poly(lactide-*co*-glycolide) used in this study was synthesized by ring-opening copolymerization of L- or D,L-lactide and glycolide using either tin(II) 2-ethylhexanoate (Sn(Oct)$_2$) or lipase *Pseudomonas cepacia* as catalyst and by polycondensation of L-lactic acid or D,L-lactic acid and glycolic acid using Ti(OBu)$_4$.

4.2 Results and Discussion

4.2.1 Polycondensation

First, we will discuss here the analysis of PLGA synthesized by polycondensation of the hydroxyacids lactic- and glycolic acid. Two samples of PLGA have been prepared in the melt with Ti(OBu)$_4$ as catalyst. PLLGA (80L/20G) synthesized with L-lactic acid and glycolic acid as monomers afforded a number average molecular weight of 18.6 kg·mol^{-1} with a polydispersity of 1.7 and the synthesis of PDLLGA (80L/20G) under similar conditions resulted in a number average molecular weight of 19.6 kg·mol^{-1} with a polydispersity of 1.8. Both copolymers were amorphous, with a T_g of 48.6 °C for PLLGA and 45.9 °C for PDLLGA. Standard MALDI-ToF-MS spectra were recorded in the reflector mode using potassium trifluoroacetate as cationization agent. A typical spectrum is shown in Figure 4-1.
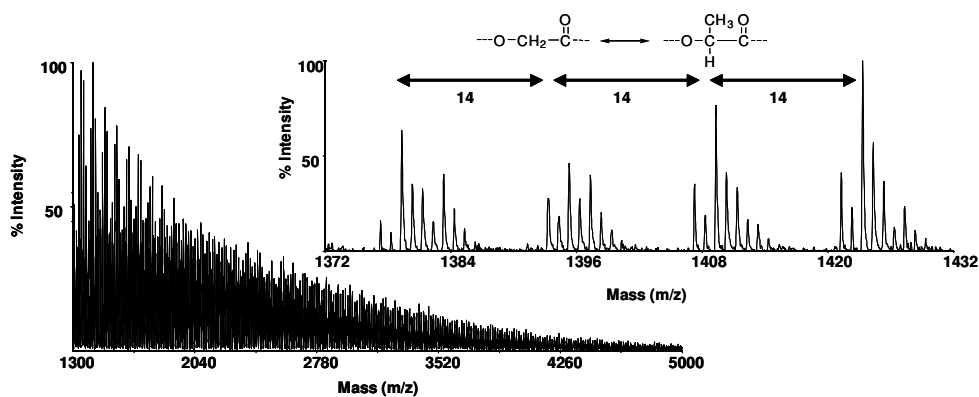
Figure 4-1. MALDI-ToF-MS spectrum and enlargement of PDLLGA synthesized by polycondensation (recorded with K$^+$).

The key issue is to assign the peaks recorded in the spectrum to a single combination of lactyl and glycolyl units and a certain end group. Generally, polymer chains obtained by polycondensation, but also by ring-opening polymerization of cyclic esters, are terminated by an alcohol and a carboxylic acid group (referred to as an H-OH end group). However, processes like end-to-end condensation and/or intramolecular transesterification are responsible for the additional presence of cyclic structures. Furthermore, the acidic proton of the carboxylic acid end group can be replaced by a cation, deriving from the synthesis glassware, solvents and/or cationization salt used in MALDI-ToF-MS, resulting in an H-OK end group.

If we zoom in on the spectrum we find several overall distributions of the isotope patterns. The differently colored stars represent these distributions. The difference between the two consecutive stars is 14 m/z, which corresponds to the exchange of one glycolyl unit (58.01 g·mol^{-1}) for one lactyl unit (72.02 g·mol^{-1}) within a single chain of a certain number of monomer residues (Figure 4-2).[***] Hopping from star to star equals the exchange of a glycolyl unit for a lactyl unit. This continues until no more glycolyl units are present. The next step is a transition towards another distribution of chains consisting of one monomer residue more in total chain length; see arrows in Figure 4-2.
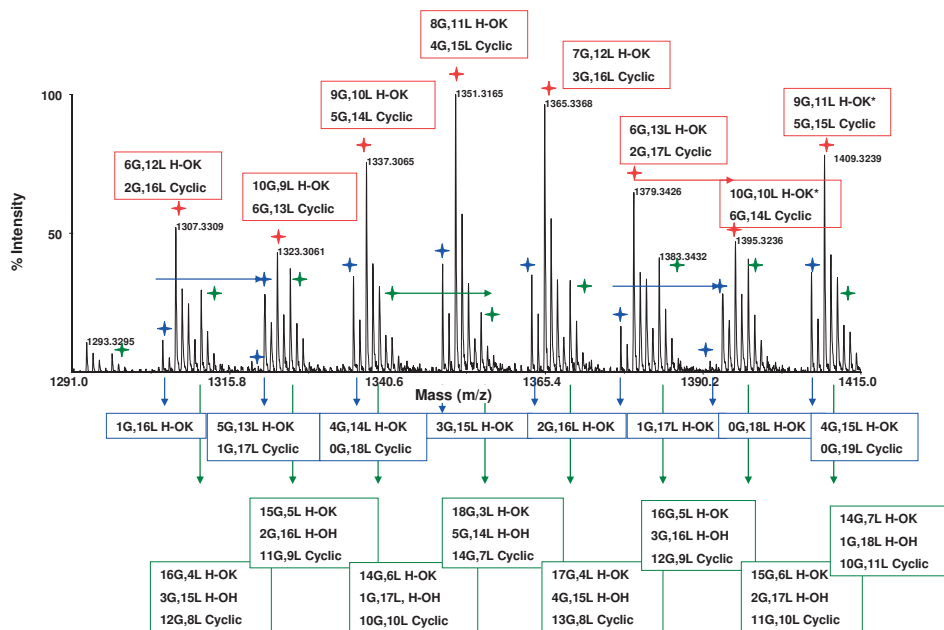
Figure 4-2. Possible combinations of lactyl and glycolyl units for the three potential end groups for the isotope distributions in a range of the spectrum of PDLLGA synthesized by polycondensation (recorded with K$^+$).

[***] Lactyl unit = -O-CH(Me)-C(O)-, Lactydyl unit = -O-CH(Me)-C(O)-O-CH(Me)-C(O)-
Glycolyl unit = -O-CH$_2$-C(O)-, Glycolydyl unit = -O-CH$_2$-C(O)-O-CH$_2$-C(O)-

Figure 4-2 also clearly illustrates that the mass of more than one combination of lactide, glycolide and end-groups match with the mass of the most abundant peak of a distribution. The complexity of the spectrum increases with increasing *m/z* and following the described pathway for the remaining part of the spectrum becomes cumbersome. Hence, pure mathematical analysis will not suffice to analyze the MALDI-ToF-MS spectra since often more probabilities are obtained than chemically possible based on the reaction conditions and reactivity ratios of the monomers. Comparison of the calculated data with the recorded peaks in the spectrum results in elimination of certain chemically unrealistic combinations. Considering the feed with a ratio of 80L/20G, some combinations are more logical than others. With this information we determined that the isotope patterns with a blue star derive from chains with an H-OK end group, the patterns with a red star correspond to cyclics and the ones with a green star derive from chains terminated by H-OH.

It is clear that manually fitting chain structures to the peaks in the MALDI spectrum is a tedious and time-consuming task. We therefore developed software, as mentioned in Chapter 2, that allows us to simulate the whole spectrum for a certain combination of end groups by constructing a complete intensity matrix with $n_{G,i}$ rows and $m_{L,j}$ columns for a given end group using Equation 4-1. Assignment of the peaks in the spectrum to a certain position in the matrix can be done employing the inequality 4-2.

$$m_{cal} = n_G M_G + m_L M_L + E_I + E_{II} \tag{4-1}$$

$$\left| m_{exp} - m_{cal} \right| \leq \frac{\Delta m}{2} \tag{4-2}$$

E_I and E_{II} in equation 4-1 represent the molar masses of the end groups at opposite sides of the chain, $n_G M_G$ and $m_L M_L$ represent the number and mass of the repeating glycolyl and lactyl units respectively, and M^+ the mass of the cation. In the inequality 4-2, m_{exp} represents the experimental mass, m_{cal} the calculated mass and Δm the accuracy (1-2 g·mol^{-1}). By calculating the natural abundance isotope distributions for each position in the matrix and rescaling it to the corresponding highest-intensity mass-peak, a full spectrum can now be simulated.[15,16] A part of the simulated spectrum is shown in Figure 4-3.
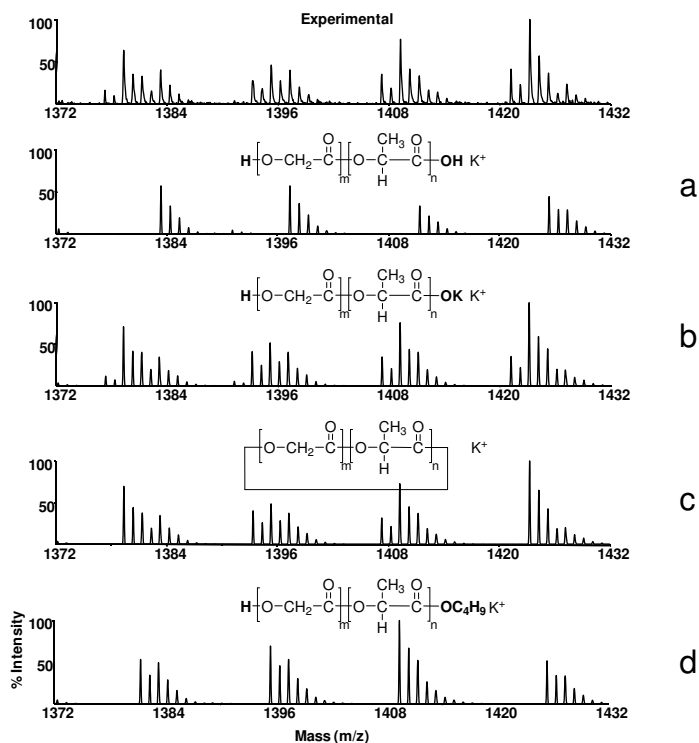
Figure 4-3. Simulated isotope patterns (a-d) derived by the in house developed software for different end groups of PDLLGA synthesized by polycondensation are compared to the experimental one.[†††] *(N.B. a complete spectrum was simulated, but for clarity only a selected range of it is shown.)*

The simulated data are in agreement with the "manual" calculations shown in Figure 4-2 but are obtained much faster. Although the software allows the simulation of full spectra, in some cases it remains very difficult to appoint a peak to a single combination of monomer residues and end groups. Comparison of the MALDI-ToF-MS spectra recorded with potassium- and sodium trifluoroacetate proved to be of great help in appointing the true end group and comonomer composition of each of the individual chains. If we translate the sodium spectrum by −16 and by −32, it can be seen which distributions coincide with distributions in the spectrum recorded with potassium. The difference of 32 *m/z* is only possible between the H-OK ended polymer chains with K^{+} adduct and the H-ONa ended chains with Na^{+} adduct. The difference of 16 *m/z* can be explained by both H-OH terminated chains and cyclics. In Figure 4-4 it is shown that both Δ*m/z*, 16 as well as 32, were detected.

[†††] In theory a butanol end group can derive from the titanium catalyst used in this condensation reaction. The occurrence of the H-OBu end group is not likely, considering the concentration of the catalyst used. In this study, this end group is therefore left out of consideration.
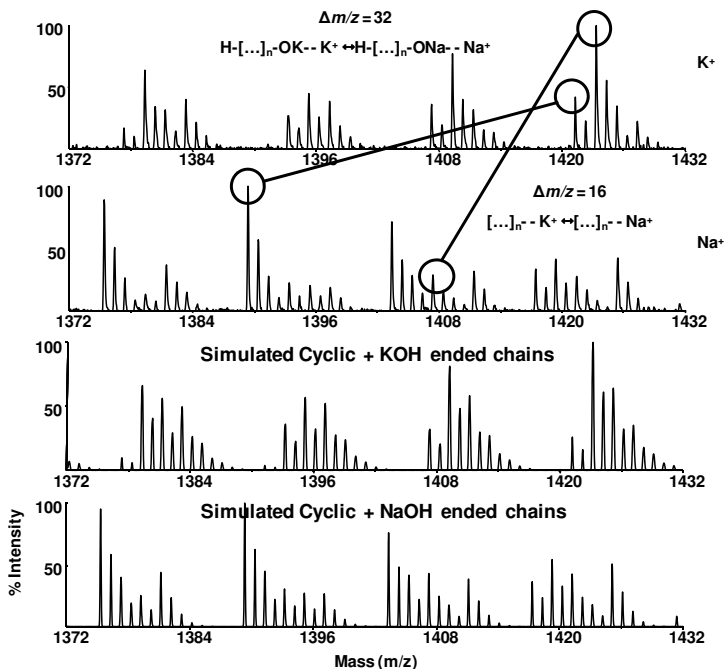
Figure 4-4. Experimental and simulated enlargement of the spectra of PDLLGA recorded with K^+ and Na^+.

The intensity of the isotope distributions differs in the spectra for the two cations (Figure 4-4). For identical sampling and measuring conditions (*e.g.* laser power), the highest intensity distributions in the spectrum measured with potassium derive from cyclic structures, but in the spectrum measured with sodium, H-ONa end capped structures dominate. This difference can originate from a difference in cationization of cyclic chains between the two salts. Therefore, the ionization of macrocyclic polyesters was further investigated by changing the cation of the salt (Li, Na, K, Cs), but no clear discrimination could be established. The effect of the choice for a particular cationization salt can reflect in the distribution of the polymers. Unfortunately, the inevitable effect of ionization efficiency limits MALDI-ToF-MS for quantitative applications. Integration of the isotope distributions and determination of the area-ratio of cyclic and linear structures is therefore not sensible. Other characterization techniques are required to determine the true ratio of cyclic to linear chains, *e.g.* liquid chromatography under critical conditions as proposed and performed by De Geus.[17]

So far we only dealt with the polycondensation of D,L-lactic acid and glycolic acid. The reaction between L-lactic acid and glycolic acid has also been carried out and the MALDI-ToF-MS recorded. The complete procedure will not be repeated for this case, but the spectra will be given along with the contour plots.

Figure 4-5 shows an apparent difference between the spectra recorded with potassium and sodium demonstrating again the better ionization efficiency for cyclic polymers with a potassium cationization agent. Simulations proved that the isotope distributions highest in intensity belonged to H-OH terminated chains for both the spectrum measured with potassium and with sodium. However, isotope distributions for linear chains, where a proton was exchanged for an extra K^+ or Na^+, were present, just as the distributions for cyclic chains.
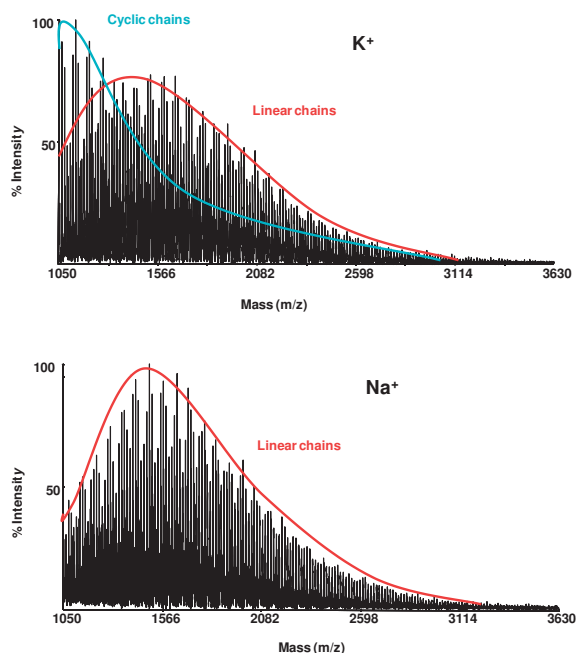
Figure 4-5. MALDI-ToF-MS spectrum of PLLGA synthesized by polycondensation (recorded with K^+ and Na^+).

Besides determining the end groups and the comonomer contribution of the chains, in most cases it is also possible to determine the topology of the polymer. To elucidate the topology of the polymer, we make use of the normalized matrix extensively discussed in Chapter 2. The matrix of poly(lactide-*co*-glycolide) can be represented conveniently in a 2D graph. By plotting the data information is provided that cannot directly be derived from the MALDI-ToF-MS spectrum. The matrix is represented as a 2D contour plot with lactyl- and glycolyl units on the axes displaying the corresponding peak intensity of the combination (n_G,m_L) in color grading. Interestingly, the position of the plot is strongly depending on the end group while the shape is hardly influenced by it. Information on the topology of the polymer is partly revealed by the shape and position of the plot as outlined in Chapter 2.

Simply put, a line drawn through the optimum of the contour plot is a measure for the average chemical composition. If this line crosses the origin and the slope remains constant the copolymer can be classified as random. When the line is curved but still crosses the origin, the plot represents a gradient copolymer. Finally, if the line does not cross the origin, we are dealing with a more blocky copolymer or a binomial random copolymer.
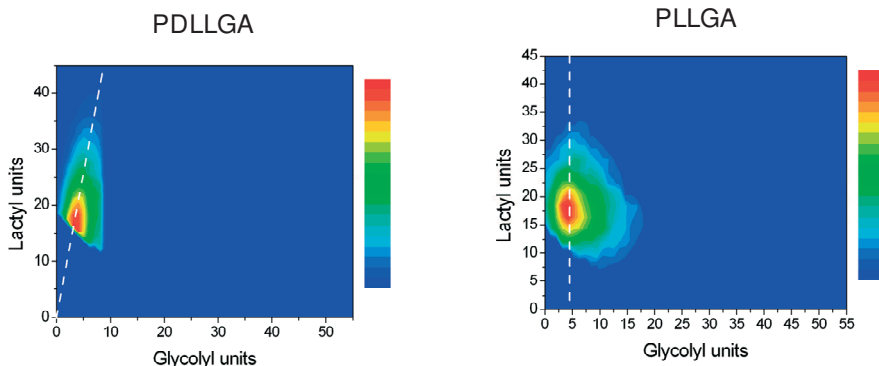
Figure 4-6. Contour plots of PDLLGA and PLLGA synthesized by polycondensation (recorded with K^+/Na^+). The colors represent the intensity with red being the most abundant chains corresponding to the isotope distributions of highest intensity in the spectrum shown in Figure 4-1.[‡‡‡]

Figure 4-6 shows the fingerprints of PDLLGA and PLLGA. The contour plot of PDLLGA seems to be cut off, but this is due to the fact that these MALDI-ToF-MS spectra were not recorded for masses lower than 1250 *m/z*. The dashed line is an indication for the average composition. The contour plot of PLLGA lies against the ordinate confirming the presence of homopolymer lactide. Therefore PLLGA tends more towards a copolymer with long sequences of lactide. On the other hand the contour plot of PDLLGA shows a higher inclination with the ordinate suggesting a more random character.

[‡‡‡] Ghost plots, *i.e.* plots deriving from multiple peak assignment or plots deriving from a match of a certain end group are not displayed here.

4.2.2. Ring-opening polymerization – Sn(Oct)$_2$

To study the difference in end groups and topology, besides polycondensation poly(lactide-*co*-glycolide) was also synthesized using ring-opening polymerization of lactide and glycolide. PLLGA (80L/20G) synthesized with L-lactide and glycolide as monomers afforded a number average molecular weight of 9.9 kg·mol^{-1} with a polydispersity of 1.5 and synthesis of PDLLGA (80L/20G) resulted in a number average molecular weight of 32.6 kg·mol^{-1} with a polydispersity of 1.6. Both copolymers were amorphous, with a T_g of 50.9 °C for PLLGA and 43.8 °C for PDLLGA. The ratio of lactide and glycolide in the polymer represented the feed ratio as determined by ^{1}H-NMR. Here, a pattern of alternating high and low intensity isotope distributions was detected for both PLLGA and PDLLGA. The difference in *m/z* between adjacent isotope distributions again equals 14, which corresponds to the exchange of one glycolyl unit for one lactyl unit within a single chain (see enlargement of Figure 4-7). The difference of 28 *m/z* between the most abundant isotope distributions corresponds to the exchange of one glycolydyl unit (116.01 g·mol^{-1}) for a lactydyl unit (144.04 g·mol^{-1}).
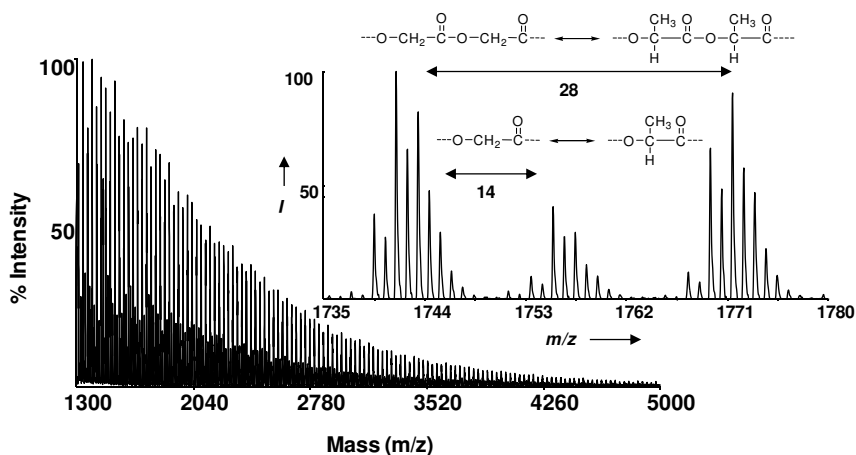
Figure 4-7. MALDI-ToF-MS spectrum and enlargement of PDLLGA.

Comparison of the MALDI-ToF-MS spectra recorded with potassium- and sodium trifluoroacetate again helped to determine the end group since the spectrum measured with the sodium cationization agent was shifted −16 in *m/z* with respect to the spectrum measured with the potassium agent (Figure 4-9). This automatically excludes the H-OK end group as a possible solution. For the difference between an H-OK terminated chain with a K$^+$ adduct and an H-ONa terminated chain with a Na$^+$ adduct, the spectrum measured with sodium should have shifted −32 in *m/z*. The occurrence of H-OH ended chains can be ruled out as well for three different reasons.

The first reason is that statistically, with the large excess of salt used, the exchange of a certain percentage acidic protons for a K^+ / Na^+ should have taken place resulting in occasionally a difference of 32. Secondly, the presence of H-OH terminated chains alone cannot explain all isotope distributions present and finally the calculated composition for H-OH terminated chains differs too much from the composition of the copolymer determined by ^{1}H-NMR. Occasionally, catalyst residues give rise to additional end groups, *e.g.* an octanoyl end group as reported by Kowalski *et al.*[18,19] (Figure 4-8d). Simulation of the experimental MALDI-ToF-MS spectrum did not afford a unique solution since cyclic structures, chains with an octanoyl end group and chains with an H-OK end group yielded virtually identical spectra (Figure 4-8). Although the presence of chains containing octanoyl end groups originating from catalyst residues cannot be excluded, their contribution is expected to be marginal due to the low catalyst concentration. Furthermore, these polymers should also undergo occasional deprotonation of the carboxylic acid end group leading to a shift of -32 *m/z*, which was not detected. Therefore, the sequential difference of 16 *m/z* observed for the K^+ and Na^+ cationized spectra, strongly suggests the presence of mainly cyclic structures. Both experimental and simulated isotope patterns of cyclic species ionized with potassium and sodium are shown in Figure 4-9.
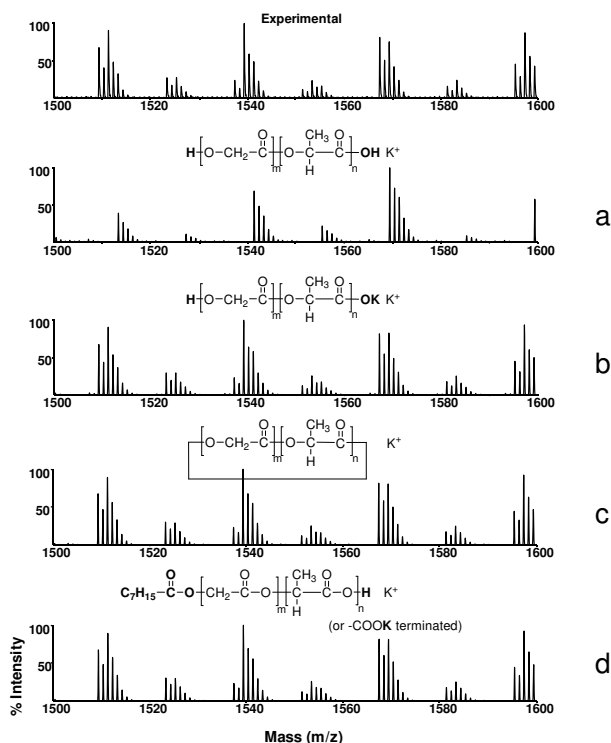
Figure 4-8. Experimental and simulated isotope patterns for different end groups.
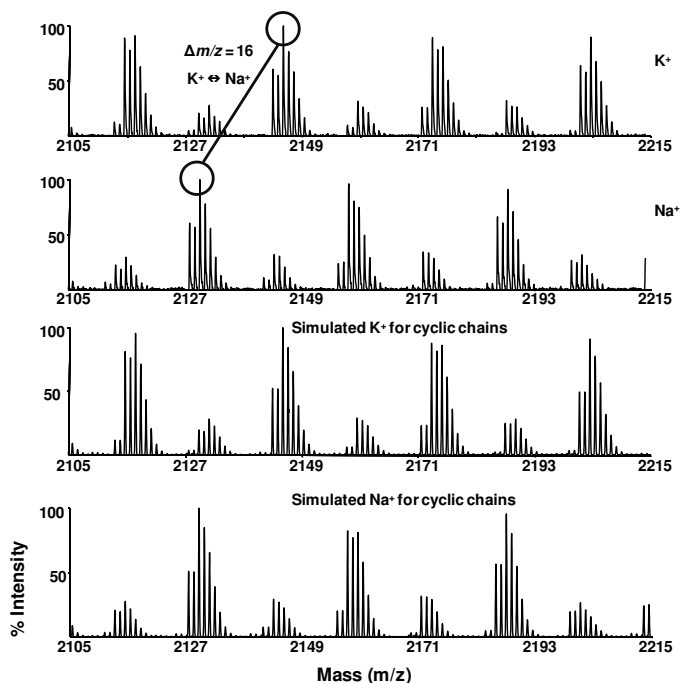
Figure 4-9. Experimental and simulated enlargement of the spectra of PDLLGA recorded with K^+ and Na^+.

It is worth mentioning that for sufficient mass resolution, MALDI-ToF-MS is restricted to lower molecular weight fractions. The fact that the MALDI-ToF-MS spectrum only shows cyclic structures does not exclude the possibility that linear chains are present in the higher molecular weight fraction of the material.

The pattern of high and low intensity isotope distributions in the MALDI-ToF-MS spectrum of PLLGA and PDLLGA (Figure 4-7) is reflected in the contour plots of the polymers (Figure 4-10). The striped pattern is characteristic for the presence of mainly chains both even- and odd-numbered in glycolyl units but only even-numbered in lactyl repeating units. The horizontal lines in the plot represent the polymer chains existing of complete lactydyl units. This suggests that the $Sn(Oct)_2$ readily transesterifies glycolydyl units, but is hardly capable of transesterifying the lactydyl ester bond under the reaction conditions applied.
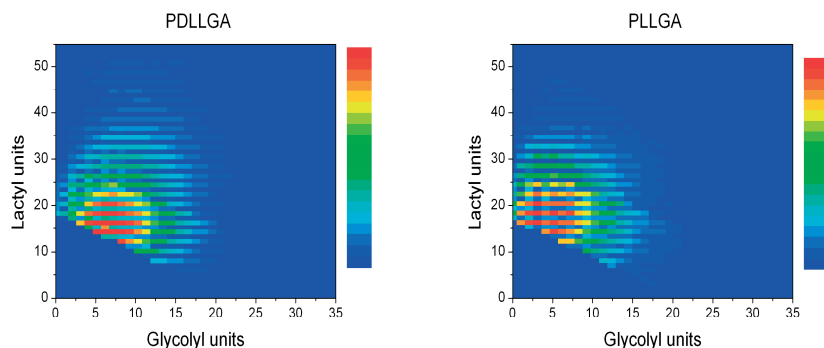
Figure 4-10. Contour plots of PDLLGA and PLLGA for cyclic structures. *(N.B. the contour plots seem to be cut off, but this is due to the fact that these MALDI-ToF-MS spectra were not recorded at m/z values lower than 1250.)*

This can be determined more clearly by looking at the chemical composition distributions (CCD as described in Chapter 2) for an even and an odd numbered chain, see Figure 4-11. The probability that the chain is odd numbered mainly derives from the glycolyl units as the highest peaks in the CCD for chain length 29 are odd numbered whereas for lactyl units for the same chain length the highest peaks are even numbered. In principle one could quantitatively determine the even and odd numbered chains by summing the area beneath the peaks in the MALDI-ToF-MS spectrum assuming that there is no difference in ionization efficiency between the even and odd numbered chains.
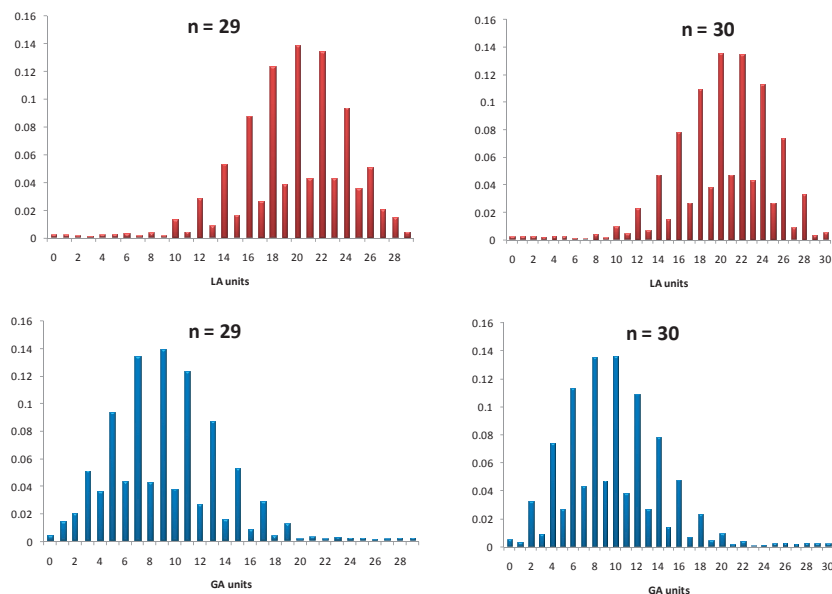
Figure 4-11. CCD for lactyl- and glycolyl units for chain lengths 29 and 30.

Expectedly, contour plots of PLGA synthesized by polycondensation of the hydroxyacids showed a homogeneous area, indicative for an equal distribution of even-numbered and odd-numbered chains. As mentioned before, the contour plot can in most cases provide significant information on the topology of the polymeric material. Due to the discontinuity in the area, the shape and position of the contour plot in Figure 4-10 do not show unambiguously if we are dealing with a more block or a more random copolymer. A better insight into the topology is obtained when the plot is simulated with complete lactydyl units instead of lactyl units (Figure 4-12).
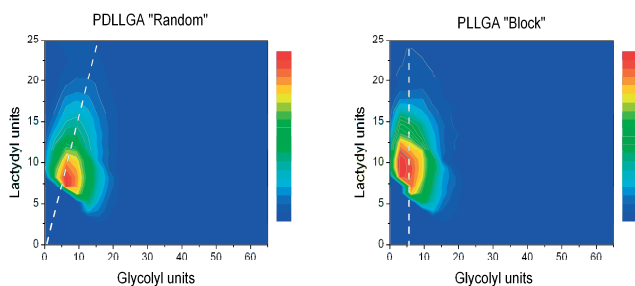
Figure 4-12. Contour plots of PDLLGA and PLLGA for cyclic structures plotted with lactydyl units.

Apparently, the configuration of lactide has an influence on the randomness of the copolymer. The more random character of PDLLGA compared to PLLGA, suggests that the topologies of both polymers are probably determined by a higher built-in rate of racemic mixture of D,D-lactide and L,L-lactide, compared to enantiomerically pure L,L-lactide. This striped pattern was not only observed for PLGA. Also for the copolymerization of lactide and ε-caprolactone using $Sn(Oct)_2$ similar patterns were found in the fingerprint deriving from the dimer-wise incorporation of lactide, see Figure 4-13.
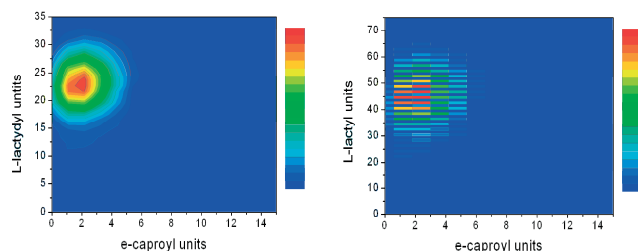
Figure 4-13. Contour plots of PLLCL for H-OH terminated structures. In the plot on the left whole lactydyl units against ε-caproyl units is portrayed, on the right lactyl units against ε-caproyl units.

4.2.3 Ring-opening polymerization – enzymatically

As PLGA is predominantly used for medical applications, there is a strong interest to obtain this polymer without the use of (toxic) metal catalysts. Enzymes might be a feasible solution to circumvent the use of metal-based catalysts. Due to their capability of stereo-, regio- and chemoselective polymerizations under mild reaction conditions, enzymes gain increasing appreciation in the world of polymer synthesis. It was first reported by both the groups of Kobayashi[20] and Gutman[21] that lipases, enzymes capable of catalyzing the hydrolysis of fatty acid esters, can polymerize various medium-sized lactones, *e.g.* ε-caprolactone and δ-valerolactone. Matsumura *et al.*[22,23] reported in 1997 the successful enzymatic polymerization of lactide using free and immobilized lipase PS. Enzymatic ring-opening polymerizations of lactide and glycolide (80L/20G) using both immobilized and free lipase PS were performed in bulk at 100 ^{o}C and 130 ^{o}C under an argon atmosphere. The copolymers were characterized by MALDI-ToF-MS, DSC, SEC and NMR. The racemic mixture of lactide (D,L-lactide) was only used at 130 ^{o}C due to the higher melting point. The results are given in Table 4-1.

Table 4-1. Results of lipase-catalyzed synthesis of PLGA.

Entry Polymer[1]	Enzyme	M_w[2] (kg mol^{-1})	PDI[2]	Conv.[3] (%)	T_g[4] (^{o}C)
1. PLLGA	PS	11.7	1.8	95	47.5
2. PLLGA	PS-D I	8.7	1.5	82	44.7
3. PLLGA	-	1.9	1.3	25	n.d.
4. PLLGA	PS	20.6	4.0	98	45.6
5. PLLGA	PS-D I	13.1	2.7	94	45.6
6. PLLGA	-	2.2	1.2	12	n.d.
7. PDLLGA	PS	13.5	3.2	94	43.7
8. PDLLGA	PS-D I	12.7	2.5	75	39.2

[1] Reaction time of 7 days at 100 ^{o}C for entries 1-3 and of 2 days at 130 ^{o}C for entries 4-8.
[2] Determined by SEC. [3] Determined by integration of methine peaks in ^{1}H-NMR. [4] Measured by DSC at a heating rate of 10 ^{o}C·min^{-1}.

To be able to discriminate between enzymatically and non-enzymatically obtained polymers, reference reactions were performed in the absence of lipase. In the blank reaction at 100 ^{o}C copolymer was formed with a molecular weight of 1.9 kg·mol^{-1} but monomer conversions were low in comparison to the enzyme-promoted reactions. Conversely, the blank reaction at 130 ^{o}C unexpectedly produced relatively high molecular weight polymer with high conversions of monomer albeit that the reaction took 7 days. A possible explanation for the polymerization in the blank reaction is the cationic

polymerization by traces of hydroxyacid present in the monomers. Fortunately, even at 130 °C the non-enzymatic ring-opening polymerization is considerably slower than the enzymatic one and is left out of consideration for reaction times up to 2 days.

As can be seen in Figure 4-14, the difference between adjacent isotope distributions equals 14 *m/z* corresponding to the exchange of a glycolyl unit (58.01 g·mol^{-1}) for a lactyl unit (72.02 g·mol^{-1}). The difference between the most abundant peaks in the spectrum of PLLGA synthesized at 100 °C, is 144 *m/z*, which corresponds to the mass of a lactydyl unit. This indicates the simultaneous presence of homopolymer poly(lactide) (Figure 4-14).

Figure 4-14. MALDI-ToF-MS spectrum and enlargement of PLLGA synthesized by lipase PS-D I at 100 °C (recorded with K$^+$).

Simulation of the isotope distributions using the in-house developed software resulted in Figure 4-15, in which Figure 4-15a, b and c are simulated spectra for H-OH, H-OK and cyclic structures, respectively. Elimination of the presence of certain chain structures due to mismatching isotope patterns appeared impossible since *the most abundant distributions* could be explained by all three possibilities.
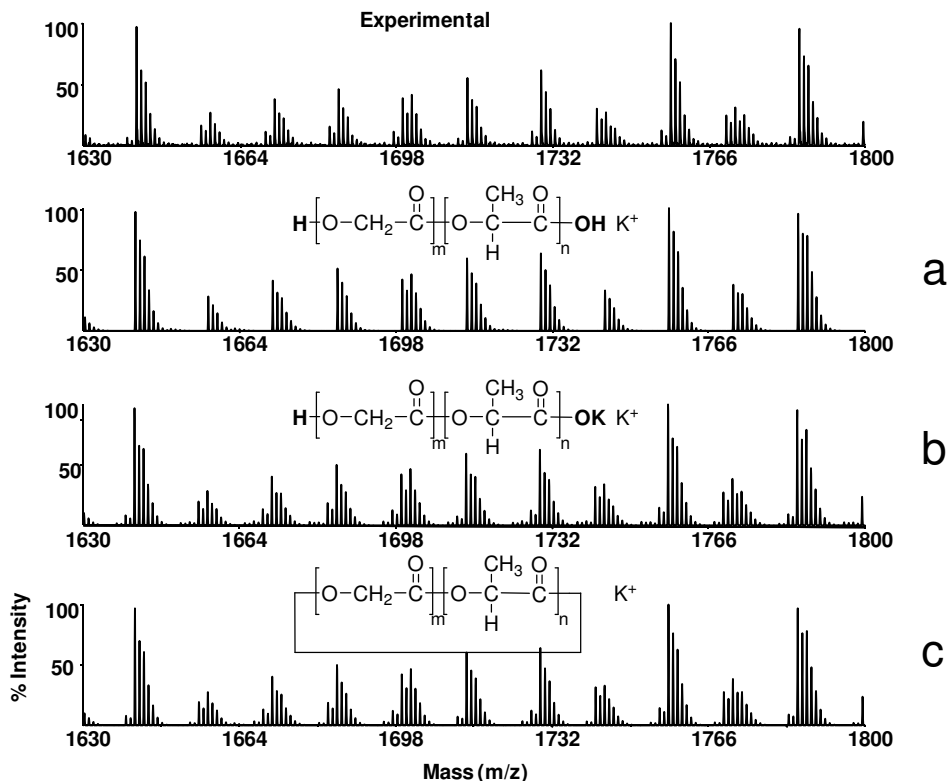
Figure 4-15. Experimental and simulated isotope patterns for different end groups of PLLGA synthesized by lipase PS-D I at 100 ^{o}C (recorded with K$^+$).

Comparison of MALDI-ToF-MS spectra recorded with both potassium- and sodium trifluoroacetate revealed a shift of −16 *m/z* between *the most abundant peaks* (Figure 4-16a and 4-16b). This automatically excludes the possibility that the highest intensity peaks derive from H-OK (or H-ONa) terminated chains. For these chains a difference of 32 *m/z* should have been detected; the difference between an H-OK terminated chain with a K$^+$ adduct and an H-ONa terminated chain with a Na$^+$ adduct. This leaves H-OH end capped and cyclic structures as the remaining possibilities for the highest intensity peaks.
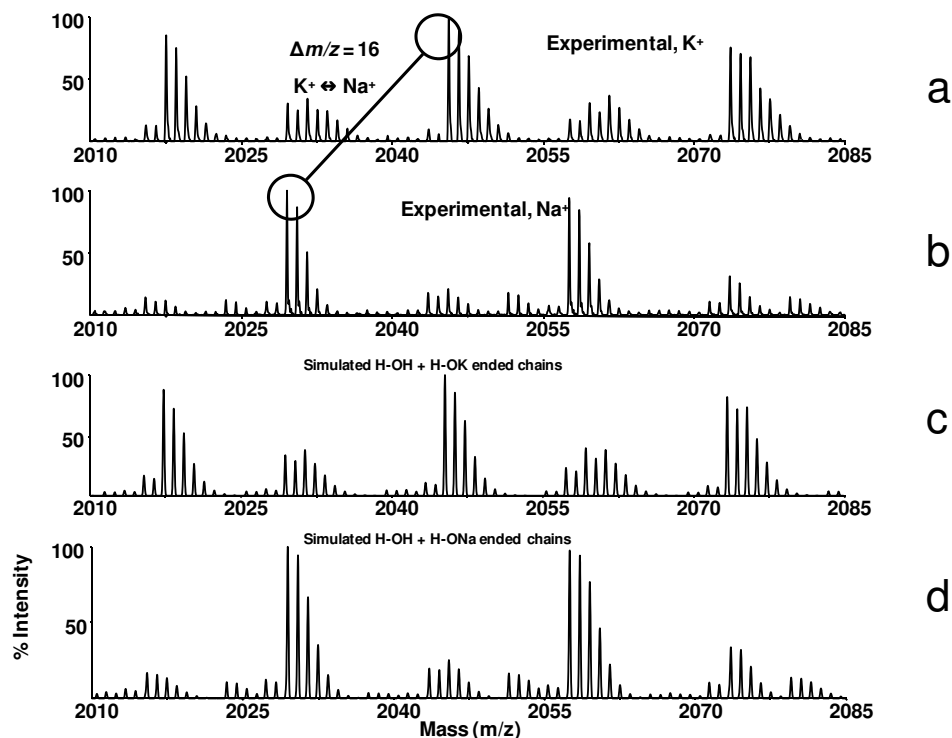
Figure 4-16. Experimental and simulated enlargement of the spectra for PLLGA (recorded with K$^+$ and Na$^+$).

To distinguish between H-OH and cyclic structures the contour plots for both types of polymers were calculated. The presence of cyclic structures can be excluded based on their contour plot (Figure 4-17a). The plot is abruptly cut off at the left of the column with red squares, which correspond to peaks of highest intensity in the MALDI-ToF-MS spectrum. Statistically this cutting off is impossible due to equal chances of the syntheses for chains with one glycolyl unit more or less than the most abundant polymer chains, unless homopolymer lactide is present. Then, subtraction of a glycolyl unit is impossible as the number of glycolyl units cannot equal −1. A plot as Figure 4-17a strongly suggests that the end group is chosen wrongly and that the plot should in fact be positioned against the y-axis. This proved to be the case for chains terminated by an H-OH group (Figure 4-17b). Therefore, it can be concluded that the major part of the polymer chains is linear and H-OH end capped. This is confirmed by the presence of low intensity peaks that correspond to H-OK (and H-ONa) terminated chains where indeed the acidic proton is exchanged for a cation of the cationization agent (Figure 4-16c and d).
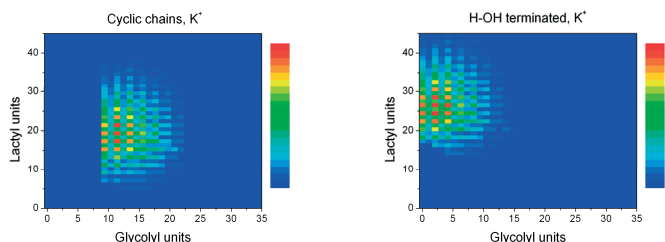
Figure 4-17. a) Contour plot for cyclic structures. b) Contour plot for H-OH terminated chains. Both plots have been derived from the spectrum recorded with K+ for PLLGA synthesized by lipase PS-D I at 100 °C.

Contour plots of copolymer synthesized by enzymatic ring-opening reactions performed at 100 °C, show a curious phenomenon. Instead of the expected homogeneously colored area, the contour plot of PLLGA resembles a Scottish tartans pattern in which regularly distributed red squares can be seen (Figure 4-17). The first column of squares, counting from left to right, corresponds to the homopolymer of lactide since no glycolyl units are present. Every second column shows the addition of a complete glycolydyl unit [-O-CH$_2$-C(O)-O-CH$_2$-C(O)-]. Similarly, every second row a complete lactydyl unit is added to the polymeric chain. This indicates a dimer-wise incorporation of both monomers and negligible transesterification by lipase. In the work of Wahlberg *et al.* lactide and *ε*-caprolactone were copolymerized in the presence of *Candida antarctica* lipase B at 70 °C. Using MALDI-ToF-MS they showed that lactide was built in dimer-wise as lactydyl units and that most chains were even-numbered in lactide. After one week a limited amount of odd-numbered chains was detected. Only after 8 weeks the initially non-random product was lost by extensive transesterification.[24]

The polymers synthesized by the lipase catalyzed reaction performed at 130 °C were examined in a similar way as the polymers obtained at 100 °C. The contour plot of this polymer showed a normal homogeneous plot instead of the tartan pattern and the difference between the distributions is 14 *m/z*, as expected. The MALDI-ToF-MS spectrum of PDLLGA, synthesized by free lipase PS, is given in Figure 4-18. The MALDI-ToF-MS spectrum of PLLGA prepared at 130 °C was found to be similar to that of PDLLGA and will therefore be left out of consideration.
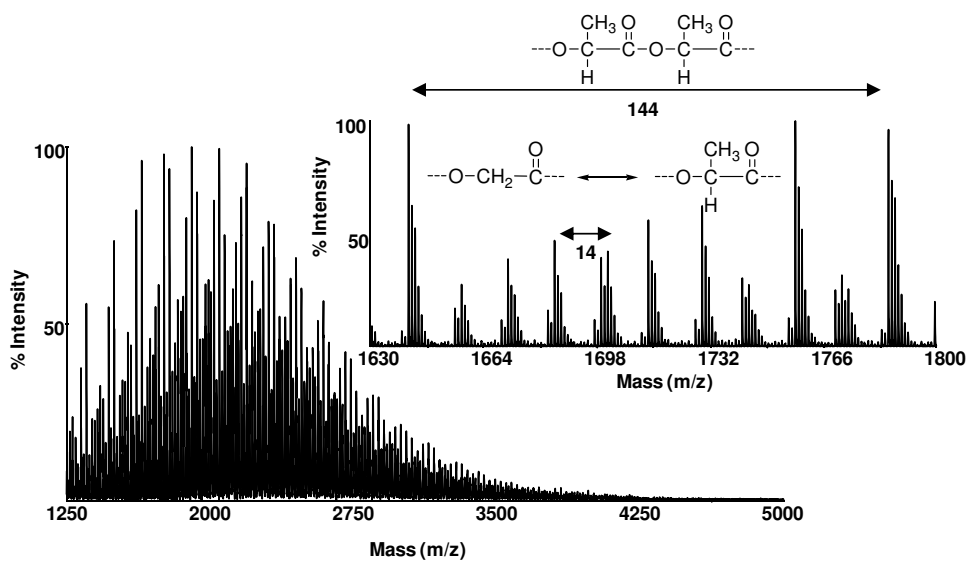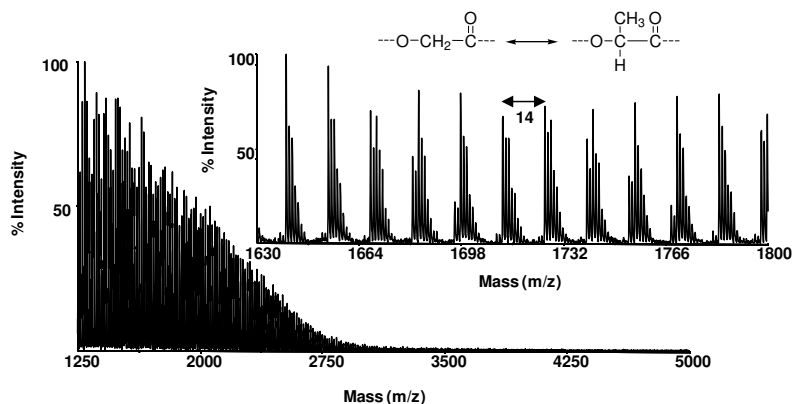
Figure 4-18. MALDI-ToF-MS spectrum and enlargement of PDLLGA synthesized by free lipase PS at 130 ^{o}C (recorded with K$^+$).

Simulation of the possible end groups, similar as for the polymerizations at 100 ^{o}C, resulted in the isotope patterns displayed in Figure 4-19. Surprisingly, while H-OH terminated chains were the main polymer structures formed at 100 ^{o}C, at 130 ^{o}C the most abundant isotope distribution does not correspond to chains with H-OH end groups. The isotope distribution in 4-19 corresponds to both cyclic structures and chains end-capped by H-OK.
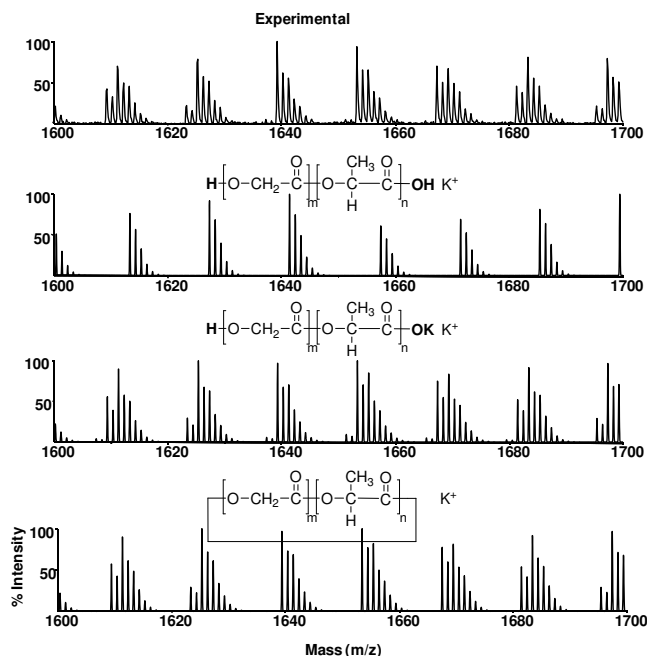
Figure 4-19. Experimental and simulated isotope patterns for different end groups of PDLLGA synthesized at 130 ^{o}C by free lipase PS (recorded with K$^+$).

Using potassium and sodium trifluoroacetate, a difference of 16 *m/z* is detected, ruling out the possibility of H-OK terminated chains as mentioned before. In the spectrum measured with sodium a few additional distributions are recorded in front of the most intense peaks which are absent in the potassium measured spectrum. These distributions are derived from polymer chains with an H-ONa end group. In Figure 4-20, the experimental and simulated isotope patterns clearly match.
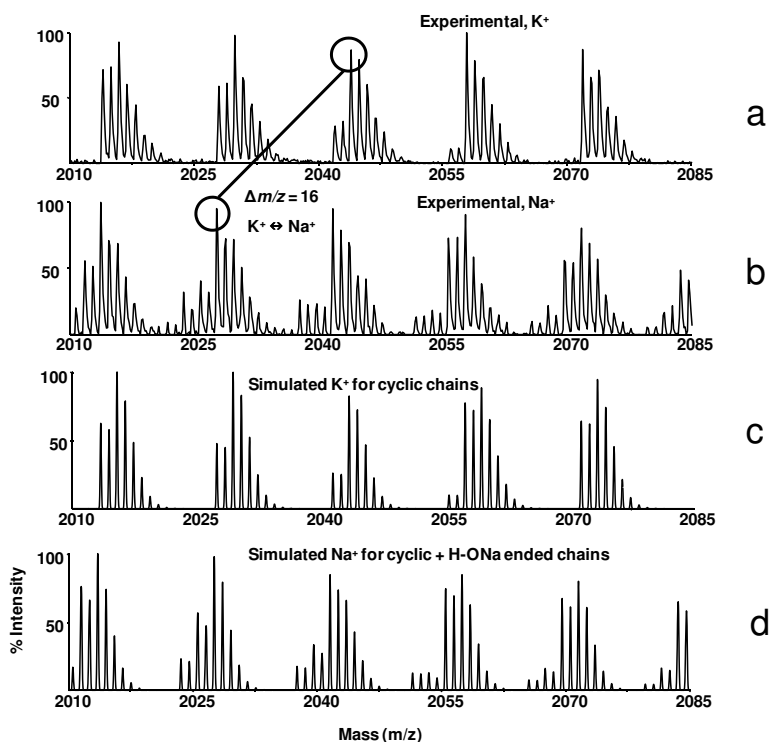
Figure 4-20. Experimental and simulated enlargement of the spectra for PDLLGA (recorded with K^{+} and Na^{+}).

In contrast to the polymer formed at 100 °C, the main structures in this case appear to be cyclic as determined by MALDI-ToF-MS. The contour plots for cyclic structures of PDLLGA and PLLGA synthesized by free and immobilized lipase respectively, are shown in Figure 4-21. Interestingly, unlike the checker board pattern observed for polymer synthesized at 100 °C, the contour plots show a homogeneous area suggesting a highly increased (enzymatic) intermolecular transesterification. The most abundant polymer is the random copolymer of PLGA as can be seen from the plot. Furthermore, no differences were observed between PLLGA and PDLLGA or between the free and immobilized lipase PS.
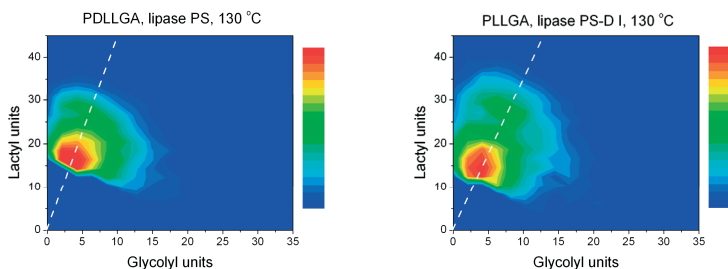
Figure 4-21. a) Contour plot of PDLLGA synthesized by free lipase PS at 130 ^{o}C. b) Contour plot of PLLGA synthesized by lipase PS-D I at 130 ^{o}C. (both plots from spectra recorded with K$^+$)

4.3 Conclusion

MALDI-ToF-MS was successfully used to determine the composition, the end groups and the topology of poly(lactide-*co*-glycolide). It was shown that the molecular characterization of copolymers using MALDI-ToF-MS is a challenging task, but by using intelligent software more information can be derived than initially seemed possible. Overlap of isotope distributions and multiple peak assignment are common and make the spectra more complicated, especially when comonomers only differ by a methyl group. The presence of mainly even numbered polymer chains in lactyl units as visualized by a 'striped' fingerprint of the MALDI-ToF-MS spectrum provided evidence for the selective and preferred transesterification by Sn(Oct)$_2$ for glycolide ester bonds over lactide ester bonds. Furthermore, the bulk polymerization of glycolide and lactide at 100 ^{o}C in the presence of lipase resulted in a tartan patterned fingerprint, strongly suggesting the absence of transesterification of both type of ester bonds. Contrarily, the enzyme supported polymerization carried out at 130 ^{o}C, resulted in a homogeneous plot indicating a completely transesterified system. Although it is clear that the enzyme promotes the ring-opening copolymerization of lactide and glycolide because of the shorter reaction time and higher conversions of both monomers, further investigation is needed to completely elucidate the mechanism and the role the enzyme is playing. The presence of a small amount of the hydroxyacids in the comonomers might be sufficient to initiate or even catalyze polymerization according to a cationic ring-opening polymerization mechanism. At this point the enzymatic polymerization is not capable to compete with metal catalyzed reactions from a molar mass and reaction time perspective.

4.4 Experimental Section

Reagents. D,L-lactic acid (Acros organics, 85 wt%), L-lactic acid (Aldrich, 85 wt%) and glycolic acid (Aldrich, 99%) were used without further purification. Titanium (IV) n-butoxide (Acros organics, 99%) was dissolved in toluene at a concentration of (0.06 mol·L^{-1}). D,L-lactide (DLL) ((+/-)-3,6-dimethyl-1,4-dioxane-2,5-dione, racemic mixture of D,D-lactide and L,L-lactide) and L-lactide (LL) ((3*S*)-*cis*-3,6-dimethyl-1,4-dioxane-2,5-dione) were purchased from Sigma-Aldrich and glycolide (G) (1,4-dioxane-2,5-dione) from Avocado. Amano lipase PS (Sigma-Aldrich) was used without further purification. Lipase PS is derived from *Burkholderia cepacia* and is also available immobilized on diatomaceous earth (lipase PS-D I). Glycolide and lipases were stored in a desiccator in the presence of P_2O_5.

ROP using Sn(Oct)$_2$. In a typical example, a three-neck flask equipped with a mechanical stirrer was charged with a mixture of an 80/20 molar ratio of lactide (5.0 g, 34.7 mmol) and glycolide (1.0 g, 8.7 mmol). Tin(II) 2-ethylhexanoate (0.1 mol‰) was added after complete melting of the monomers. The mixture was stirred for 6 hours under argon atmosphere at 160 ^{o}C. Finally, the polymer was dissolved in chloroform and precipitated with diethyl ether. The purified product was dried *in vacuo* at 40 ^{o}C for 48 hours.

ROP using lipase *Pseudomonas cepacia*. A mixture of lipase PS (8 wt%), lactide (2.0 g, 13.9 mmol) and glycolide (0.4 g, 3.4 mmol) was reacted in an ampule placed in a thermostated oil bath at either 100 ^{o}C or 130 ^{o}C under an argon atmosphere for 7 or 2 days, respectively. Next, the viscous mixture was dissolved in chloroform and the enzyme was removed by filtration. The crude polymer was then precipitated by pouring the solution into methanol under continuous stirring. The precipitate was removed by filtration and dried in vacuo at 40 ^{o}C for 48 hours.

Polycondensation with Ti(OBu)$_4$. In a typical example, an 80/20 molar ratio of an 85 wt% aqueous solution of lactic acid and glycolic acid was charged into a three-neck flask equipped with a mechanical stirrer, a Dean-Stark and a reflux condenser. The mixture of aqueous lactic acid and glycolic acid was then pre-polymerized at a constant temperature of 150 ^{o}C as follows: first, the reaction system was maintained at atmospheric pressure for 0.5 hours, then at a reduced pressure of 0.1-0.2 bar for 2 hours and finally, after addition of the catalyst Ti(OBu)$_4$ (0.01 mol%) , the pressure was reduced to 0.01-0.02 bar for 4 hours. Viscous oligomers were formed and the amount of water removed from the system was measured. After cooling to room temperature, the oligomers were dissolved in acetone and precipitated with ethanol (isolated yield 40%). The purified products were dried *in vacuo* at 40 ^{o}C for 12 hours. Next, the oligomers were gradually heated to 180 ^{o}C at a pressure of 0.1 mbar for 6 hours or longer depending on the desired molecular weight. The reaction was stopped by cooling to room temperature under an argon atmosphere.

The obtained polymer was dissolved in chloroform and precipitated with diethyl ether. The purified product was dried *in vacuo* at 40 ^{o}C for 48 hours.

NMR Analysis. NMR spectra were recorded on a Varian Mercury Vx (400 MHz) and a Varian Gemini 2000 (300 MHz) spectrometer. The solvents used were dimethylsulfoxide-d_6 and chloroform-d_1.

DSC Analysis. The glass transition temperatures of the purified material were measured using a TA Instruments Q100 DSC equipped with a refrigerated cooling system (RCS) and autosampler. The DSC cell was purged with a nitrogen gas flow of 50 mL·min^{-1}. Experiments were performed in aluminum hermetic pans using a heating and cooling rate of 10 ^{o}C·min^{-1}. The T_g was determined from the second heating curve by applying the half-extrapolated tangent method.

SEC Analysis. SEC analysis was carried out using a Waters model 510 pump, a model 410 refractive index detector (at 40 ^{o}C) and a model 486 UV detector (at 254 nm) in series. Injections were done by a Waters model WISP 712 autoinjector, using an injection volume of 50 µL. The columns used were a PLgel guard (5 µm particles) 50 × 7.5 mm column, followed by two PLgel mixed-C (5 µm particles) 300 × 7.5 mm columns at 40 ^{o}C in series. THF (Biosolve, 'non-stabilized') was used as eluent at a flow rate of 1.0 mL·min^{-1}. For calibration polystyrene standards were used (Polymer Laboratories, M_n = 580 to 7.1 × 10^6 g·mol^{-1}). Data acquisition and processing were performed using Waters Millennium 32 (v4.0) software.

MALDI-ToF-MS Analysis. MALDI-ToF-MS analysis was performed on a Voyager DE-STR from Applied Biosystems equipped with a 337 nm nitrogen laser. An accelerating voltage of 25 kV was applied. Mass spectra of 1000 shots were accumulated. The polymer samples were dissolved in THF at a concentration of 1 mg·mL^{-1}. The cationization agents used were potassium trifluoroacetate (Fluka, >99%) or sodium trifluoroacetate (Fluka, >99%) dissolved in THF at a concentration of 1 mg·mL^{-1}. The matrix used was *trans*-2-[3-(4-*tert*-butylphenyl)-2-methyl-2-propenylidene]malononitrile (DCTB) (Fluka) and was dissolved in THF at a concentration of 40 mg·mL^{-1}. Solutions of matrix, salt and polymer were mixed in a volume ratio of 10:1:5, respectively. The mixed solution was hand-spotted on a stainless steel MALDI target and left to dry. The spectra were recorded in the reflector mode. Baseline corrections and data analyses were performed using Data Explorer version 4.0 from Applied Biosystems.

References

[1]   M. Chasin, R. Langer, *Biodegradable Polymers as Drug Delivery Systems*, Marcel Dekker Inc, New York, p1-41, **1990**.

[2]   H.R. Kricheldorf, I. Kreiser, *Makromol. Chem.* **1987**, *188*, 1861.

[3]   H.R. Kricheldorf, I. Kreiser-Saunders, *Makromol. Chem.* **1990**, *191*, 1057.

[4]   O. Dechy-Cabaret, B. Martin-Vaca, D. Bourissou, *Chem. Rev.* **2004**, *104*, 6147.

[5]   A. Dumitrescu, B. Martin-Vaca, H. Gornitzka, J.-B. Cazaux, D. Bourissou, G. Bertrand, *Eur. J. Inorg. Chem* **2002**, *8*, 1948.

[6]   C.-M. Dong, K.-Y. Qiu, Z.-W. Gu, X.-D. Feng, *Polymer* **2001**, *42*, 6891.

[7]   I. Kreiser-Saunders, H.R. Kricheldorf, *Macromol. Chem. Phys.* **1998**, *199*, 1081.

[8]   H.R. Kricheldorf, G. Behnken, *J. Macromol. Sci., Pure Appl. Chem.* **2007**, *44*, 795.

[9]   H.R. Kricheldorf, J.M. Jonté, M. Berl, *Makromol. Chem. Suppl.* **1985**, *12*, 25.

[10]   M. Bero, P. Dobrzynski, J. Kasperczyk, *Polym. Bull.* **1999**, *42*, 131.

[11]   P. Dobrzynski, J. Kasperczyk, H. Janeczek, M. Bero, *Macromolecules* **2001**, *34*, 5090.

[12]   P. Dobrzynski, J. Kasperczyk, H. Janeczek, M. Bero, *Polymer* **2002**, *43*, 2595.

[13]   S. Huijser, B.B.P. Staal, J. Huang, R. Duchateau, C.E. Koning, *Angew. Chem. Int. Ed.* **2006**, *45*, 4104.

[14]   S. Huijser, B.B.P. Staal, J. Huang, R. Duchateau, C.E. Koning, *Biomacromolecules* **2006**, *7*, 2465.

[15]   B.B.P. Staal, *PhD Thesis*, University of Technology Eindhoven, **2005**, ISBN 90-386-2826-9, http://alexandria.tue.nl/extra2/200510540.pdf.

[16]   R.X.E. Willemse, *PhD Thesis*, University of Technology Eindhoven, **2005**, ISBN 90-386-2816-1, http://alexandria.tue.nl/extra2/200510293.pdf.

[17]   M. de Geus, *PhD Thesis*, University of Technology Eindhoven, **2007**, ISBN-10 90-386-2709-2, http://alexandria.tue.nl/extra2/200710129.pdf.

[18]   A. Kowalski, A. Duda, S. Penczek, *Macromolecules* **2000**, *33*, 7359.

[19]   A. Kowalski, A. Duda, S. Penczek, *Macromolecules* **2000**, *33*, 689.

[20]   H. Uyama, S. Kobayashi, *Chem. Lett.* **1993**, *22*, 1149.

[21]   D. Knani, A.L. Gutman, D.H.J. Kohn, *J. Polym. Sci. Part A: Polym. Chem.* **1993**, *31*, 1221.

[22]   S. Matsumura, K. Mabuchi, K. Toshima, *Macromol. Rapid Commun.* **1997**, *18*, 477.

[23]   S. Matsumura, K. Mabuchi, K. Toshima, *Macromol. Symp.* **1998**, *130*, 285.

[24]   J.P. Wahlberg, P-V. Persson, T. Olsson, E. Hedenström, T. Iversen, *Biomacromolecules* **2003**, *4*, 1068.

Polyesters formed by ring-opening polymerization of epoxides and anhydrides.

Abstract. *Copolymerization of oxirane with alicyclic anhydrides applying chromium and zinc catalysts resulted either in polyesters or poly(ester-co-ether)s, depending on the type of nature of the catalyst, presence of a cocatalyst, solvent and type of anhydride. The combination of TPPCrCl as catalyst and 4-N,N-dimethylamino-pyridine as cocatalyst in the copolymerization of cyclohexene oxide with different anhydrides invariably resulted in a completely alternating topology and therefore a pure polyester. Contrarily, the salophenCr(III) complex used with 4-N,N-dimethylamino-pyridine did not afford pure polyesters for the copolymerization of succinic anhydride or cyclopropane dicarboxylic acid anhydride with cyclohexene oxide but did achieve the alternating topology when the alicyclic anhydrides cyclobutane-1,2-dicarboxylic acid anhydride and cyclopentane-1,2-dicarboxylic acid anhydride were used as comonomers. Similar results were obtained when the bisphenoxy zinc catalyst was employed, yet the copolymerization with cyclobutane-1,2-dicarboxylic acid anhydride did show the presence of a few ether bonds. When CO_2 was introduced as termonomer, not only for TPPCrCl and aforementioned cocatalyst perfect poly(ester-co-carbonate)s without ether bonds were obtained, but also a salenCr(III) complex in combination with 4-N,N-dimethylamino-pyridine resulted in ether-free poly(ester-co-carbonate)s.*

5.1 Introduction

Aliphatic polyesters gained increasing attention the past decades due to their good biodegradability. Moreover, the biocompatibility of several aliphatic polyesters has augmented their use as drug delivery vesicles within the human body.[1] Generally, aliphatic polyesters are obtained by either polycondensation or ring-opening polymerization of cyclic esters. The latter route limits the polymer properties to those of the cyclic esters that are available. While the nearly endless choice of diols and diacids gives access to a much larger range of polymer properties for AABB polyesters, their synthetic procedure of polycondensation is disadvantageous. Usually, drastic conditions are required to remove water and to drive the reaction towards high conversion, required to obtain high molecular weight products. Ring-opening polymerization of oxiranes and anhydrides is an alternative way to synthesize AABB type polyesters. The catalytic coupling of oxiranes with acid anhydrides was first reported in the 1950s,[2] but the undesirable side-reaction of homopolymerization of the oxirane and the low molecular weights generally obtained impeded its popularity and its development towards a routine pathway. The finding of selective catalysts to optimize this route is the key to a wide variety of monomers for the production of aliphatic polyesters with a broad span of physical properties. Until recently, the best results in terms of alternating character and molecular weight were achieved by Inoue[3] and Maeda[4] with an aluminum porphyrinato complex and magnesium diethoxide as catalysts, respectively. During our study on the copolymerization of oxiranes with anhydrides, a similar study was reported by the group of Coates. They reported high molecular weight material synthesized from various alicyclic oxiranes and anhydrides using a zinc 2-cyano β-diketiminato complex. Molecular weights up to 55,000 g·mol^{-1} were achieved in a perfectly alternating microstructure.[5] This study marked a breakthrough in the polyester synthesis via the oxirane/anhydride route as not earlier such results have been reported. Additionally, Coates and coworkers reported the successful terpolymerizations of oxirane/anhydride and CO_2 with as result a one pot synthesis of di-block poly(ester-*co*-carbonate)s.[6] Other terpolymerizations of carbon dioxide, propylene oxide and maleic anhydride were reported to occur in an alternating repetition of CO_2-propylene oxide-maleic anhydride by a polymer supported bimetallic complex.[7] Not only metal-based catalysts but also enzymes have been reported to copolymerize oxiranes and anhydrides, but activities were generally rather low.[8,9]

5.2 Results and Discussion ~ Polyesters

In this chapter we report on some mechanistic aspects of the alternating copolymerization of the alicyclic epoxide cyclohexene oxide (CHO) with succinic anhydride (SA), cyclopropane-1,2-dicarboxylic acid anhydride (CPrA), cyclobutane-1,2-dicarboxylic acid anhydride (CBA) and cyclopentane-1,2-dicarboxylic acid anhydride (CPA) using chromium porphyrinato (**1**), salophen (**2**) complexes and bis(2,6-difluoro-phenoxy) zinc (**3**) as catalysts (Scheme 5-1). The polymer products were subjected to an intensive MALDI-ToF-MS study to determine the polymer's topology and to derive information on chain termini. The catalysts were selected based on their known ability to copolymerize cyclohexene oxide with carbon dioxide to afford polycarbonates.[10] Next to these complexes, also Coates' β-diketiminato zinc catalyst ({HC[C(Me)NC$_6$H$_3$Et$_2$]$_2$}ZnO^{i}Pr)[11] was applied but unfortunately the complex decomposed in the presence of anhydrides.
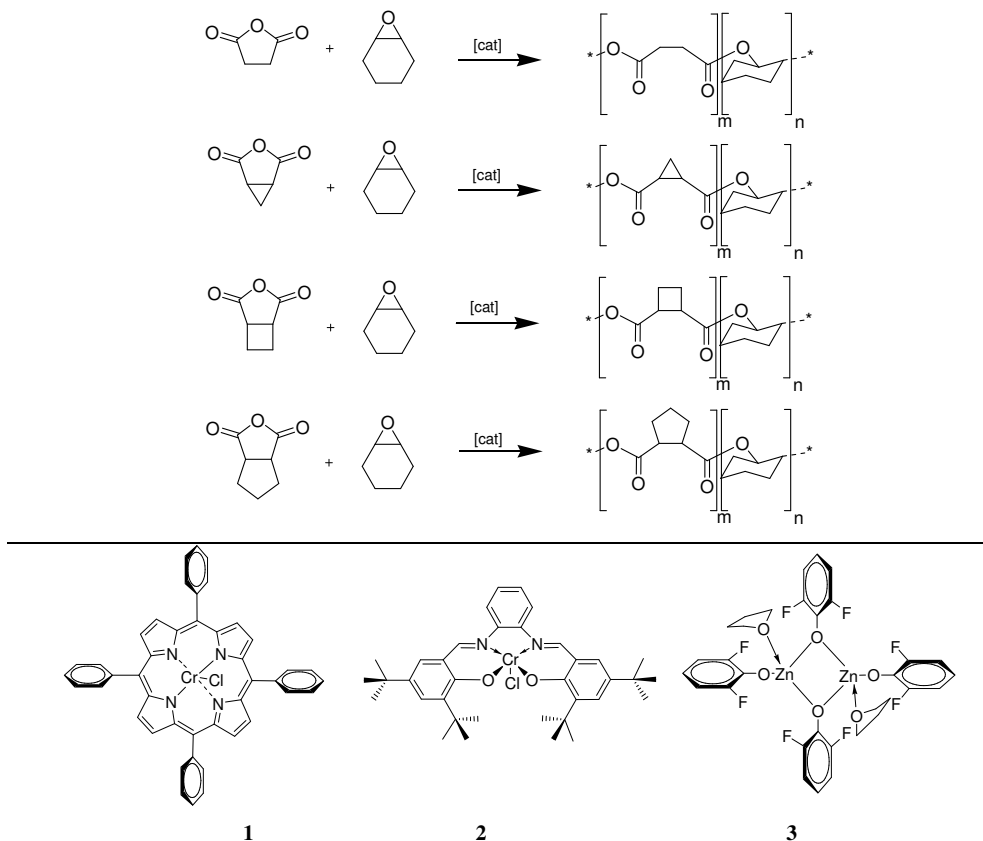
Scheme 5-1. a) Synthesis of polyester from cyclohexene oxide and dicarboxylic acid anhydrides (succinic anhydride, cyclopropane-, cuclobutane- and cycopentane-1,2-dicarboxylic acid anhdyride. b) Complexes used in the copolymerization of cyclohexene oxide and dicarboxylic acid anhydrides.

The copolymerizations were performed in bulk as well as in a toluene solution at 100 ^{o}C with a monomer to initiator ratio of 500:1. The results of the reactions are depicted in Table 5-1. Evidently, only few ester linkages were formed in the reactions where only the chromium porphyrinato or salen complexes were applied, resulting in mainly polyether with negligible incorporation of anhydride units. A similar observation was made by Inoue *et al.* who reported mainly oligoether formation when aluminum porphyrinato complexes were employed without phosphonium salts as cocatalysts.[12] It was reported that most metal salen and porphyrinato complexes used for the oxirane – CO_2 copolymerization gave far higher activities in the presence of nucleophilic cocatalysts such as DMAP (4-N,N-dimethylamino-pyridine) or MeIm (N-methyl-imidazole).[10,13-17] We therefore explored the use of DMAP as cocatalyst for the chromium systems. The presence of DMAP as cocatalyst not only accelerated the copolymerization of succinic anhydride with cyclohexene oxide, it also strongly stimulated the formation of ester linkages.

Table 5-1. Results of solution and bulk polymerizations.[a]

Entry	Catalyst (+ cocatalyst)	Anhydride	Time (min)	Conv. CHO/%[b]	Ester bonds/%[b]	$\overline{M}_n$ g/mol[e]	PDI[c]
1	DMAP	SA (bulk)	140	33	53	700	1.2
2	DMAP	SA (solution)	300	<5	-	-	-
3	DMAP	CPA (bulk)	140	52	100	1600	1.1
4	DMAP	CPA (solution)	300	0	-	-	-
5	1	SA (bulk)	140	85	14	2300	1.9
6	1	SA (solution)	300	<10	0	-	-
7	1 + DMAP	SA (bulk)	140	89	100	1300	1.6
8	1 + DMAP	SA (solution)	300	81	100	1500	1.8
9	1 + DMAP	CPrA (bulk)	60	100	100	5600	1.5
10	1 + DMAP	CPrA (solution)	300	100	100	6600	1.6
11	1 + DMAP	CBA (bulk)	30	100	100	10000	5.2[§§§]
12	1 + DMAP	CPA (bulk)	140	100	100	5600	1.5
13	1 + DMAP	CPA (solution)	300	100	100	4900	1.3
14	2	SA (bulk)	140	57	11	1800	4.2
15	2	SA (solution)	300	0	-	-	-
16	2 + DMAP	SA (bulk)	140	60	67	1500	1.6
17	2 + DMAP	SA (solution)	300	43	73	1000	1.3
18	2 + DMAP	CPrA (bulk)	140	55	70	4700	1.4
19	2 + DMAP	CPrA (solution)	300	65	85	5700	1.3
20	2 + DMAP	CBA (bulk)	140	76	100	6500	1.3
21	2 + DMAP	CPA (bulk)	140	72	100	8400	1.3
22	2 + DMAP	CPA (solution)	300	23	100	3200	1.3
23	3	SA (bulk)	140	100	30	2800	1.9
24	3	SA (solution)	300	100	80	5800	1.3
25	3	CPrA (bulk)	140	100	26	2200	2.3
26	3	CPrA (solution)	300	87	57	3200	1.6
27	3	CBA (bulk)	140	100	n.d.	3300	1.7
28	3	CPA (bulk)	140	100	100	7900	1.4
29	3	CPA (solution)	300	83	100	6600	1.3

[a] [M]/[I]=500/1, [DMAP]/[cat]=1/1, T = 100 ^{o}C, [b] determined by ^{1}H-NMR/MALDI, [e] determined by SEC.

[§§§] Unexpectedly high PDI.

The copolymerization with **1**/DMAP afforded perfectly alternating oxirane-anhydride copolymers. With 73% ester linkages **2**/DMAP showed a similar trend, although the activity and selectivity were lower than for **1**/DMAP. Interestingly, the blank experiments with DMAP alone also afforded polymer products but the yields were significantly lower than with **1** or **2**, especially when carried out in solution.

MALDI-ToF-MS spectra were recorded of all crude products prepared by **1**, **2** and **3**. End group determination was performed by comparing the recorded MALDI-ToF-MS spectra with simulations of the isotope patterns for given polymer structures. The recorded MALDI-ToF-MS spectra along with the simulated isotope patterns for the most abundant peaks are for the major part given in the appendix on the CD-R included. The MALDI-ToF-MS spectra of polymers prepared by **1** and **2** in bulk in the absence of DMAP clearly show isotope patterns for chains with higher cyclohexene oxide content. Furthermore, two distinct distributions, one corresponding to cyclic polymers and one consisting of linear polymer chains with -OH end groups, were observed. Cyclic products are most probably formed by intramolecular transesterification during the polymerization. Hydroxy-terminated polymers are assumed to be formed via water initiation. The MALDI-ToF-MS spectrum of the products formed by **1**/DMAP showed an *m/z* interval of 198 between the consecutive peaks corresponding to the addition of a cyclohexene oxide and succinic anhydride repeating unit, thus indicating a completely alternating microstructure (Figure 5-1). For **2**/DMAP, still isotope patterns for chains with a higher cyclohexene oxide content are present albeit the poly(ester-*co*-ether)s mainly contain ester linkages. In the copolymerizations catalyzed by **1** and **2** where DMAP is used as cocatalyst, the determination of the end groups appeared not to be straightforward. The expected Cl-terminated chains, or cyclics and OH-terminated chains as found in the bulk, were not found.

In order to obtain a better idea about possible chain termini more information was gathered by recording MALDI-ToF-MS spectra with different cationization salts. Surprisingly, the most abundant peaks in the spectrum recorded with potassium were also the most abundant peaks in the spectrum recorded with sodium, *i.e.* the peaks remained at exactly the same *m/z*. Normally, a shift of −16 *m/z* is found between the distributions recorded with K⁺ and Na⁺, the difference in atomic mass between both atoms. Moreover, even in the absence of any additional cationization salt a clear MALDI-ToF-MS spectrum was obtained with identical isotope distributions at the same position in the spectrum as when Na⁺ or K⁺ were used (Figure 5-2). Apparently, the chains were already ionized beforehand. Using N-MeIm as cocatalyst instead of DMAP, the spectrum shifted in total −40 *m/z*, which is equal to the molar mass difference of DMAP and N-MeIm (Figure 5-3). This implies that the Lewis base cocatalysts remain strongly attached to the polymer. Simulation of the isotope patterns for a chain endcapped at one site with the cationic cocatalyst fragment (DMAP or MeIm) and a proton as the other end group afforded a perfect fit of the isotope distributions. This observation strongly suggests

the existence of zwitterionic structures. The polymer prepared with **1**/DMAP showed a similar structure but interestingly enough with exactly n SA and n+1 CHO units (Figure 5-4).
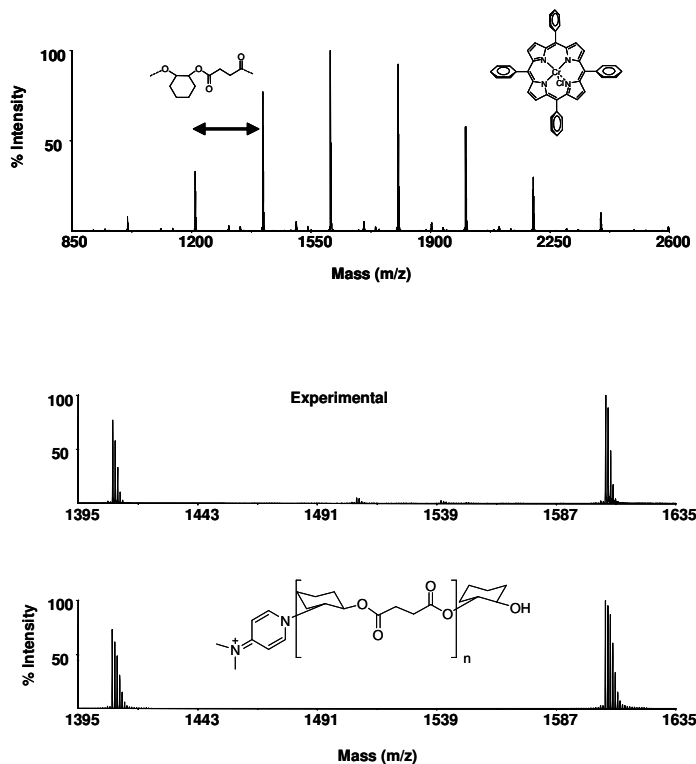
Figure 5-1. MALDI-ToF-MS spectrum of product synthesized in bulk from succinic anhydride and cyclohexene oxide in the presence of **1**/DMAP.
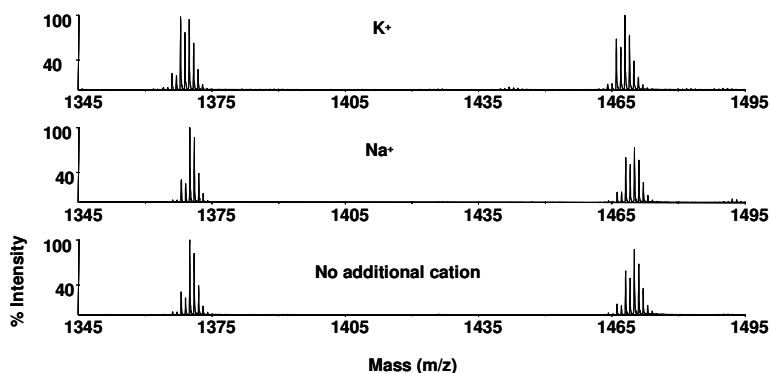
Figure 5-2. MALDI-ToF-MS spectra recorded with different salts and without an additional salt for copolymers polymerized of cyclohexene oxide and succinic anhydride in presence of **2**/N-MeIm.
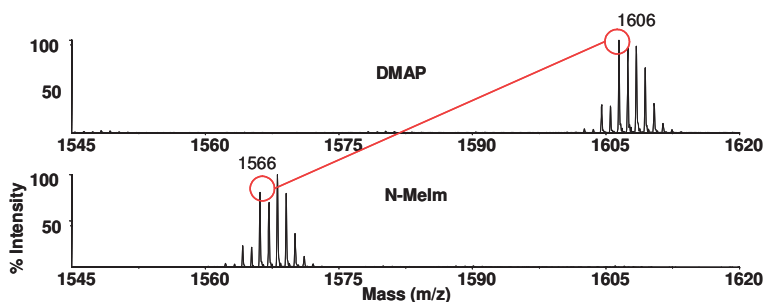
Figure 5-3. Comparison of MALDI-ToF-MS spectra of product synthesized in bulk from succinic anhydride and cyclohexene oxide in the presence of **2**/DMAP and **2**/N-MeIm. Peaks shift –40 *m/z.*
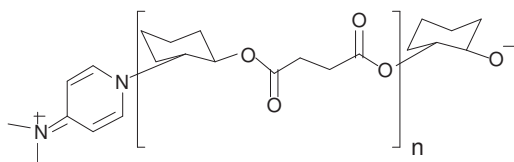
Figure 5-4. Possible structures of zwitterionic polyester synthesized by succinic anhydride and cyclohexene oxide in the presence of **1**/DMAP.

Darensbourg *et al.* already proposed the possible existence of a zwitterionic polymer for the copolymerization of carbon dioxide and cyclohexene oxide (Figure 5-5).[10,18] It was believed that the DMAP reacts with carbon dioxide to form a carbamate unit which initiates the polymerization. To verify whether a DMAP end group would indeed remain attached to a *polycarbonate* chain, the MALDI-ToF-MS spectrum of poly(cyclohexene carbonate), synthesized using a salen chromium chloride with DMAP as cocatalyst, was recorded with K^+, Na^+ and without an additional cation. Again, the isotope patterns remain at the same position regardless of which cationization agent is used and simulation of the DMAP-endcapped polymer gave a perfect fit with the recorded spectrum. Based on the MALDI-ToF-MS spectrum it can be concluded that all polycarbonate chains correspond to a perfectly alternating polymer with one additional cyclohexene oxide unit. Since it is highly unlikely that all chains contain exactly one additional ether linkage, it is therefore most probable that the DMAP has reacted with cyclohexene oxide rather than carbon dioxide. The extra cyclohexene moiety was also confirmed by the poly(ester-*co*-carbonate)s discussed in paragraph 5.3.
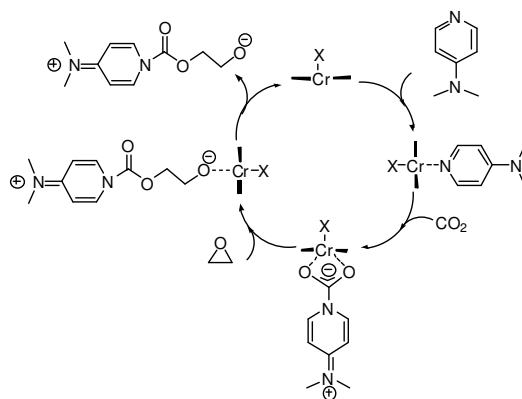
Figure 5-5. Zwitterionic mechanism for copolymerization of CO_2 with CHO proposed by Darensbourg.[10,18]

As explained in detail in Chapter 2, a MALDI-ToF-MS spectrum of a copolymer can be converted into a so-called finger print or contour plot. The shape and position of the plot are characteristic for the topology of the polymer. Contour plots constructed from the recorded MALDI-ToF-MS spectra of polymers obtained from SA/CHO catalyzed by **1**/DMAP reveal their perfectly alternating character, while the polymers prepared with **2**/DMAP clearly show a higher content of cyclohexene oxide units, resulting in a random poly(ester-*co*-ether) (Figure 5-7). An apparent difference in the amount of ester linkages was found between the reactions in bulk and in solution using the bis(2,6-difluoro-phenoxy) zinc complex. In bulk the zinc complex produced polymers with only approximately 30% ester bonds whereas in solution this amount increased to 80%. The reason for this behavior is as yet not understood. From the contour plots it can be seen that in bulk a more gradient-like topology is obtained with enrichment of cyclohexene oxide in the high molecular weight fraction (Figure 5-7). The end groups of the polymer prepared with **3** in solution are the expected phenoxides. In contrast, the polymers produced by **3** in bulk also show cyclic and hydroxide terminated chains besides these phenoxide end groups. With polydispersities ranging from 1.3 to 1.9, the polymerizations catalyzed by **3** are well-controlled, as opposed to the very broad PDIs for polycarbonates obtained from the copolymerization of CHO and CO_2 catalyzed by **3**.[19]

From the results discussed above it is clear that the chromium and zinc complexes, known to catalyze the oxirane – CO_2 copolymerization, are also effective catalysts for the oxirane – anhydride copolymerization affording either poly(ester-*co*-ether)s or polyesters. Unfortunately, the molecular weights obtained are rather low, a common feature for most catalysts.[2-4] It was assumed that increasing the ring strain in the anhydride would increase its reactivity, which might lead to more alternating copolymers with higher molecular weights.

The influence of increasing the reactivity of the anhydride monomer was studied for the different catalysts by replacing the aliphatic succinic anhydride by the alicyclic anhydrides cyclopropane-1,2-dicarboxylic acid anhydride, cyclobutane-1,2-dicarboxylic acid anhydride and cyclopentane-1,2-dicarboxylic acid anhydride. Similarly as for succinic anhydride, cyclopropane-1,2-dicarboxylic anhydride only afforded a completely alternating polymer when **1**/DMAP was used in solution as well as in bulk, but for both complex **2**/DMAP and **3** still ether bonds could be found (Figure 5-7). On the other hand in the copolymerization with cyclobutane-1,2-dicarboxylic acid anhydride in bulk using **2**/DMAP an alternating topology was discovered whereas **3** still showed a few ether bonds. Evidently, using cyclopentane-1,2-dicarboxylic acid anhydride as comonomer, all the catalysts afforded perfectly alternating polymer chains with significantly higher molecular weights than with succinic anhydride. Furthermore, also when the reaction was carried out in bulk perfectly alternating copolymers were afforded. The fingerprints derived from the MALDI-ToF-MS spectra confirmed again the alternating topology (Figure 5-7). The contour plots of the polymer derived from **2**/DMAP and **3** are slightly broader than the plot of the polymer prepared by **1**/DMAP. This is due to the fact that the possibility exists of having two anhydride units but also two cyclohexene oxide units at the chain termini.

Surprisingly, the molecular weights are an order of magnitude lower than theoretically expected from the monomer to initiator ratio although in some cases 100% conversion is achieved. We exclude here the possibility of transesterification, by for example unbound DMAP, as the main cause of this discrepancy since the molar mass distributions of the oligomers synthesized are relatively narrow. However, the size exclusion chromatograms did reveal bimodality as shown in Figure 5-6 for all three catalysts for amongst others the comonomer pair CHO/CPA.
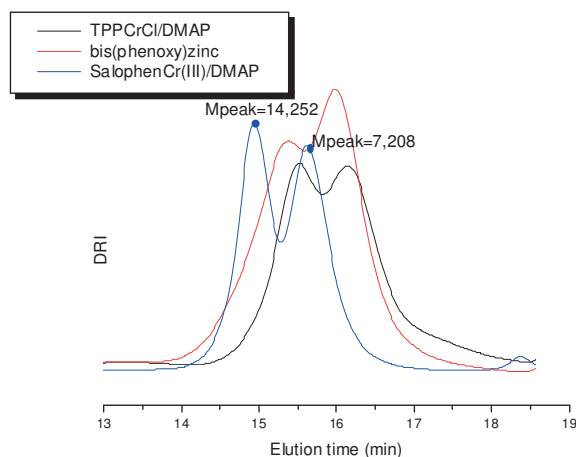
Figure 5-6. Bimodality in GPC chromatograms of the bulk polymerization of CPA and CHO for all three complexes (Entries, 12, 21, 28, Table 5-1).
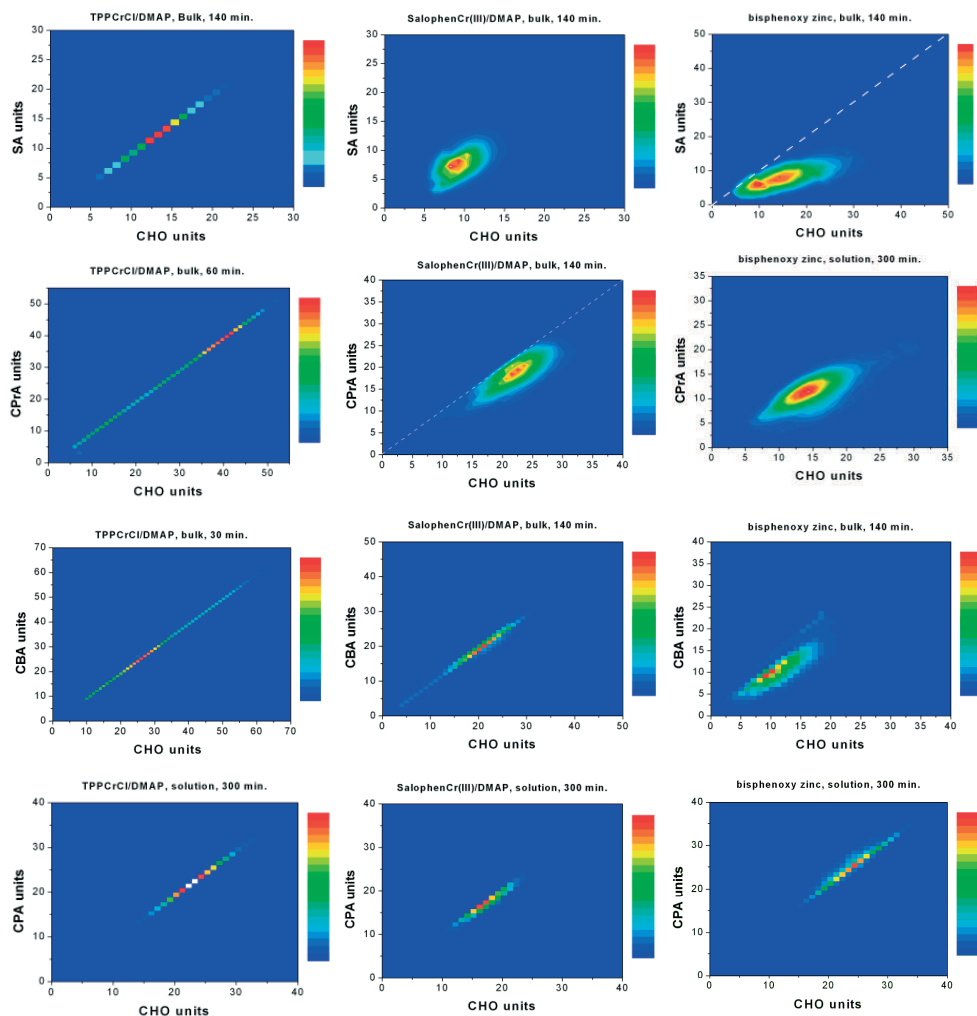
Figure 5-7. Contour plots of MALDI-ToF-MS spectra of polyesters synthesized from a) SA/CHO by **1**/DMAP (Entry 7), b) SA/CHO by **2**/DMAP (Entry 16), c) SA/DMAP by **3** (Entry 23), d) CPrA/CHO by **1**/DMAP (Entry 9), e) CPrA/CHO by **2**/DMAP (Entry 18), f) CPrA/CHO by **3** (Entry 26), g) CBA/CHO by **1**/DMAP (Entry 11), h) CBA/CHO by **2**/DMAP (Entry 20), i) CBA/CHO by **3** (Entry 27), j) CPA/CHO by **1**/DMAP (Entry 13), k) CPA/CHO by **2**/DMAP (Entry 22), l) CPA/CHO by **3** (Entry 29). *(N.B. Entries of Table 5-1 are given between parentheses.)*

The observation of bimodal behavior is not new and has been observed for oxirane-anhydride as well as for oxirane-CO_2 copolymerizations.[20,21] Inoue and Darensbourg raised the possibility that the bimodal behavior can derive from the simultaneous growth of two polymer chains on each side of respectively a metalloporphyrin and metallosalen plane.[10] The longer chain was expected to grow on the side of the axial ligand rather than on the side of the organic salt. Recently, a similar bimodality has been reported and studied by Sugimoto and Kuroda in the alternating polymerization of cyclohexene oxide with CO_2 using DMAP/TPPCoCl.[22] They attributed this behavior to water initiation occuring even after intensive drying. In addition, the bimodality in molecular weight distributions is not limited to porphyrin and salen complexes only, but also zinc diiminate complexes disclose this behavior. Eberhardt *et al.* reported a narrow yet bimodal molecular weight distribution for the polymerization of cyclohexene oxide with CO_2 employing a zinc(II) sulfinate complex.[23]

To obtain a better understanding of the origin of this phenomenon, an intensive end group study by MALDI-ToF-MS was extended by a comparison with SEC. For the copolymers synthesized by the **1**/DMAP catalyst system, an overlay of the size exclusion chromatograms with the MALDI-ToF-MS spectra confirms that the bimodality was indeed detected without structural discrimination by MALDI-ToF-MS (Figure 5-8).
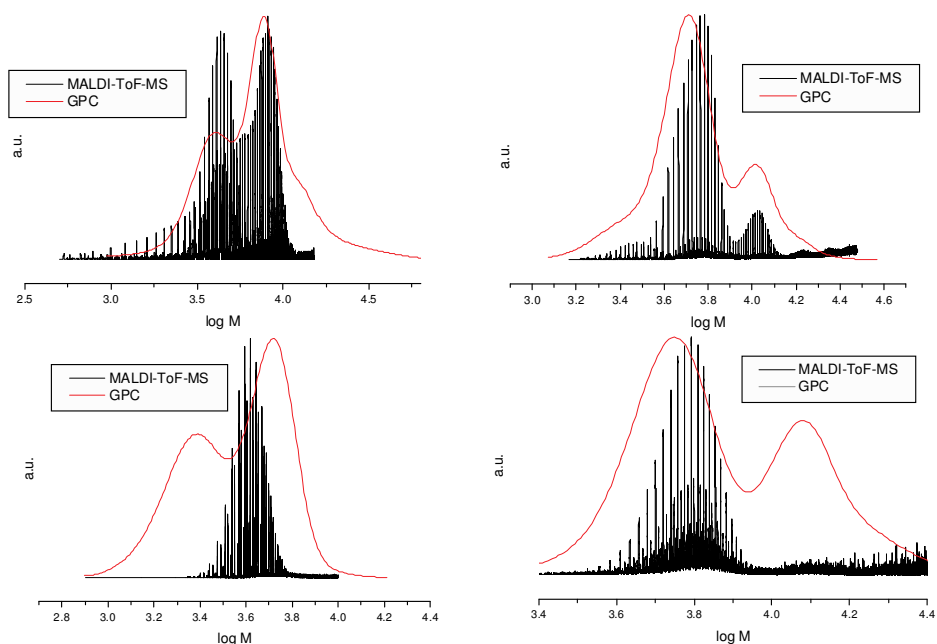
Figure 5-8. Overlay SEC and MALDI-ToF-MS a) CPrA/CHO by **1**/DMAP (Entry 9), b) CPA/CHO by **1**/DMAP (Entry 13), c) CPA/CHO by **2**/DMAP (Entry 22), d) CPA/CHO by **3** (Entry 29). *(N.B. Entries of Table 5-1 are given between parentheses.)*

In contrast to the copolymer synthesized from cyclohexene oxide and the aliphatic succinic anhydride, the beforehand-ionized DMAP terminated chains were not recorded for the copolymers synthesized from the *alicylic* anhydrides and cyclohexene oxide employing the catalytic system **1**/DMAP. A narrow, low molecular weight, low intensity distribution was attributed to H-Cl terminated chains, but H-OH terminated chains appeared to dominate the spectrum. These hydroxy-terminated species were attributed to the presence of concomitant water. An interesting observation is that these hydroxy-terminated chains are not restrained to a single distribution. This is clearly visible in the MALDI-ToF-MS spectrum for the comonomer pair CPA/CHO, in which two distributions differing by approximately a factor of 2 in molecular weight can be appointed to these chain termini. On the other hand, the copolymers synthesized by **2**/DMAP did show DMAP terminated chains even for the higher molar masses as can be seen in the appendix on the CD-R. Unexpectedly, the bimodality was not recorded by MALDI-ToF-MS for the comonomer pair CPA/CHO in case of **2**/DMAP and **3**, suggesting end group discrimination. Presumably, the signal deriving from polymer chains of the second distribution is completely suppressed by the excellent ionization of chains terminated by DMAP synthesized by the catalytic pair **2**/DMAP. We expect that the ionization of DMAP terminated chains is similar to the ionization of polymer chains with covalently bounded ammonium cations which are known to display excellent resolved MALDI-ToF-MS spectra. Likewise, the discrimination in polymer chains synthesized by **3** was thought to derive from a difference in ionization. According to our simulations, the polymer chains belonging to the distribution detected by MALDI were terminated by a phenoxy moiety. Furthermore, an overlay of the DRI and UV signals of the size exclusion chromatogram of the polymer synthesized from CPA/CHO by **3**, showed only one peak in the UV signal which is in agreement with the presence of the UV active phenoxy moiety at the chain end.

Summarizing, no conclusive evidence was found to attribute the established bimodality to a consistency in end group formation or to a certain mechanism, partially as the result of discrimination by MALDI-ToF-MS. Nevertheless, the finding of charged DMAP terminated chains supports the zwitterionic formation reported by Darensbourg. Moreover, the formation of this end group stresses the possibility of growth of a polymer chain on both sides of the complexes' plane. Probably, a combination of simultaneous growth of two chains and water initiation resulted in an ensemble of DMAP, H-Cl and H-OH terminated chains which in their turn are responsible for the multimodal distributions recorded.

5.3 Results and Discussion ~ Poly(ester-*co*-carbonate)s

Carbonate segments in polyesters gained interest in the biomedical sector due to the ability to tune the hydrolytic degradation rate of these materials and to reduce the autocatalytic effect.[24] Poly(ester-*co*-carbonate)s are generally synthesized by the reaction of cyclic esters with cyclic carbonates. The most prominent materials are obtained by the polymerizations of lactide, glycolide and ε-caprolactone with trimethylene carbonate.[25] Intriguingly, the synthesis of poly(ester-*co*-carbonate)s by employing CO_2 as reactant has not been extensively investigated whereas the copolymerization of oxiranes and CO_2 is known since the 1970s.[26] Only a few studies report on the synthesis of poly(ester-*co*-carbonate)s by the addition of a cyclic ester as lactide or lactone to the polymerization of epoxide and CO_2. Along with the possibility to synthesize homopolymer polyesters by oxiranes and dicarboxylic anhydrides as described in the previous paragraphs, the door to the terpolymerization of oxirane, CO_2 and dicarboxylic acid anhydride has been opened. Coates and coworkers reported the successful terpolymerizations of oxirane/anhydride and CO_2 with as result a one pot synthesis of di-block poly(ester-*co*-carbonate)s.[6] Other terpolymerizations of carbon dioxide, propylene oxide and maleic anhydride were reported to occur in an alternating repetition of CO_2-propylene oxide-maleic anhydride by a polymer supported bimetallic complex.[7] Here, we report on the successful terpolymerization of cyclohexene oxide, carbon dioxide and alicyclic dicarboxylic anhydrides (Scheme 5-2). Terpolymerizations were performed overnight at 80 °C in toluene using 50 bar of CO_2 pressure. The results of the terpolymerizations of cyclohexene oxide, carbon dioxide and either cyclopropane-1,2-dicarboxylic acid anhydride or cyclopentane-1,2-dicarboxylic acid anhydride using ditertbutylSalenCrCl (**4**) with DMAP as cocatalyst are given in Table 5-2.
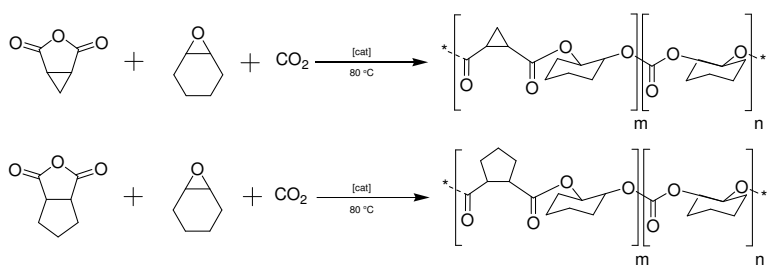
Scheme 5-2. Synthesis of poly(ester-*co*-carbonate) from cyclohexene oxide, carbon dioxide and alicylic dicarboxylic acid anhydrides.

Table 5-2. Results of terpolymerizations of CHO, CPrA or CPA and CO_2.[a]

Entry	Catalyst (+ cocatalyst)	Anhydride	Ratio CHO/ANH	Conv.[b] (CHO %)	$\overline{M}_n$ g/mol[e]	PDI[c]	Ratio[d] CHO_CO_2/ CHO_ANH
1	**1**+DMAP	CPrA	2/1	100	3200	1.13	~1/2
2	**1**+DMAP	CPA	2/1	100	10260	1.2	~1/2
3	**4**+DMAP	CPrA	1/1	90	1100	1.14	~0/1
4	**4**+DMAP	CPrA	2/1	96	2600	1.12	~1/2
5	**4**+DMAP	CPrA	4/1	97	3800	1.13	~1.5/1
6	**4**+DMAP	CPrA	8/1	93	5800	1.14	~2.5/1
7	**4**+DMAP	CPA	1/1	100	7000	1.2	~0/1
8	**4**+DMAP	CPA	2/1	87	6600	1.3	~1/2
9	**4**+DMAP	CPA	2/1	96	8300	1.4	~1/2
10	**4**+DMAP	CPA	4/1	87	7500	1.3	~1/1
11	**4**+DMAP	CPA	8/1	95	7700	1.4	~4/1

[a] Conditions: 50 bar CO_2, [M]/[I]=500, [DMAP]/[Cat]=1/1, T= 80 °C, Toluene, [b] determined by ^{1}H-NMR,
[c] determined by SEC, [d] ratio of carbonate to ester in the copolymer determined by MALDI-ToF-MS.

The polymer products were characterized by ^{1}H-NMR, SEC and MALDI-ToF-MS. Analysis of the terpolymers by ^{1}H-NMR spectroscopy proved difficult as the polyester and polycarbonate signals overlapped. Characterization by MALDI-ToF-MS was more successful. The difference between two consecutive peaks in the MALDI-ToF-MS spectrum of the terpolymer with cyclopropane dicarboxylic acid anhydride equals 68 *m/z*, being the direct difference between a [CHO_CO_2] unit and a [CHO_CPrA] unit. This concomitantly discloses that no additional ether linkages are present whereas the copolymerization under similar conditions but in the absence of CO_2 did give ether linkages. Simulation of the end groups showed the presence of beforehand-ionized DMAP terminated chains, as was also observed for epoxide-anhydride and epoxide-CO_2 copolymers, as well as water initiated chains. An overlay of the MALDI spectrum recorded with and without cationization salt and the size exclusion chromatogram revealed that the seemingly unimodal distribution is in fact a bimodal distribution. One distribution is the zwitterionic DMAP terminated chain, the other, the H-OH terminated chain (Figure 5-9).
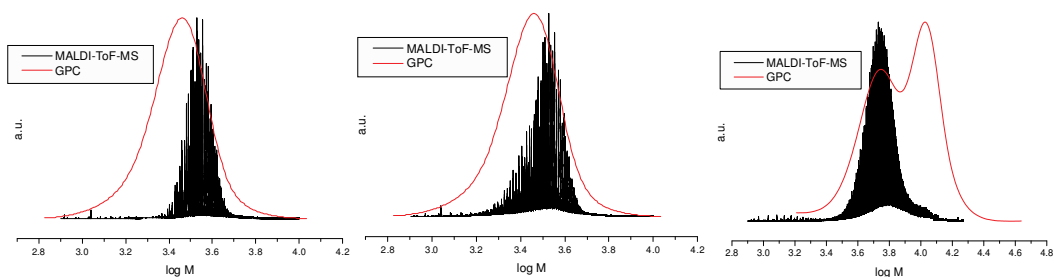
Figure 5-9. Overlay of SEC and MALDI-ToF-MS of a) CPrA/CHO/CO_2 recorded without doping agent, b) CPrA/CHO/CO_2 recorded with doping agent, c) CPA/CHO/CO_2 recorded with doping agent.

Interestingly, the presence of an additional cyclohexene oxide unit, as shown in Figure 5-4 for the analogues polyesters, was confirmed by the position of the contour plot for the terpolymer of cyclopropane anhydride, cyclohexene oxide and CO_2. An extra cyclohexene oxide unit in our simulations resulted in a completely different composition. The composition without this extra unit displayed an excess of carbonate bonds to ester bonds, whereas the presence of the unit showed the opposite. The true plot was appointed with the knowledge that the anhydride reacts faster and by ^{1}H-NMR. Figure 5-10 shows both contour plots together with the chemical structures for which the MALDI-ToF-MS spectra were simulated.
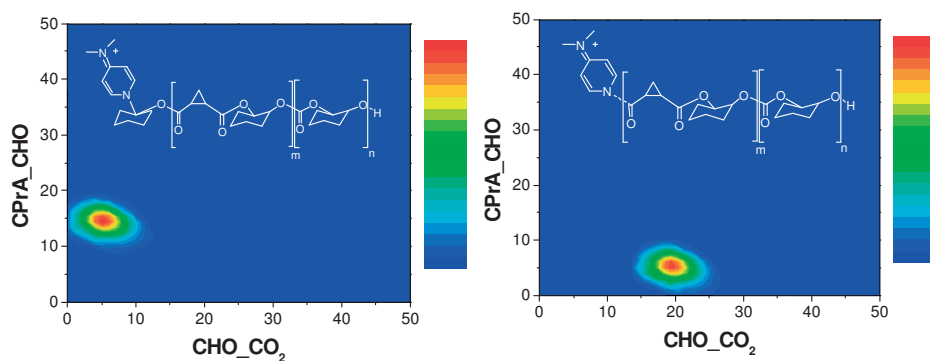
Figure 5-10. a) Contour plot of CPrA/CHO/CO_2 poly(ester-*co*-carbonate) with additional cyclohexene oxide unit. b) Contour plot of CPrA/CHO/CO_2 poly(ester-*co*-carbonate) without additional cyclohexene oxide unit.

For the terpolymer set CPA/CHO/CO$_2$, the MALDI-ToF-MS spectrum shows a difference between consecutive peaks of 46 *m/z*. This equals the difference between two [CHO_CO$_2$] units (284 g·mol^{-1}) and one [CHO_CPA] unit (238 g·mol^{-1}) and corresponds to an ether-free polymer. Whereas, *in analogy to the copolymerizations*, the SEC showed a bimodal distribution (Figure 5-9), the MALDI of the same sample displays a unimodal distribution of chains end-capped by a proton on one side and chloride on the other side of the chain. MALDI measurements without additional cationization salts did not reveal the existence of DMAP end-capped polymers as was observed for the corresponding CPrA/CHO/CO$_2$ system. Why, in this case, the second bimodal distribution in SEC was not observed with MALDI is not clear. Possibly, the second distribution originates from chains with different end-groups that prevent the polymer to 'fly'.

The contour plots derived from the MALDI-ToF-MS spectra of the terpolymerizations of both cyclopropane dicarboxylic acid anhydride and cyclopentane dicarboxylic acid anhydride are depicted in Figures 5-11 and 5-12. It can be seen that upon decreasing the loading of anhydride, more carbonate bonds are present and that even pure polycarbonate is found for the polymerizations in which CPA was employed as termonomer. Surprisingly, pure *polyester* was produced when applying a 1:1 ratio of anhydride to epoxide, indicating a much higher reactivity of the anhydride in comparison to CO$_2$. The effect of this difference in reactivity was expected to result in a blocky microstructure in line with the findings of Jeske *et al*., who reported on the one-step di-block copolymer formation for the terpolymerization of diglycolic anhydride, cyclohexene oxide and CO$_2$.[6] Unfortunately as mentioned in Chapter 2 on page 35, the shape and position of the contour plot in case of a living polymerization do not reveal whether the topology is block or random unless samples are taken over time. Identical reactions performed at different reaction times for the terpolymerization of CPA/CHO/CO$_2$ show that the average composition remains constant both for one night and two nights of reaction time, (Figure 5-12) indicating a random microstructure. This is most likely the result of the relatively high CO$_2$ pressure needed for salen complexes and, evidently, a lowering of the pressure to 10 bar CO$_2$, resulted in pure *polyester*. Further research is currently conducted on terpolymerizations and the polymers' related microstructures.

A discrepancy between the conversion and the ratio of carbonate to ester bonds was found. Despite the fact that the conversion reached nearly 100%, the ratio did not equal 1:1. This inconsistency can be explained by the presence of some free polycarbonate and/or polyether. The free polycarbonate was detected by MALDI whilst NMR showed some free polyether. Furthermore the difference in conversion and molecular weight between the first and second night of reaction time suggests that cyclohexene oxide was lost during or after the reaction. This might well be due to the formation of cyclohexene carbonate as side product.

Figure 5-11. MALDI-ToF-MS spectra and matching contour plots of poly(ester-*co*-carbonate) synthesized by CO_2 and different loadings of CHO/CPrA. Contour plots of spectra show the changing ratio of ester to carbonate bonds in the terpolymer with decreasing anhydride to epoxide ratio (Entries 3-6, Table 5-2).
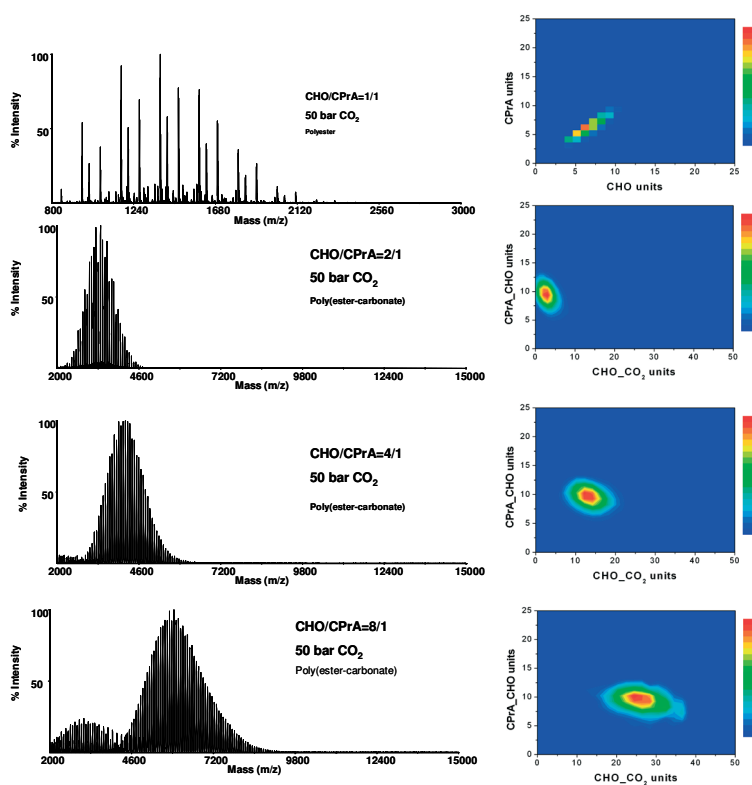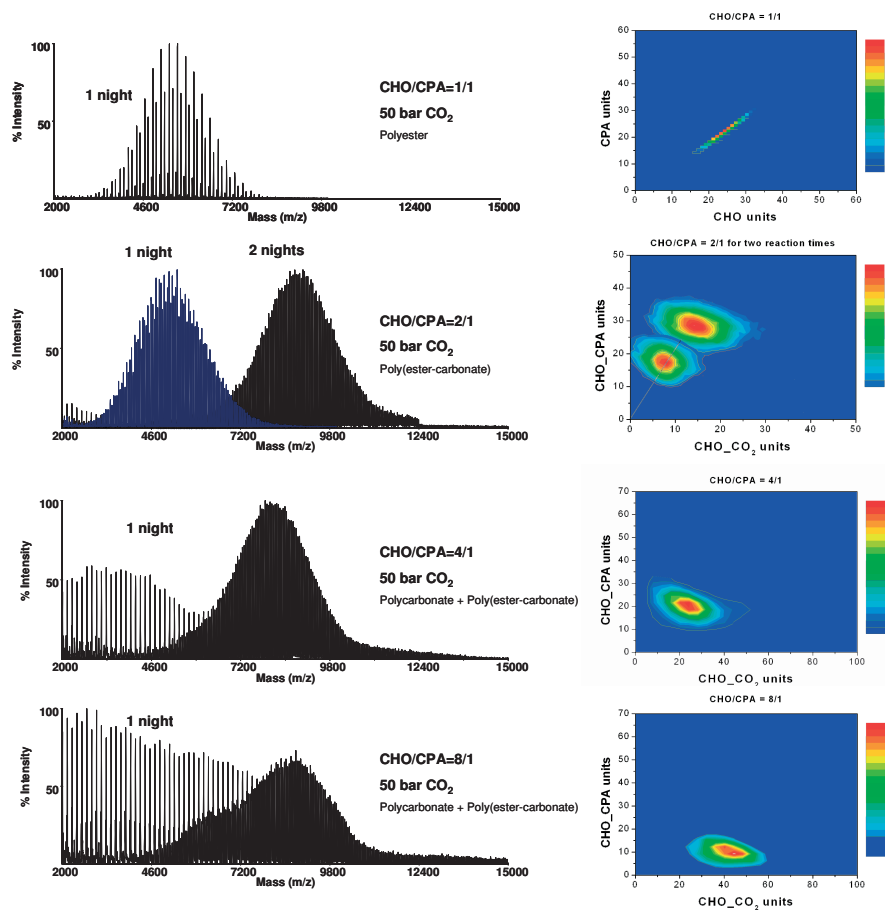
Figure 5-12. MALDI-ToF-MS spectra and matching contour plots of poly(ester-*co*-carbonate) synthesized by CO_2 and different loadings of CHO/CPA. Contour plots of spectra with an anhydride to epoxide ratio of 1:2 after one night and two nights of reaction time, showing the same overall composition indicating a random incorporation (Entries 7-11, Table 5-2).

5.4 Conclusion

In conclusion, it was shown that in absence of a cocatalyst, **1** and **2** showed little or no activity in the copolymerization of oxiranes and anhydrides and produced mainly polyether. The presence of DMAP as cocatalyst dramatically increased both the activity and the copolymerization selectivity of the catalysts. Moreover, **1**/DMAP is more active and selective than **2**/DMAP for the copolymerization of cyclohexene oxide with succinic anhydride whereas the opposite was observed during cyclohexene oxide – CO_2 copolymerization. As was already proposed by Darensbourg and coworkers for the copolymerization of oxiranes and carbon dioxide, MALDI-ToF-MS proved that also during oxirane – anhydride copolymerization the DMAP (or MeIm) cocatalyst is attached to the polyester as a cationic end group of a zwitterionic polymer. Interestingly, complex **3**, which proved to be an ill-defined multi-site catalyst system for the oxirane – CO_2 copolymerization, turned out to be a single-site catalyst for the copolymerization of CHO and anhydrides. It was proven that for anhydrides with different ring strain, **1**/DMAP resulted always in a completely alternating structure in contrast to **2**/DMAP and **3**. Complex **2**/DMAP afforded the pure polyester from 1,2-cyclobutane dicarboxylic acid anhydride whereas **3** still showed a few ether linkages. Ultimately, also complex **3** achieved a perfectly alternating topology when cyclopentane-1,2-dicarboxylic acid anhydride was employed as comonomer. Introduction of a third monomer, CO_2, resulted in poly(ester-*co*-carbonate)s without the presence of ether bonds for both **1**/DMAP and **4**/DMAP. Furthermore, the reactivity of the anhydride exceeds the reactivity of CO_2 as can be concluded from the fact that no carbon dioxide is built in when the anhydride:epoxide ratio equals 1:1. This difference in reactivity however does not result in di-block copolymers but in random copolymers as indicated by sampling over time. Further mechanistic research is in progress on the effect of using different solvents, cocatalysts to catalyst ratios and different comonomers.

5.5 Experimental Section

Reagents. Succinic anhydride (SA), cyclopropane-1,2-dicarboxylic acid anhydride (3-Oxabicyclo[3.1.0]hexane-2,4-dione) (CPrA) and cyclohexene oxide (CHO) were purchased from Aldrich. Cyclobutane-1,2-dicarboxylic acid anhydride (perhydrocyclobuta[c]furan-1,3-dione) (CBA) was purchased from Maybridge. Cyclopentane-1,2-dicarboxylic acid anhydride (CPA) was purchased from CHESS GmbH. Cyclohexene oxide was dried over CaH_2, distilled and stored under argon. Succinic anhydride was sublimed prior to use. DMAP (4-(N,N-dimethylamino)pyridine) was used without further purification. All manipulations were performed under an inert atmosphere or in a nitrogen-filled glovebox unless stated otherwise. TPPCrCl (**1**) was purchased from STREM. The bis(phenoxy) zinc complex [(2,6-$F_2C_6H_3O)_2$Zn·THF]$_2$ (**3**),[19] the *N,N'*-Bis(3,5-di-*tert*-butylsalicylidene)-1,2-phenylenediamine chromium(III) chloride (**2**),[27] the *N,N'*-Bis(3,5-di-*tert*-butylsalicylidene)-1,2-meso-diphenyl-1,2-ethylenediimine chromium(III) chloride[13,28] and the *N,N'*-Bis(3,5-di-*tert*-butylsalicylidene)-1,2-ethylenediimine chromium(III) chloride[29] (**4**) were prepared according to literature procedures. Toluene was dried over an alumina column and stored on molecular sieves under argon.

Synthesis copolymers. *Bulk:* A mixture of anhydride (2.5 mmol), oxirane (2.5 mmol) and catalyst (10 μmol) (+cocatalyst 10 μmol) was reacted in a crimp lid vial placed into an aluminum heating block at 100 °C for 140 min. *Solution:* A mixture of anhydride (2.5 mmol), oxirane (2.5 mmol) and catalyst (10 μmol) (+cocatalyst 10 μmol) in 0.9 mL toluene was reacted in a crimp lid vial placed into an aluminum heating block at 100 °C for 300 min. Crude samples were taken for all analyses.

Synthesis terpolymers. A stainless steel 7 mL reactor was dried at 150 °C in an oven overnight together with the glass insert. After introduction in the glove-box, the glass insert was charged with a certain ratio of the complex, the anhydride, cyclohexene oxide and 2 mL toluene. Next, the reactor was closed and removed from the glove-box. The reactor was pressurized to 50 bar CO_2 and placed into a pre-heated aluminum block at 80 °C under stirring overnight. After venting, crude samples for NMR and MALDI-ToF-MS were taken.

NMR Analysis. NMR spectra were recorded on a Varian Mercury Vx (400 MHz) spectrometer. The solvent used was chloroform-d_1.

SEC Analysis. SEC analysis was carried out using a Waters 2695 Alliance pump and injector, a model 2414 refractive index detector (at 40 °C) and a model 2487 UV detector (at 254 nm) in series. The columns used were a PLgel guard (5 μm particles) 50 × 7.5 mm column, followed by two PLgel mixed-C (5 μm particles) 300 × 7.5 mm columns at 40 °C in series. THF (Biosolve 'non-stabilized') was used as eluent at a flow rate of 1.0 mL·min^{-1}. Samples were filtered through a 0.2 μm PTFE syringe filter (13 mm, PP housing, Alltech). Calibration was carried out using narrow *MWD* polystyrene standards (Polymer

Laboratories, M_n = 580 to 7.5 × 10^6 g·mol^{-1}). Data acquisition and processing were performed using Waters Empower 1 software.

MALDI-ToF-MS Analysis. MALDI-ToF-MS analysis was performed on a Voyager DE-STR from Applied Biosystems equipped with a 337 nm nitrogen laser. An accelerating voltage of 25 kV was applied. Mass spectra of 1000 shots were accumulated. The polymer samples were dissolved in THF at a concentration of 1 mg·mL^{-1}. The cationization agent used was potassium trifluoroacetate (Fluka, >99%) dissolved in THF at a concentration of 5 mg·mL^{-1} unless stated otherwise. The matrix used was trans-2-[3-(4-tert-butylphenyl)-2-methyl-2-propenylidene]malononitrile (DCTB) (Fluka) and was dissolved in THF at a concentration of 40 mg·mL^{-1}. Solutions of matrix, salt and polymer were mixed in a volume ratio of 4:1:4, respectively. The mixed solution was hand-spotted on a stainless steel MALDI target and left to dry. The spectra were recorded in the reflector mode. All MALDI-ToF-MS spectra were recorded from the crude products.

References

[1]   M. Chasin, R. Langer, *Biodegradable Polymers as Drug Delivery Systems*, Marcel Dekker Inc, New York, **1990**.

[2]   R.F. Fischer, *J. Polym. Sci.* **1960**, *44*, 155.

[3]   T. Aida, K. Sanuki, S. Inoue, *Macromolecules* **1985**, *18*, 1049.

[4]   Y. Maeda, A. Nakayama, N. Kawasaki, K. Hayashi, S. Aiba, N. Yamamoto, *Polymer* **1997**, *38*, 4719.

[5]   J.C. Jeske, A.M. DiCiccio, G.W. Coates, *J. Am. Chem. Soc.* **2007**, *129* , 11330.

[6]   J.C. Jeske, J.M. Rowley, G.W. Coates, *Angew. Chem. Int. Ed.* **2008**, *47*, 6041.

[7]   Y. Liu, K. Huang, D. Peng, H. Wu, *Polyme*r **2006**, *47*, 8453.

[8]   S. Matsumura, T. Okamoto, K. Tsukada, K. Toshima, *Macromol. Rapid Commun.* **1998**, *19*, 295.

[9]   R. Rajkhowa, I.K. Varma, A.-C. Albertsson, U. Edlund, *J. Appl. Polym. Sci.* **2005**, *97*, 697.

[10]   D.J. Darensbourg, *Chem. Rev.* **2007**, *107*, 2388.

[11]   M. Cheng, D.R. Moore, J.J. Reczek, B.M. Chamberlain, E.B. Lobkovsky, G.W. Coates, *J. Am. Chem. Soc.* **2001**, *123*, 8738.

[12]   T. Aida, S. Inoue, *Macromolecules* **1982**, *15*, 682.

[13]   R.L. Paddock, S.T. Nguyen, *J. Am. Chem. Soc.* **2001**, *123*, 11498.

[14]   D.J. Darensbourg, J.C. Yarbrough, *J. Am. Chem. Soc.* **2002**, *124*, 6335.

[15]   D.J. Darensbourg, J.C. Yarbrough, C. Ortiz, C.C. Fang, *J. Am. Chem. Soc.* **2003**, *125*, 7586.

[16]   R. Eberhardt, M. Allmendinger, B. Rieger, *Macromol. Rapid Commun.* **2003**, *24*, 194.

[17]   W.J. Kruper, D.V. Dellar, *J. Org. Chem.* **1995**, *60*, 725.

[18]   D.J. Darensbourg, R.M. Mackiewicz, *J. Am. Chem. Soc.* **2005**, 127, 14026.

[19]   D.J. Darensbourg, J.R. Wildeson, J.C. Yarbrough, J.H. Reibenspies, *J. Am. Chem. Soc.* **2000**, *122,* 12487.

[20]   H. Sugimoto, H. Ohtsuka, S. Inoue, *J. Polym. Sci., Part A: Polym. Chem.* **2005**, *43*, 4172.

[21]   T. Aida, S. Inoue, *J. Am. Chem. Soc.* **1985**, *107*, 1358.

[22]   H. Sugimoto, K. Kuroda, *Macromolecules* **2008**, *41*, 312.

[23]   R. Eberhardt, M. Allmendinger, G.A. Luinstra, B. Rieger, *Organometallics* **2003**, *22*, 211.

[24]   P. Dobrzynski, J. Kasperczyk, *J. Polym. Sci., Part A: Polym. Chem.* **2006**, *44*, 98.

[25]   P. Dobrzynski, *Polymer* **2007**, *48*, 2263.

[26]   S. Inoue, H. Koinuma, T. Tsuruta, *J. Polym. Sci., Part B: Polym. Lett.* **1969**, *7*, 287.

[27]   J. Wöltinger, J.-E. Bäckvall, A. Zsigmond, *Chem. Eur. J.* **1999**, *5*, 1460.

[28]   D.J. Darensbourg, R.M. Mackiewicz, J.L. Rodgers, C.C. Fang, D.R. Billodeaux, J.H. Reibenspies, *Inorg. Chem.* **2004**, *43*, 6024.

[29]   D.J. Darensbourg, E.B. Frantz, J.R. Andreatta, *Inorg. Chim. Acta* **2007**, *360*, 523.

6

Technology Assessment.

Abstract. *The research described in this thesis was part of a project that deals with the possibility to use the glass transition temperature as a control for pulsatile drug administration, for example to be employed in cancer breakthrough pains. An implantable device releases drug on-demand by heating through the glass transition and closes upon cooling back to the glass state. The importance of this project is evident as cancer became death cause number one in The Netherlands in January 2009 above cardiovascular diseases. In this chapter we discuss the possibility of the glass transition temperature as a switch with the emphasis on its relation to the chemical parameters topology and composition. Furthermore we very briefly highlight the most recent and promising developments on pulsatile controlled drug delivery.*

Polyesters are potential candidates for both medicine in their role as vehicles for local drug administration as well as material for 'green' packaging. Owing these potentials, polyester research intensified during the 80s and 90s. The areas of research are mainly focused on the synthesis of new polyesters, the characterization thereof, the thermal and mechanical properties of these materials and the design and synthesis of new catalysts to improve synthetic routes. This thesis covered the synthesis and analysis of mainly *copolymers* and specifically copolyesters. The syntheses were confined to the ring-opening copolymerization of lactides and lactones and the possibility to synthesize polyesters from epoxides and anhydrides. MALDI-ToF-MS was employed as the characterization tool to determine the polymer's topology and reactivity ratios.

In this closing chapter we discuss the position of this research as part of a bigger project which deals with the possibility and the problems arising to use these polyesters in a drug delivery device that governs the glass transition temperature as an on and off switch.[1] The device is open and the drug is released in its rubbery state; in its glassy state the device is closed and the drug is captured inside. At first instance, the use of the glass transition seemed straightforward as we felt confident with the term and the actual meaning of the glass transition temperature. However, as R. J. Seyler reports in his opening discussion of the book 'Assignment of the Glass Transition', when surveying a random selection of material scientists and ask them to determine the glass transition temperature of a given specimen, the data reported back can very well be widely scattered.[2] This is related to the fact that our language was created before the physical phenomenon was actually well understood as correctly stated by B. Wunderlich.[2] Different experiments exist to measure the glass transition, *e.g.* calorimetry, dilatometry, dielectric measurements and thermal plus dynamic mechanical analyses. In the scope of this project, with heat as the triggering of the device once implanted in the human body, calorimetry seemed actually the most logical option.

The starting choice of the polymeric medium in which the drug was dispersed or encapsulated was poly(lactide-*co*-glycolide). This material ultimately had all the desired requirements: an amorphous polymer, biocompatible and biodegradable, with a glass transition just above the human body temperature. The latter is of high importance as no surrounding tissue burns might occur and the drug may not be released if someone is struck by the flu. Furthermore, the possibility of slightly tuning the glass transition existed by changing the lactide to glycolide ratio. The material however did not give the desired in-vitro release results and degraded relatively fast even with a low glycolide content. Moreover, a drop in glass transition could be expected upon degradation of the material, not yet to speak about plasticizing effects of body liquids and possibly the drug.[3,4] The synthesis of a new amorphous material, preferably, biodegradable and biocompatible with a glass transition temperature around 42 $^{\circ}$C was required. Although being a well defined goal, the task appeared cumbersome once the many physical parameters that practice an influence on the glass transition temperature are met.

Figure 6-1 shows schematically the division of the effects on the glass transition temperature in four major categories.
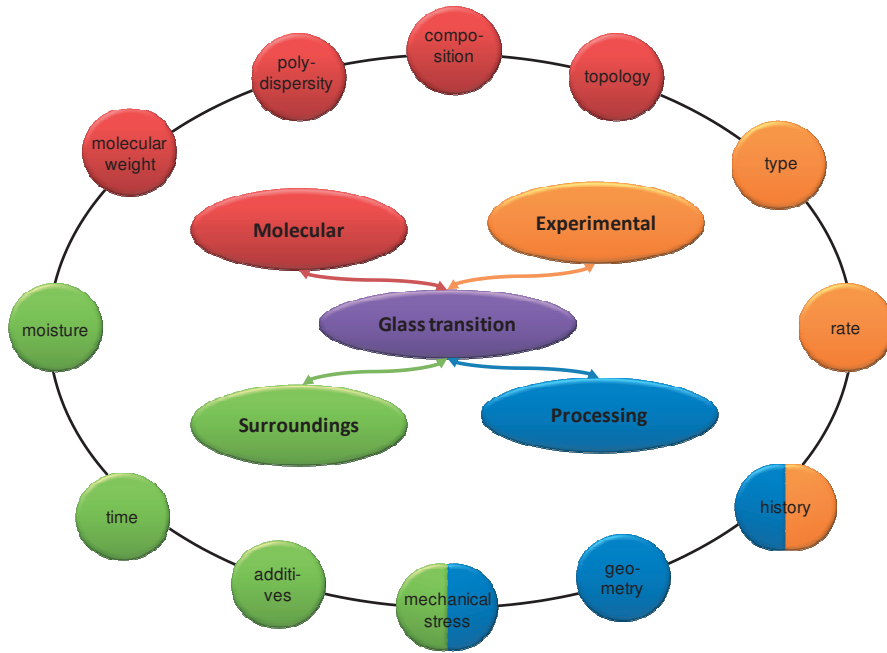
Figure 6-1. The many chemical and physical parameters affecting the glass transition have been divided into four categories.

The parameters a polymer chemist can play with are type of building blocks, molecular weight, polydispersity, topology, end groups etc. The starting point can be considered the most difficult because it requires a deep understanding of chemical structure in correlation to the physical property. In reality it requires even the power of a prediction of the property. Different relations exist to predict the glass transition temperature of a copolymer, yet many of them require the knowledge of the homopolymers and assume linearity and complete randomness of the building blocks, *e.g.* the Fox[5] equation, the Gordon-Taylor[6] equation and the DiMarzio-Gibbs[7] equation. Evidently, many copolymers do not exhibit a random topology with as result a deviation of the predicted or theoretical glass transition temperatures.[8,9] Figure 6-2 shows a general example of the differences in glass transition temperatures for a certain copolymer and its different topologies.
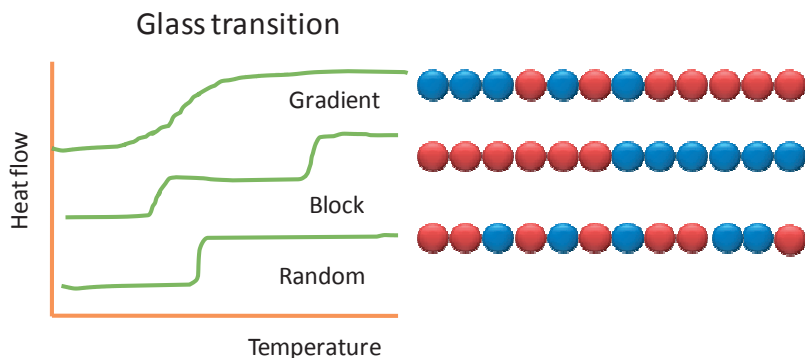
Figure 6-2. Glass transition temperature is depending on microstructure.

The Johnston equation makes use of the diad sequence contribution to the instantaneous glass transition temperature, but requires knowledge of the glass transition temperature of both homopolymers and the strictly alternating polymer, see equation 6-1. Notwithstanding, this equation does show the importance of the influence of the intramolecular microstructure on the physical properties (*e.g.* the glass transition) and confirms the need for the controllability of these properties on molecular level.[10-12]

$$\frac{1}{T_g} = \frac{w_1 P_{11}}{T_{g1}} + \frac{w_2 P_{22}}{T_{g2}} + \frac{(w_1 P_{12} + w_2 P_{21})}{T_{g12}}$$

(6-1)

(In which P_{ij} are the propagation probabilities and w_i the instantaneous weight fractions of monomer i.)

Other equations[13,14] make use of extensions of the aforementioned equations or of the triad sequences instead, yet it is beyond the scope of this assessment to treat them all. Nevertheless, we would like to mention a recently reported new equation by Liu *et al.*[15] which expresses the glass transition in terms of the glass transition of periodic polymers and the mole fractions of different diads, emphasizing the effect not only of composition but also once more of sequence distributions. The latter show the relation to the reactivity ratios.

$$T_g = n_{AA} T_{gA} + n_{BB} T_{gB} + 2n_{AB} T_{g[AB]}$$

(6-2)

with for example:

$$n_{AA} = n_A P_{AA} = \frac{r_A \frac{[A]}{[B]}}{r_A \frac{[A]}{[B]} + r_B \frac{[B]}{[A]} + 2}$$

(6-3)

Liu *et al.* reported even an extension taking into account chain tacticity. They obtained excellent fitting of the equation for the copolymer systems STY/MMA, E/MMA and E/VAc.

Clearly, an easy and reliable characterization of a copolymer's topology with respect to a better understanding of this particular physical parameter in the framework of this project is of vital importance. The contribution of the method as described in Chapter 3 is considered a valuable and helpful asset in the correlation of the glass transition temperature to a polymer's fine structure. It not only helps in an easy determination of end groups, composition and to some extent topology but also of the reactivity ratios. With this a big part of the category 'molecular' in Figure 6-1 is covered. An overview of this method is given in Figure 6-3 for sake of clarity.
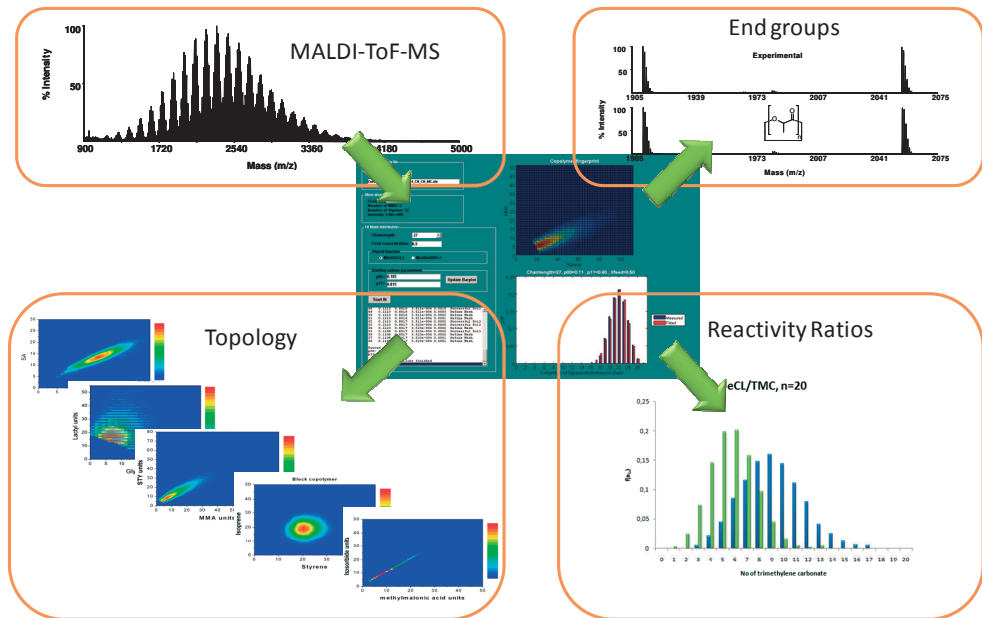
Figure 6-3. Overview of chemical information obtained via characterization by MALDI-ToF-MS.

Assumable, all the above mentioned parameters can be controlled; still the 'jump' in C_p of the glass transition might be weak. It is well-known that the breadth of the transition broadens *i)* for miscible blends, *ii)* for copolymers relative to their homopolymers or *iii)* for a highly cross-linked material.[2] It was believed that a large ΔC_p correlates to a more well-defined release pattern. Unfortunately, no scientific proof of this idea has been found. Other effects that can obstruct the use of the transition as switch are the presence of moisture or other molecules (including the drug) that can work plasticizing or anti-plasticizing. An example is given in Figure 6-4, in which ibuprofen and lidocaine invoke a profound drop of the glass transition temperature of poly(lactide).
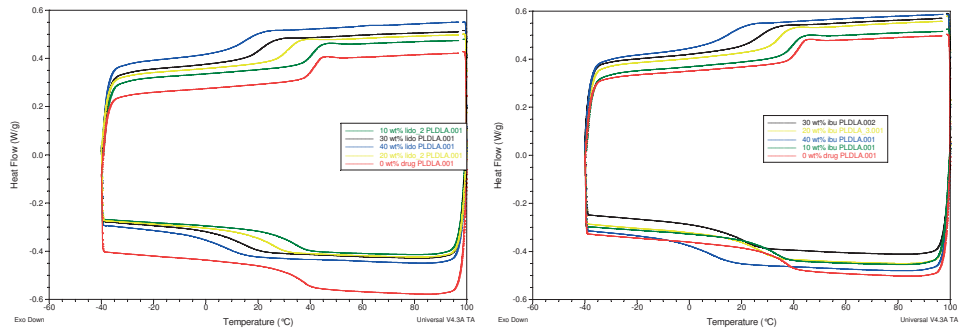
Figure 6-4. Plasticizing effect on poly(lactide) of ibuprofen and lidocaine.

Subsequently, the effect of the drug is subject to its release, not only establishing a profile in concentration but also in glass transition.

The category 'processing' covers mainly the manufacturing of the device, its shape and not to forget the sterilization prior to implantation. Moreover, the time the device is in storage before usage is an important factor that can alter the glass transition considerably. The glass transition is a function of 'thermal history' and consequently depends highly on the rate with which the material is cooled. Additionally, thermodynamic effects on the transition by repeatedly turning the device 'on' are subject to a patients' need for the drug and add an extra dimension to the prediction and therefore to the controllability of the transition. Conclusively, erasing of the thermal history directly before implantation is a necessity as well as knowledge of the frequency in relation to time intervals a patient will make use of the device. Thinkable, a preset number of times a patient may turn the device 'on' with a certain time interval as is the case for many tablets, can make predictions on the physical behavior of the transition easier but allows not a single exception. This brings us to the marketing concept of the drug delivery device and any statement on this matter is beyond the intention of this assessment. Yet, we would like to quote M. Staples *et al.*[16] in *Pharmaceutical Research*, who stated that an ideal implant would:

- protect the drug or biosensor from the body until needed,
- allow continuous or pulsatile delivery
- of both liquid and solid drug formulations,
- and be controllable by the physician or patient.

Possibly, the confidence in the idea that the glass transition would relatively easy allow for a controllable, pulsatile delivery, might have been misplaced. Unfortunately, the dependence of the glass transition on many physical and chemical parameters make it a much more complex system to be used as a switch as simple as the word itself implies. Moreover, the glass transition exhibits bidirectional hysteresis depending on time, which does not allow for a prediction of the output without complete knowledge of the input's history.[2] Even if all parameters of influence could separately be controlled, this would not mean that the transition overall can be controlled. Therefore, more research is necessary to better understand the influence and mutual dependence of the physical parameters on the glass transition temperature in order to pursue an application that deals with something as precarious as the health of people.

A note on the biocompatibility and biodegradability of the material cannot be bypassed in this assessment. Many scientists dealing with polyesters know that the term biodegradable is often used incorrectly as an equivalent to hydrolysis. Moreover, the use of monomers extracted from a natural source (plants, algae, invertebrates etc.) does not guarantee biocompatibility. With the same reasoning, one could state that any plant growing on this planet is non-toxic. In many scientific papers related with the synthesis of new polyesters or polycarbonates, the authors highlight the possibility of the applicability of the material in a drug delivery device. This statement demands for a scientific proof which requires the input of another discipline like biotechnology. In the given case, even if the material meets these demands, the stability of the glass transition can be questioned for the molecular weight changes. Of course, the degradability should be tuned such that it starts after the treatment is finished. Nonetheless, in the context of this project, it is advisable to mostly exclude macromolecular chemical effects by choosing a non-degradable, commercially available material with a controlled, continuous supply. The polyesters described in Chapter 5 have not yet proven to be biocompatible.

A relatively new prosperous direction in pulsatile administration is the use of electromechanical based drug delivery devices. These devices have the ability to fulfill the shortcomings of 'regular' polymeric drug delivery implants in terms of controllability and pulsatile delivery. Moreover, the possibility of wireless data transmission enables the implementation of an alert system or biosensor. At the beginning of this year Elman *et al.* reported on the first implantable device based on the micro-electrical mechanical systems (MEMS) technology for ambulatory emergency care.[17] The focus of their research was on rapid but reliable delivery, something that was not achieved before by implants based on other technologies. Likewise, the latest invention of an implantable system-on-a-chip (SoC) was presented on this year's IEEE's international Solid State Circuit conference by researchers of the National Taiwan University. Their device releases drugs from reservoirs by the rupture of membranes on demand by employing a wireless circuit.[18] These fast uprising new developments in the field of drug delivery can be called nothing but promising and cast a shadow over the pursuit of a device controlled by a phenomenon as dynamic as the glass transition temperature.

References

[1]   H. Bruinewoud, J.T.F. Keurentjes, M.F. Kemmere, US Patent Application, US 2005/0025830 A1, **2005**.

[2]   R.J. Seyler, *Assignment of the Glass Transition*, American Society for Testing and Materials, Philadelphia, **1994**.

[3]   P. Blasi, S.S. D' Souza, F. Selmin, P.P. DeLuca, *J. Controlled Release* **2005**, *108*, 1.

[4]   N. Passerini, D.Q.M. Craig, *J. Controlled Release* **2001**, *73*, 111.

[5]   T.G. Fox, P.J. Flory, *J. Appl. Phys.* **1950**, *21*, 581.

[6]   M. Gordon, J.S. Taylor, *J. Appl. Chem.* **1952**, *2*, 493.

[7]   E.A. Dimarzio, J.H. Gibbs, *J. Polym. Sci.* **1959**, *40*, 121.

[8]   J. Kim, M.M. Mok, R.W. Sandoval, D.J. Woo, J.M. Torkelson *Macromolecules* **2006**, 39, 6152.

[9]   C.L.H. Wong, J. Kim, J.M. Torkelson, *J. Polym. Sci. Part B: Polym. Phys.* **2007** *45*, 2842.

[10]   N.W. Johnston, *Macromolecules* **1973**, *6*, 453.

[11]   G. Févotte, T.F. McKenna, A.M. Santos, *Chem. Eng. Sci.* **1998**, *53*, 2241.

[12]   M. Fernández-García, J.L. de la Fuente, E.L. Madruga, *Polym. Bull.* **2000**, *45*, 397.

[13]   J.M. Barton, *J. Polym. Sci. Part C: Polym. Sym.* **1970**, *30*, 573.

[14]   H. Suzuki, N. Kimura, Y. Nishio, *J. Therm. Anal.* **1996**, *46*, 1011.

[15]   G. Liu, Z. Meng, W. Wang, Y. Zhou, L. Zhang, *J. Phys. Chem. B* **2008**, *112*, 93.

[16]   M. Staples, K. Daniel, M. Cima, R. Langer, *Pharm. Res.* **2006**, *23*, 847.

[17]   N.M. Elman, H.L. Ho Duc, M.J. Cima, *Biomed Microdevices*, Springer, **2009**.

[18]   Y.-J. Yang, Y.-J. Huang, H.-H. Liao, T. Wang, P.-L. Huang, C.-W. Lin, Y.-H. Wang, S.-S. Lu, National Taiwan University, IEEE Solid State Circuit Conference, February **2009**.

Abbreviations

DSC	differential scanning calorimetry
GPC	gel permeation chromatography
SEC	size exclusion chromatography
MALDI	matrix assisted laser desorption ionization
ToF	time of flight
MS	mass spectrometry
LCCC	liquid chromatography under critical conditions
CCD	chemical composition distribution
CLD	chain length distribution
BLD	block length distribution
MC	Monte Carlo method
LSSQ	least sum of squares
PLLA	poly(L-lactide)
PDLA	poly(D-lactide)
PDLLA	poly(D,L-lactide)
PLDLA	poly(D,L-lactide-*co*-L-lactide)
PLGA	poly(lactide-*co*-glycolide)
PLLGA	poly(L-lactide-*co*-glycolide)
PDLGA	poly(D-lactide-*co*-glycolide)
PDLLGA	poly(D,L-lactide-*co*-glycolide)
PCL	poly(ε-caprolactone)
PPDL	poly(ω-pentadecalactone)
ROP	ring-opening polymerization
eROP	enzymatic ring-opening polymerization
cROP	chemical ring-opening polymerization
D-LA	D-lactide
L-LA	L-lactide
ε-CL	ε-caprolactone
δ-VL	δ-valerolactone
PDL	ω-pentadecalactone
4-MeCL	4-methyl-ε-caprolactone
DXO	1,5-dioxepan-2-one

TMC	trimethylene carbonate
BA	butyl acrylate
EA	ethyl acrylate
MA	methyl acrylate
BMA	butyl methacrylate
EMA	ethyl methacrylate
MMA	methyl methacrylate
STY	styrene
VAc	vinyl acetate
AIBN	2,2'-azobisisobutyronitrile
DDT	1-dodecanethiol
ANH	anhydride in general
SA	succinic anhydride
CPrA	cyclopropane-1,2-dicarboxylic acid anhydride
CBA	cyclobutane-1,2-dicarboxylic acid anhydride
CPA	cyclopentane-1,2-dicarboxylic acid anhydride
CHO	cyclohexene oxide

Summary

The understanding of the physical behavior of polymers leads back to the knowledge on chemical structure. The main chemical parameters determining the physical properties of a polymer are molar mass, molar mass distribution, composition and microstructure (random, block, alternating, gradient). An easy, reliable and above all fast analytical method is highly desirable to obtain a good estimate of these parameters. In this thesis it will be demonstrated that MALDI-ToF-MS is an analytical tool that can provide these parameters in a single measurement. Composition and microstructure can only indirectly be obtained by a deconvolution of the MALDI spectra in case of polymers with more than one different monomer residue. Along with the deconvolution into its monomer residues, an indirect access to homo-propagation and cross-propagation probabilities becomes available by the simulation of a first order Markov chain using either the Monte Carlo method or the much faster analytical solution as discussed in this thesis.

Mainly driven by the discussion on environmental pollution by non-degrading stray garbage, aliphatic polyesters gained increasing attention the past decades due to their good biodegradability. Moreover, the biocompatibility of several aliphatic polyesters has augmented their use as drug delivery vesicles within the human body. Also the research described in this thesis has been carried out within the framework of drug delivery. The finding of a polymeric medium that can be used in a device that governs the glass transition temperature as an on and off switch is the key issue. Probably the most important polymers for medicinal purposes are poly(lactide) and its copolymers like poly(lactide-*co*-glycolide). Ring-opening polymerizations of the comonomer pair lactide/glycolide by lipase and Sn(Oct)$_2$ were performed and a step growth polymerization of lactic and glycolic acid in the presence of Ti(OBu)$_4$. The topology of poly(lactide-*co*-glycolide), the distribution of lactyl and glycolyl units along the individual chains, was determined by creatively exploiting MALDI-ToF-MS analysis. We observed a difference in topology between L-lactide and D,L-lactide with glycolide for PLGA synthesized by both metal-based catalysts applied, namely tin for ring-opening polymerization and titanium for polycondensation. Moreover, in this thesis we demonstrate the difference in transesterification of PLGA synthesized according to the diverse pathways by converting a MALDI-ToF-MS spectrum into a so-called fingerprint or contour plot. We discovered three types of fingerprints, a striped fingerprint showing dimer-wise incorporation of one of the cyclic di-ester monomers, a checkerboard pattern deriving from a dimer-wise incorporation of both monomers and a homogeneous plot as a result of complete transesterification or using the hydroxyacids as monomers.

Besides by the commonly used polycondensation, polyesters can be obtained by ring-opening polymerization of cyclic esters. However, the polymer structures and properties are limited to the commercial availability of these cyclic esters.

While the nearly endless choice of diols and diacids gives access to a much larger range of polymer properties for AABB polyesters, their synthetic procedure of polycondensation is disadvantageous due to the required drastic conditions. Ring-opening polymerization of oxiranes and anhydrides is an alternative way to synthesize these AABB type polyesters. The undesirable side-reaction of homopolymerization of the oxirane and the low molecular weights generally obtained impeded its popularity and its development towards a routine pathway. Finding selective catalysts to optimize this route will allow access to a wide variety of monomers for the production of aliphatic polyesters with a broad span of physical properties. In this thesis we report on some mechanistic aspects of the alternating copolymerization of the alicyclic epoxide cyclohexene oxide (CHO) with succinic anhydride (SA), cyclopropane-1,2-dicarboxylic acid anhydride (CPrA), cyclobutane-1,2-dicarboxylic acid anhydride (CBA) and cyclopentane-1,2-dicarboxylic acid anhydride (CPA) using chromium porphyrinato, chromium salen and bis(2,6-difluoro-phenoxy) zinc complexes as catalysts. Interestingly, the synthesis of the pure polyester not only depended on type of catalyst, but also on the presence of a cocatalyst, solvent and type of anhydride. The chromium porphyrinato complex resulted always in a completely alternating structure in contrast to the salen complex and bis(2,6-difluoro-phenoxy) zinc complex employed. The chromium salen complex afforded the pure polyester from cyclobutane-1,2-dicarboxylic acid anhydride whereas the bisphenoxy zinc complex still showed a few ether linkages. Ultimately, also the zinc complex achieved a perfectly alternating topology when cyclopentane-1,2-dicarboxylic acid anhydride was employed as comonomer. Moreover, the introduction of a third monomer, CO_2, resulted in poly(ester-*co*-carbonate)s without the presence of ether bonds for both a chromium porphyrinato as a salen complex. Further mechanistic research is in progress on the effect of using different solvents, cocatalysts to catalyst ratios and different comonomers.

Samenvatting

Om achterliggende oorzaken van het fysische gedrag van polymeren te ontsluiten, is kennis op moleculair niveau een vereiste. De belangrijkste chemische parameters die de fysische eigenschappen van een polymeer bepalen zijn molecuulgewicht, molecuulgewichtsverdeling, samenstelling en microstructuur (random, blok, gradiënt). Een gemakkelijke, betrouwbare en vooral snelle analyse methode is hoogst wenselijk om een goede schatting van deze parameters te verkrijgen. In dit proefschrift wordt aangetoond dat MALDI-ToF-MS een analytisch hulpmiddel is dat deze parameters uit één enkele meting kan verstrekken. In het geval van polymeren met meer dan één verschillend monomeer residu, kunnen de samenstelling en de microstructuur slechts indirect worden verkregen door het deconvolueren van de MALDI spectra. Samen met het deconvolueren naar zijn monomeer eenheden, wordt een indirecte toegang verleend tot de homo-propagatie en cross-propagatie kansen door simulatie van een eerste orde Markov keten gebruikmakende van de Monte Carlo methode of de veel snellere analytische oplossing zoals die in dit proefschrift besproken is. Vervolgens kunnen uit de verkregen kansen, de reactiviteitverhoudingen worden berekend wanneer de voedingssamenstelling bekend is.

Hoofdzakelijk gedreven door milieuvervuiling veroorzaakt door niet degradeerbaar zwerfvuil, is er de afgelopen decennia een toenemende interesse voor alifatische polyesters waargenomen, die kan worden toegeschreven aan hun goede biologische afbreekbaarheid. Daarnaast heeft de biocompatibiliteit van verscheidene alifatische polyesters hun gebruik als drug toedieningimplantaten in het menselijk lichaam sterk doen toenemen. Ook het werk omschreven in dit proefschrift is uitgevoerd in het kader van drug toediening en wel gepulseerde drug toediening. Het zoeken naar een polymeer materiaal dat gebruikt kan worden in een implantaat dat de glasovergangstemperatuur van het materiaal gebruikt als aan- en uit schakelaar stond centraal. Waarschijnlijk zijn de belangrijkste polymeren voor medicinale doeleinden poly(lactide) en zijn copolymeren zoals poly(lactide-*co*-glycolide). In dit proefschrift zijn zowel de ringopening polymerisaties van het comonomeren paar lactide/glycolide door lipase en $Sn(Oct)_2$ bestudeerd, als ook een polymerisatie door polycondensatie van melkzuur en glycolzuur in aanwezigheid van $Ti(OBu)_4$. De microstructuren van poly(lactide-*co*-glycolide), de intramoleculaire verdeling van de monomeer eenheden, zijn bepaald door MALDI-ToF-MS analyse creatief te exploiteren. Door een ontrafeling van de spectra naar de comonomeer eenheden, gebruikmakende van in-huis ontwikkelde slimme software, wordt een zogenaamde vingerafdruk of contour plot geconstrueerd. Aan de hand van deze afdrukken is het mogelijk iets te zeggen over de topologie, maar vooral ook over het optreden van transesterificaties zoals besproken in dit proefschrift. Het verschil in transesterificatie van PLGA gesynthetiseerd volgens de eerder genoemde routes kon duidelijk worden afgelezen uit de verkregen contour plots.

Drie typen 'vingerafdrukken' werden geconstateerd, namelijk een gestreepte vingerafdruk die dimeer-wijze incorporatie van één van de cyclische di-esters vertoond, een schaakbordpatroon dat voortkomt uit een dimeer-wijze incorporatie van beide monomeren en een homogene vingerafdruk als resultaat van volledige transesterificatie of door het gebruik van de corresponderende hydroxyzuren als bouwstenen.

Naast polycondensatie kunnen AB-type polyesters verkregen worden door ringopening polymerisaties van cyclische esters. Echter de polymeereigenschappen worden daarbij beperkt door de commerciële verkrijgbaarheid van deze cyclische esters. Terwijl de bijna eindeloze keuze aan diolen en dizuren toegang verschaft tot een veel groter scala aan polymeereigenschappen voor AABB type polyesters, is hun synthetische procedure door middel van polycondensatie nadelig door de vereiste drastische condities en vaak beperkte molecuulmassa's. De ringopening polymerisatie van epoxiden en anhydriden is een alternatieve methode om deze AABB-typen polyesters te synthetiseren. Ongewenste nevenreacties zoals de homopolymerisatie van het oxiraan en de over het algemeen laag verkregen molecuulgewichten, hebben de populariteit en de ontwikkeling naar een routine synthese methode belemmerd. Het vinden van selectieve katalysatoren om deze route te optimaliseren zal dan ook de toegang verschaffen tot een grote verscheidenheid aan monomeren voor de productie van alifatische polyesters met een brede range aan fysische eigenschappen. In dit proefschrift worden enige mechanistische aspecten beschreven van de copolymerisaties van het alicyclische epoxide cyclohexeen oxide (CHO) met barnsteenzuur anhydride (SA), cyclopropaan-1,2-dicarbonzuur anhydride (CPrA), cyclobutaan-1,2-dicarbonzuur anhydride en cyclopentaan-1,2-dicarbon zuur anhydride (CPA) gebruik makend van chromoporphyrinato en salen complexen en een bis(2,6-difluoro-phenoxy) zink complex als katalysatoren. Het chromoporphyrinato complex resulteerde voor alle comonomeer paren in een volledig alternerende structuur in tegenstelling tot de aangewende salen en bis(2,6-difluoro-phenoxy) zink complexen. Het chromosalen complex katalyseerde de synthese van zuiver polyester uit de comonomeer cyclohexeen oxide en cyclobutaan-1,2-dicarbonzuur anhydride terwijl het polymeer verkegen met het bisphenoxy zink complex nog een paar opeenvolgende ether-aaneenschakelingen vertoonde. Uiteindelijk, werd in de aanwezigheid van het zink complex ook een volkomen alternerend polyester geproduceerd wanneer het cyclopentaan-1,2-dicarbonzuur anhydride als comonomeer werd gebruikt. Tenslotte resulteerde de introductie van een derde monomeer, CO_2, in poly(ester-*co*-carbonaat) zonder de aanwezigheid van etherbindingen voor zowel een chromoporphyrinato als een salen complex. Voortschrijdend mechanistisch onderzoek loopt evenals het onderzoek naar het effect van het gebruik van verschillende oplosmiddelen, co-katalysatoren, katalysatorverhoudingen en verschillende comonomeren.

Dankwoord

In fact, this journey started in an internet café in Greece during a great summer holiday where I, for unknown reasons, felt the urge to check my university email. Curiously, I had received an email from a former colleague informing me about a very interesting Ph.D. project at the Polymer Chemistry Group of the very same University at which I was participating in the TOIO program. After some weeks of consideration, I finally decided to apply for the position. The rest is history as the result is lying in front of you, yet it would not have been possible without the help from a lot of people.

Allereerst wil ik Cor Koning bedanken voor de mogelijkheid binnen zijn groep te promoveren en voor het vertrouwen dat hij in mij had. Rob Duchateau wil ik bedanken voor de directe en bijna dagelijkse begeleiding. Rob, ondanks dat je hart ligt bij de organometaalchemie, was je altijd zeer geïnteresseerd in mijn gedachte kronkels over polymeren en analyse. Je hebt mij hierin altijd gesteund en met raad en daad bijgestaan. Bedankt! Alex wil ik bedanken voor zijn rol als tweede promotor. Alex, je hebt al twee prachtige MALDI promoties achter de rug, maar ik hoop dat deze mooi in het rijtje mag aansluiten.

I would like to thank the reading committee for their effort to correct my manuscript: prof. dr. Cor Koning, prof. dr. Alex van Herk, dr. Rob Duchateau, prof. dr. Bert Meijer, prof. dr. Hans Kricheldorf and prof. dr. Philip Mountford.

Daarnaast wil ik SenterNovem en Dolphys Medical bedanken voor de financiële ondersteuning van mijn onderzoek als onderdeel van een maatschappelijk zeer interessant project.

De bijnaam 'miss time-of-flight' met dank aan prof. Lemstra, had ik nooit gekregen zonder de hulp van een aantal zeer inspirerende mensen. Bastiaan, mijn hartelijke dank voor alle hulp aangaande MALDI-ToF-MS en voor de samenwerking vooral in het begin van mijn promotie onderzoek. Iedere keer dat je weer eens in Eindhoven was, was een verademing vanwege je begrip en enthousiasme. Gerben, jij verdient een speciale dankbetuiging. Zonder jouw nimmer aflatende optimisme, gedrevenheid en enorme hulp op mathematisch vlak met al mijn MALDI problemen was hoofdstuk 3 er niet geweest. Bedankt! Prof. Remco van der Hofstad wil ik bedanken voor de geweldige hulp bij de afleidingen van de Markov chain en voor de prachtige eindsprint. Hans Heuts wil ik bedanken voor de discussies op het gebied van de vrije radicaal polymerisatie en de goede tips! Hans, ondanks dat ik je vaker lastig viel op momenten dat je eigenlijk geen tijd had, maakte je toch even tijd voor me. Mijn dank hiervoor.

Achter ieder proefschrift schuilt een hoop werk, dat er niet direct uit kan worden afgelezen, maar dat minstens even belangrijk is. Hieronder vallen voornamelijk de inspanningen van de ondersteunende en wetenschappelijke staf. Caroline en Pleunie bedankt voor alle administratieve hulp, geestelijke ondersteuning en vooral gezelligheid.

Marion en Wieb zonder jullie analytische kennis, uitvoering van chromatografie en MALDI-ToF-MS analyse en inspanning was dit boekje er nooit gekomen. Verder Henk en Petra, het LCCC clustertje, bedankt! Carin en Friso, we hebben maar kort samengewerkt, maar het was me een waar genoegen! Wouter G, bedankt voor alle technische ondersteuning gedurende mijn promotie onderzoek met van alles en nog wat, gewoonweg te veel om op te noemen. Rinske wil ik bedanken voor de hulp in het laatste jaar van mijn promotie. Martin F. bedankt voor de introductie in de chemie van de oxazolines!

My office mates in chronological order Jelena, Wouter vM, Rutger, Jenny, David, Ali, Timo, Jens, Gözde and finally Bahar thanks for the fun discussions and good time. Our bumping SKA Rutger, especially for you: *it is nice to be important, but it is more important to be nice!* Jenny, we started not too far apart from one another and spent until the very last day in the same office. We shared all the good and bad times. Thanks for your support and all the very best to you wherever you decide to go. Syed alias Ali, you joined somewhat later, but we have spent at least two to three years in the same office. Thank you for the discussions and jokes! Timo, if I ever need someone to produce animal sounds, you are on the top of my list! Jens, du hast dein Schuh verloren…. The Turkish ladies, both of you just came in the last half a year of my Ph.D., but thank you and all the best to you!

Martin O. bedankt voor alle zinvolle en leuke discussies aangaande het management van de afdeling en de zin en onzin van wetenschappelijk onderzoek. Maurice bedankt voor de fijne samenwerking op het vlak van de CO_2 chemie. Inge, Jenny, Ali and Patricia thanks for some purified monomers! Donglin, thank you for the polycondensation sample. Gözde and Hector, thank you for the help with ATRP. MC thanks for the short introduction in carbonanotubes. Although nothing can be found back of that work, it was not in vain! Rafael, you were the 'former colleague' giving me the hint. We go back quite some years to the time that I was still messing around in the labs of SKA where already then you were giving me advice. Thank you for all your help over the years! To all my other not previously mentioned colleagues from SPC: thanks! I wish all of you the very best and good luck!

Next, I had the privilege to supervise several students and want to thank them for all their efforts and work. Juan, you were my first student, thank you! I hope your stay in The Netherlands was a good and educated experience. I also wish that holds for both my Turkish Erasmus exchange students. Thanks, guys! Alaaf Chris, je hebt me grijze haren bezorgd. Jon, al die kilo's drop die wij geconsumeerd hebben, blijken toch hun vruchten afgeworpen te hebben. Veel succes met je master.

Collaborations are a key issue to a successful finishing of a Ph.D. Although, most of the time it concentrated itself around myself measuring MALDI, in some cases it was a little more than that. Hellen, the discussions with you and Philip were a great pleasure. Thank you for involving me. Przemek, I had great admiration for the patience you had with your experiments. Thousand hours or longer waiting for results, but finally it paid off. Thank you.

Tot slot wil ik hier van de gelegenheid gebruik maken om de mensen die me op het thuisfront er doorheen gesleept hebben zoals familie en vrienden, te bedanken.

René, jou wil ik bedanken voor je nimmer aflatende steun. Al begreep je soms niet waar ik het over had, jouw onvoorwaardelijke vertrouwen kreeg ik zonder slag of stoot. Ik heb bewondering voor jouw opgewekte karakter en gouden hart. Mijn dank gaat ook uit naar Pascha.

My beloved bunch of foreign but mainly Greek friends: Thanks guys, for all the understanding and support! Apart from the parties and dinners, those numerous discussions on practicing science and research helped me to put things in perspective.

Αγόρι μου, χωρίς εσένα ίσως να μην είχα καν ξεκινήσει αυτό το διδακτορικό! Ευχαριστώ για όλη την υποστήριξη & τη βοήθεια όλα αυτά τα χρόνια. Εκτός από αγάπη, οι δύο λέξεις που περιγράφουν καλύτερα τα αισθήματα μου για σένα είναι εκτίμηση & θαυμασμός. Γνωρίζω ότι οι περιστάσεις δεν ήταν εύκολες για κανέναν από τους δυο μας, μιας που αμφότεροι πεθαίναμε στη δουλειά, αλλά είμαι βέβαιη ότι διανύουμε ήδη καλύτερες μέρες. Τα αυτιά σου μπορούν τώρα να ξεκουραστούν - το νανάκι τελείωσε.

Lieve pap en mam: jullie wil ik bedanken voor al die jaren waarin jullie mij financieel en moreel hebben bijgestaan. En dat zijn er heel wat! Daarnaast had ik ook nog eens het geluk dat jullie mij beide in al mijn ontevreden discussies over het onderzoek vaak volledig konden volgen. Broertje, jou wil ik bedanken voor alle steun en vooral hulp met de nodige computer rompslomp.

Curriculum Vitae

Saskia Huijser was born on the 1st of March 1977 in Eindhoven, The Netherlands. She attended the Augustinianum in Eindhoven, where she obtained her degree for University entrance in 1995. Nevertheless, she started at the Higher Technical School West-Brabant in Etten-Leur/Breda where she obtained a bachelor degree in Environmental Science in 1999. In the same year she attended the shortened version of the Chemical Engineering study at the University of Technology Eindhoven from which she graduated in 2003. At the same institute, she joined the postmaster program Process and Product Design, which she left after a little more than half a year, to start a Ph.D. project at the Laboratory of Polymer Chemistry in Eindhoven under guidance of prof. dr. C.E. Koning and dr. R. Duchateau. The most important results of this doctoral research are described in this thesis.

Saskia Huijser werd geboren op 1 maart 1977 te Eindhoven. Aan scholengemeenschap het Augustinianum te Eindhoven behaalde zij in 1995 haar VWO diploma waarna zij datzelfde jaar begon met de studie Milieukunde aan de Hogeschool West-Brabant te Etten-Leur/Breda. In 1999 sloot zij met succes deze opleiding af om vervolgens te starten met de verkorte opleiding Scheikundige Technologie aan de Technische Universiteit Eindhoven. In 2003 behaalde zij haar diploma en besloot de ontwerperopleiding Proces- en Productontwerp te gaan volgen aan de Technische Universiteit Eindhoven. Na een half jaar maakte zij de overstap naar de Polymeerchemie groep om te gaan promoveren onder leiding van prof. dr. C.E. Koning en dr. R. Duchateau. De belangrijkste resultaten van dit promotieonderzoek staan beschreven in dit proefschrift.

Scientific Papers:

S. Huijser, B.B.P. Staal, J. Huang, R. Duchateau, C.E. Koning, **Chemical composition and topology of poly(lactide-*co*-glycolide) revealed by pushing MALDI-TOF MS to its limit,** Angew. Chem. Int. Ed., 45, 4104-4108, (2006).

S. Huijser, B.B.P. Staal, J. Huang, R. Duchateau, C.E. Koning, **Topology characterization by MALDI-ToF-MS of enzymatically synthesized poly(lactide-co-glycolide),** Biomacromolecules, 7(9), 2465-2469, (2006).

S. Huijser, G.D. Mooiweer, J. Feenstra, R. Duchateau, C.E. Koning, **Complete copolymer characterization by the click of a button; reactivity ratios of comonomers from a single MALDI-ToF-MS measurement,** to be submitted.

S. Huijser, M.L.J. Frijns, C. de Jong, R. Duchateau, C.E. Koning, **Ring opening copolymerization of an alicyclic oxirane with carboxylic acid anhydrides in the presence of chromium and zinc catalysts,** to be submitted.

R. Duchateau, W.J. van Meerendonk, S. Huijser, B.B.P. Staal, M.A. Van Schilt, G. Gerritsen, A. Meetsma, C.E. Koning, M.F. Kemmere, J.T.F. Keurentjes, **Silica-grafted diethylzinc and a silsesquioxane-based zinc alkyl complex as catalysts for the alternating oxirane-carbon dioxide copolymerization,** Organometallics, 26(17), 4204-4211 (2007).

H.E. Dyer, S. Huijser, A.D. Schwarz, C. Wang, R. Duchateau, P. Mountford, **Zwitterionic bis(phenolate)amine lanthanide complexes for the ring-opening polymerization of cyclic esters,** Dalton Trans., 1, 32–35 (2008).

P. Malanowski, S. Huijser, F. Scaltro, R.A.T.M. van Benthem, L.G.J. van der Ven, J. Laven, G. de With, **Molecular mechanism of photolysis and photooxidation of poly(neopentyl isophthalate),** Polymer, in press.

P. Malanowski, S. Huijser, R.A.T.M. van Benthem, L.G.J. van der Ven, J. Laven, G. de With, **Photodegradation of poly(neopentyl isophthalate) Part I: Laboratory and outdoor conditions,** submitted.

T. Yashiro, H.R. Kricheldorf, S. Huijser, **Syntheses of biodegradable polyesters from succinic anhydride and various diols catalyzed by metal triflates,** submitted.